

University of Minnesota  
St. Anthony Falls Hydraulic Laboratory

Project Report No. 187

CULVER-GOODMAN TUNNEL  
DROPSHAFT EXIT CONDUIT MODEL STUDIES

by

Warren Q. Dahlin

and

Joseph M. Wetzel

Conducted for

LOZIER ENGINEERS, INC.  
Rochester, New York

and

HARZA ENGINEERING COMPANY  
Chicago, Illinois

Sponsored by the

DIVISION OF PURE WATERS  
Monroe County, New York

September, 1979  
Minneapolis, Minnesota

## Preface

Inherently, most metropolitan areas of the United States have storm water and sanitary sewage handling problems. Due to population growth and ever increasing industrialization the problems are becoming more severe. One solution to the problem being developed by several large cities is the use of tunnels excavated or bored into rock layers beneath the ground surface for conveyance, storage, and purification of the storm water and sanitary sewage. The effluent is stored during periods when the capacity of the treatment plants is exceeded and pumped out of storage and treated as the demands on the plants diminish.

One of these projects is the combined sewer overflow and abatement plan being developed by the City of Rochester, New York. The Culver-Goodman Tunnel, a part of the overall project, was the subject of this model study. Conduits near the surface collect storm water runoff and sewage and convey it to vertical dropshafts of various diameters; the diameter is determined by the design flow for the particular shaft. The water drops about 150 ft into a sump where energy is dissipated and entrained air removed. The air is returned to the surface through an air vent and the water is conveyed at a reduced velocity through an exit conduit to a 16 ft diameter storage and conveyance tunnel.

The purpose of the Culver-Goodman model studies was to provide some hydraulic insight into what occurs at the junctions of the exit conduits and storage tunnel, the effect of tunnel flow on conditions in the sump and at the junction, the effect of angularity of the incoming surface conduit, and the effect of exit conduit length and slope. To study these problems a model was constructed at the St. Anthony Falls Hydraulic Laboratory.

The model tests described in this report were conducted for Lozier Engineers, Inc. of Rochester, New York, represented by Salvatore LaBella, Robert Plecash, and Howard Shapiro; and Harza Engineering Company of Chicago, Illinois, represented by Dr. David Louie, Frank DeFazio, and Wayne Coleman. The model tests were sponsored by the Division of Pure Waters, Monroe County, New York, represented by Gerald McDonald and John Davis. During the course of the model studies, several meetings were held at the St. Anthony Falls Hydraulic Laboratory to demonstrate the model, discuss

various aspects of the project, outline the required tests, and discuss the results. Meetings were attended by representatives of the above organizations and the Laboratory. The study was under the immediate direction of Warren Dahlin, Scientist, and tests were conducted by Keith Anderson, Research Assistant. Various aspects of the project were reviewed by Joseph Wetzel, Assistant Director. A silent-color motion picture summarizing the pertinent tests was prepared by Warren Dahlin and reviewed by Joseph Wetzel. This final report summarizes the results of the test program.

TABLE OF CONTENTS

Preface .....	i
I.. INTRODUCTION .....	1
II. CONCLUSIONS .....	3
III. TYPE A DROPSHAFT .....	5
A. Description of Model .....	5
B. Model Observations .....	7
C. Piezometric Pressures .....	8
D. Fluctuating Pressures .....	8
IV. TYPE B DROPSHAFT .....	12
A. Description of Model .....	12
B. Model Observations .....	12
C. Piezometric Pressures .....	13
D. Fluctuating Pressures .....	13
V. TYPE C DROPSHAFT .....	14
A. Description of Model .....	14
B. Model Observations .....	14
C. Piezometric Pressures .....	14
D. Fluctuating Pressures .....	15
VI. TYPE C-1 DROPSHAFT .....	16
LIST OF PHOTOS .....	17
PHOTOS .....	21
LIST OF CHARTS .....	42
CHARTS .....	47

Project Report No. 187

CULVER-GOODMAN TUNNEL  
DROPSHAFT EXIT CONDUIT MODEL STUDIES

I. INTRODUCTION

The City of Rochester plans to excavate the Culver-Goodman tunnel and connect it to the existing Cross-Irondequoit tunnel through a control structure. Several dropshafts will convey the effluent from surface collection facilities to the storage and conveyance tunnel. The function of these dropshafts is to transport the water from one elevation and energy level to a lower elevation and energy level and, in the process, to dissipate energy and remove the entrained air. The term "dropshaft" is sometimes used collectively to include the various components of the structure. Conduits at or near the ground surface collect the water and convey it to an elbow which deflects the flow about 90 degrees into the vertical drop shaft. The vertical shaft is divided by a slotted wall which separates the falling water-air mixture and the released air returning to the surface. In the elbow and vertical shaft the falling water entrains considerable amounts of air and gains kinetic energy. The vertical shaft terminates in a sump, which is a large excavated and lined chamber. The purpose of the sump is to dissipate some of the energy, to remove and collect the entrained air, and to direct the water at a reduced velocity into the exit conduit. The sloping roof of the sump guides the collected air back to the vent side of the vertical shaft. A portion of the rising air is drawn through the slots in the divider wall and re-entrained in the falling water; the excess air returns to the surface. The exit conduit conveys the water into the tunnel.

A typical model including all of these components was fabricated at the St. Anthony Falls Hydraulic Laboratory and installed in the Laboratory's gravity flow system as shown in Photos 1 and 2. The model was built to a scale of 1:21.5. This scale was selected so that 4 inch diameter plastic tubes could be used to represent 7.17 ft diameter prototype conduits and dropshafts and 9 inch diameter plastic tubes to approximate the 16 ft diameter storage and conveyance tunnel. The study conducted was based upon steady state uniform flow approaching the dropshaft.

Gravity is the predominant motion-producing force in both the prototype and model. For this kind of system the greatest degree of dynamic similarity is obtained when the model-prototype relationships are established by the Froude Law. The following expressions were used to convert dimensions and hydraulic quantities from model to prototype or vice versa. The subscripts m and p refer to model and prototype, respectively, and the subscript r denotes the ratio of model to prototype.

<u>Quantity</u>	<u>Ratio</u>	<u>Scale Relation</u>
Length, L	$L_r = L_m/L_p$	1:21.5
Discharge, Q	$Q_r = L_r^{5/2}$	1:2143.37
Velocity, v	$V_r = L_r^{1/2}$	1:4.637
Pressure, P	$P_r = L_r$	1:21.5
Time, T	$T_r = L_r^{1/2}$	1:4.637
Frequency, f	$f_r = \frac{1}{L_r^{1/2}}$	1:0.216

For example, if the velocity in the model is 1.0 ft/sec, the corresponding velocity in the prototype will be 4.637 ft/sec.

Complete similarity for the air entrainment and air removal processes cannot in general be obtained because the mechanism of entrainment, the sizes of bubbles, and the relative movement of the bubbles through the water are subject to forces other than gravity and depend more on such forces as surface tension and viscosity. However, the processes are qualitatively similar and it is believed that the observations made in the model regarding the flow characteristics of the aerated mixture will be qualitatively correct. That is, the model indicates a large amount of air entrainment in the vertical shaft and effective air removal in the sump, then the prototype behavior is expected to be similar, even though the quantities of air do not obey Froude Law scaling.

## II. CONCLUSIONS

1. The type A dropshaft functioned quite effectively for all flows up to and including the design dropshaft flow of 300 cfs. Air removal was no problem for tailwater elevations below 16 ft, the elevation of the crown of the main tunnel and exit conduit, as the free water surface was continuous throughout the entire system and escaping air could easily return to the air vent. With tailwater elevations above 16 ft the main tunnel and exit conduit were full. The escaping air rose to the top of the sump and returned up the sloping top to the air vent. Very little air was carried into the exit conduit and main tunnel. The dropshaft had the capacity to convey a flow of 400 cfs, but with tailwater elevations of 20 and 40 ft the air removal was not as effective and some air was carried into the main tunnel. Hydraulic conditions at the 30 degree junction between the exit conduit and the main tunnel appeared acceptable. The disturbance was minimal and static pressures were positive. Instantaneous pressure fluctuations were also minimal at the junction. Instantaneous pressure fluctuations in the impact area were substantial. A maximum peak of 745 ft was recorded with several peaks in the 600 - 700 ft range. Several dips down to -250 ft were also recorded. These values were measured at a "point" with the 1/16 in. tap and chamber mounted transducer. With the same transducer flush-mounted and the 1/2 in. diameter diaphragm sensing the pressure fluctuations, much lower values were measured. Although these studies indicated that cavitation is likely in the impact area, prototype experience has shown that aeration will probably reduce the severe surface erosion. With a discharge in the main tunnel, no visually significant changes in the flow characteristics were observed. The instantaneous pressure fluctuations in the junction area increased somewhat both in frequency and magnitude.
2. The type B dropshaft, with the inlet turned 30 degrees, functioned quite effectively. The tests showed that the hydraulic characteristics were quite similar to type A in the main tunnel, exit conduit, and sump. Increased vorticity occurred in the upper elbow and dropshaft. Instantaneous fluctuating pressures on the floor of

the sump under the dropshaft were reduced considerably from those of type A. One possible reason for these lower pressures was the increased vorticity. Also, with the elbow turned, the flow pattern was different and the higher fluctuating pressures could have occurred at another area away from the tap location.

3. The type C dropshaft, with the shorter exit conduit, functioned quite effectively and the performance was similar to type A.
4. The type C-1 dropshaft included a cutoff plate installed at the crown of the exit conduit. This plate reduced the movement of air towards the main tunnel, but also blocked the trapped air in the main tunnel from escaping back through the dropshaft. For this reason the use of the cutoff plate is not recommended.



### III. TYPE A DROPSHAFT

#### A. Description of Model

The 1 to 21.5 scale model used in these studies was fabricated from transparent Lucite so that flow characteristics in the structure could be observed and photographed. The first geometry investigated was designated as the type A dropshaft. The dimensions and layout of this type are specified on Chart 1 and the model is shown in Photos 1 and 2. The design of the dropshaft is similar to that developed at the Laboratory in previous studies for the Lawrence Avenue sewer system in Chicago (1). The components modeled were the 7.17 ft diameter horizontal conduit at the ground surface, an elbow with a curved invert, a 7.17 ft diameter vertical shaft with a slotted divider wall, a sump, an exit conduit, a junction with the main tunnel, and a portion of the 16 ft diameter main tunnel. The inlet conduit pipe, sump, and exit conduit were in a straight line and made a 30 degree angle junction with the upstream section of the main tunnel. Close-up views of the junction from the left and right sides are shown in Photos 3 and 4. The top of the exit conduit was horizontal with the bottom at a slope of 12.5 per cent, with the conduit height expanding to match the 16 ft diameter of the tunnel. A tunnel length of 600 ft was modelled, with 200 ft upstream of the junction and 400 ft downstream. The components were fabricated in the laboratory shops and then assembled at the model site. Connections between the elbow, inlet pipe, and vertical shaft, and vertical shaft and top of the sump were provided with O-ring seals to facilitate changing inlet angle as required in future tests. Other sections such as the exit conduit were provided with flanges for connecting to the sump and junction for convenience in assembling and making revisions later in the program.

The water supply was obtained from the Mississippi River through the Laboratory's gravity flow supply system. A 4 inch supply line with a 1-5/8 inch diameter orifice meter and control valve was installed for larger flows. For lower flows a 2 inch by-pass line with a 7/8 inch

---

(1) Anderson, Alvin G. and Dahlin, Warren Q., "Model Studies - Lawrence Avenue Sewer System, City of Chicago," Project Report No. 100, University of Minnesota, St. Anthony Falls Hydraulic Laboratory, October 1968.

diameter orifice and control valve was provided. To control the tailwater level in the system, a butterfly valve was installed at the downstream end of the tunnel. The butterfly valve was installed with its axis horizontal so that the valve plate opened at the crown of the tunnel, thus, air collecting there would be swept out simulating air movement in the prototype tunnel.

Initial tests on the type A dropshaft were made with no tunnel flow. As the test program progressed, it was deemed desirable to investigate the effect tunnel flow would have on the flow conditions in the junction, exit conduit, and sump. Consequently, a 10 inch supply line with an 8 inch diameter orifice meter and control valve was connected to the model tunnel. The model was provided with numerous pressure taps at selected locations (Chart 1). These taps were connected by flexible plastic tubes to a manometer board where the static pressures were observed (Photos 1 and 2). The taps were provided with fittings to which the plastic tubes were attached. In making pressure fluctuation measurements these fittings were removed and a similar fitting, attached to a Lucite block containing a pressure transducer, was installed.

The design discharge of the prototype dropshaft was 300 cfs with an anticipated tailwater range of 0-40 ft. Initial tests were made with no tunnel flow. Later tests were made with tunnel flow. The flow conditions were determined from a mathematical model of the overall system which was developed for Lozier Engineers in another research program at the Laboratory. The following table summarizes the flow conditions investigated on the physical model, with  $Q_{DS}$  denoting dropshaft flow and  $Q_T$  denoting tunnel flow. The tailwater elevations used were also based on results of the mathematical model.

Flow Conditions Investigated

<u><math>Q_{DS}</math></u>	<u><math>Q_T</math></u>	<u>T.W. Elevation</u>
cfs	cfs	ft
400, 300, 200, 100	0	0, 4, 8, 12, 20, 40
400, 300, 200	800	8
400, 300, 200	2400	11
400, 300, 200	4000	40

## B. Model Observations

Overall views of the model in operation with the design dropshaft discharge of 300 cfs, no tunnel flow, and 0 ft tailwater are shown in Photos 5 and 6. As the flow conditions in the junction of the exit conduit and tunnel were the primary concern of these tests, particular attention was focused on this section. Photos 7 through 10 show closeup views of the junction with a dropshaft flow of 300 cfs and no tunnel flow. Photos 7 and 9 show these flows with a tailwater of 0 ft, and Photos 8 and 10 with tailwaters of 12 ft and 8 ft, respectively. With zero tailwater the hydraulic jump occurs in the main tunnel. As the tailwater level increases, the hydraulic jump is forced upstream so that, for a tailwater of 8 and 12 ft, it is located in the exit conduit as shown in Photos 8 and 10.

For comparison of various flow conditions and geometries, the camera was set up and kept in a chosen location and a series of pictures taken. The pictures include the lower section of the dropshaft, sump, exit conduit, and junction with the tunnel. A series of these pictures with the design flow of 300 cfs and tailwater elevations from 0 to 40 ft are shown in Photos 11 through 16. Photos 17 through 19 show flows of 400, 200, and 100 cfs with a tailwater of 20 ft and may be compared to Photo 15, which shows the design flow of 300 cfs and 20 ft tailwater. It appears that the flow conditions in the junction and exit conduit are hydraulically acceptable. For flows up to the design discharge of 300 cfs, the sump is quite effective in dissipating energy and air removal. A small quantity of minute air bubbles occasionally pass into the exit conduit at 300 cfs. These bubbles gradually collect to form a larger bubble at the crown, which eventually moved back into the sump. At a discharge of 400 cfs, the sump was not as efficient as indicated by the amount of air collecting at the crown of the exit conduit (Photo 17).

Operation of the model with tunnel flow did not appear to affect the flow conditions in the exit conduit and sump appreciably. Photos 20 through 22 show flow conditions with the dropshaft flow of 300 cfs and the tunnel discharge and tailwater varying according to the values given in the previous table. These may be compared to Photos 13, 14, and 16 which were taken with no tunnel flow. Observations were made with dropshaft discharges of 400 and 200 cfs with the same comparable results.

C. Piezometric Pressures

Piezometric pressures were measured throughout the structure at locations shown on Chart 1 and for various flow conditions. Charts 2 through 5 show the pressure values for dropshaft flows of 300 and 400 cfs, no tunnel flow, and various tailwater elevations. The values plot in a systematic order and show no negative pressures. Charts 6 through 9 show the pressure values for dropshaft flows of 300 and 400 cfs with the 3 tunnel flows and corresponding tailwater elevations. In comparing Charts 6 through 9 (with tunnel flow) and Charts 2 through 5 (no tunnel flow) the pressure readings when the tunnel has a discharge are somewhat higher in the upstream sections of the tunnel, exit conduit, and sump.

D. Fluctuating Pressures

Pressure fluctuation measurements were made at most of the taps in the sump, exit conduit, and junction between the exit conduit and main tunnel. The pressure transducer assembly was connected to the selected tap with a rigid connector and recordings made of the pressure fluctuations. The fluctuations were sensed on the diaphragm of the chamber-mounted transducer, and the output was transmitted to a Sanborn amplifier and a strip chart recorder which utilized a Thermo pen to trace the record on heat sensitive paper. This method was used on all taps, where the frequency of the fluctuations was relatively low, and outside of the impact area under the dropshaft. The frequency response of the 10 and 25 psi-pressure transducers used was 4 kHz, the Sanborn amplifier 600 Hz, and the Thermo pen 125 Hz for one-half scale deflection. Some records of typical pressure fluctuations recorded in this manner are shown on Charts 10 through 22. Chart 10 shows typical fluctuations at tap 24, which is on the main tunnel wall opposite from the exit conduit, for the design dropshaft flow of 300 cfs, no tunnel flow, and various tailwater elevations. For tailwater elevations from 0 to 12 ft practically no fluctuations were recorded and the fluctuations would probably remain low for tailwater elevations up to the crown of the main tunnel and exit conduit which is at elevation 16 ft. Some minor fluctuations are noticeable at a tailwater of 40 ft. One possible explanation for these fluctuations is that the system is full of water at tailwater elevations above 16 ft. The impact forces of the falling water in the

dropshaft impinging on the water surface in the sump are transmitted through the system and detected at the various tap locations. Chart 11 shows typical pressure fluctuations for the same flow conditions at tap 27, which is located on the left tunnel wall immediately downstream of the junction. Again minor fluctuations are noted with a 40 ft tailwater elevation. For a flow of 300 cfs and various tailwater elevations, some typical pressure fluctuations in the sump and outside of the impact area are shown on Chart 12, in the exit conduit on Chart 13, and on the left tunnel wall immediately downstream of the junction on Charts 14 and 15. Some fluctuations of relatively low amplitude and frequency are noted at some taps. Higher frequencies are noted at taps 12 - 14 near the impact area. Some typical fluctuations at taps 24 and 27 for a higher discharge of 400 cfs are presented on Charts 16 and 17, and these fluctuations may be compared to those shown on Charts 10 and 11. The records appear similar, with the only noticeable difference being slightly higher fluctuations at a 20 ft tailwater elevation and 400 cfs. On Charts 16 and 17 no records are shown for a tailwater elevation of 0 ft as this is a condition of no tailwater control. The tailwater is actually close to 4 ft and the records would be similar to those shown for 4 ft.

To investigate the effect of tunnel flow on pressure fluctuations, the model was operated with the three tunnel discharges and corresponding tailwater elevations and measurements made. The dropshaft discharge was also varied from 200 - 400 cfs. Charts 18, 19, and 22 show typical fluctuations at the junction, Chart 20 in the sump, and Chart 21 in the exit conduit. Comparisons of records at the same taps and similar dropshaft discharges and tailwater elevations show that the pressure fluctuations are noticeably higher in the junction area when the main tunnel has flow.

Charts 23 through 30 show summaries of pressure fluctuations for the various taps surveyed and various flow conditions established in the model. The summary includes values that may occur on charts presented in this report, and others are not presented for the sake of brevity. The pressure fluctuations in the impact area under the dropshaft, that is taps 8-11, were of a higher frequency and recorded by a different technique. The signal from the Sanborn amplifier was fed into a Tektronix Type 564 storage oscilloscope with a frequency response of 300 kHz instead of

the Thermo pen strip chart recorder. The scope was adjusted so that the trace would sweep across the screen in one second, flyback, and start another sweep. Each succeeding trace was superimposed and stored over the previous traces. A one minute record was made in this manner, after which a photograph was taken of the stored record on the face of the scope.

Charts 31 through 38 show typical records of this type for taps 8-11 and various flow conditions. Charts 31 and 32 show typical pressure fluctuations at tap 10 (center of dropshaft) with the design discharge of 300 cfs and tailwater elevations from 0 ft (not controlled) to 40 ft. A maximum peak of 745 ft was observed at a tailwater of 12 ft with several in the 600 - 700 ft range, and dips down to -250 ft. These prototype values were transposed from model values by the  $L_r$  according to the Froude Law of model studies. Thus, negative values in the model when transposed to prototype may go below -34ft (vapor pressure) when in reality this would not be possible as cavitation would occur. Cavitation is defined as the formation of the vapor phase of a liquid when the local pressure falls below the vapor pressure determined by the bulk temperature of the liquid. The vapor bubbles so formed collapse as they move into regions of higher pressure. The collapse pressures are very intense, and erosion of the solid surface can take place. Charts 33, 34, and 35 show typical pressure fluctuations at taps 8, 9, and 11, respectively, with a flow of 300 cfs. In examining the records for taps 8-11, it may be observed that the pressure levels vary from tap to tap indicating the water-air mixture falling down the dropshaft is not uniform. Chart 36 shows typical records at tap 10 for a flow of 400 cfs, which is similar to those for a flow of 300 cfs. Chart 37 shows records at tap 10 for a flow of 200 cfs, which shows a lower average pressure and fewer peaks and dips than for the 300 cfs flow. This is rather misleading because, with a lower flow, the pressure pattern on the sump floor shifts, thus higher pressures and fluctuations would occur elsewhere. Chart 38 shows the records when tunnel flow was established and may be compared to Charts 31 and 32. In comparing records with similar tailwater elevation, the records indicate somewhat lower fluctuations with tunnel flow. Whether this occurs as a result of the tunnel flow or a pressure variation with time in the system is not known.

Charts 39 through 41 summarize the pressure fluctuations study for taps 8-11.

The fluctuations in the impact area were relatively high and thus were the subject of much scrutiny and conjecture. One possibility investigated was the resilience and mass of the sump floor in the model. The floor of the original model was fabricated from 1/2-inch thick Lucite. To provide more rigidity, this floor was reinforced with 2-inch thick Lucite and supported from the concrete floor of the building. Pressure fluctuations were recorded with this arrangement. Another test was conducted in which sandbags were placed around the sump to give the structure more mass. Records of fluctuations with these modifications to the model were quite similar to those recorded on the original model.

Another possibility would be resonance of the transducer diaphragm as a source of the extreme pressure fluctuations recorded. This is probably not a factor as the manufacturer specifies the frequency response of the transducers to be higher than 4 kHz with a flat response to 3.6 kHz which is considerably higher than the pressure fluctuation frequencies in the model.

In addition to the above, an independent study was sponsored by Harza in an attempt to verify the model pressure readings. This study determined the following:

1. Vibration of the model structure does not affect the pressure readings.
2. Model pressure fluctuation readings vary with the size of the pressure tap. That is, the typical St. Anthony Falls Hydraulic Laboratory connection with the 1/16 inch tap and chamber mount transducer shows high frequency, high amplitude fluctuations at a "point." The same transducer flush-mounted with 1/2 inch diameter diaphragm shows much lower amplitude fluctuations. This indicates that the large "point" pressure fluctuations would not produce a large load variation over large areas. Also these studies indicate that cavitation is likely even with the aeration produced by this dropshaft design. However, prototype experience has shown that aeration will probably prevent the severe surface erosion which would be present without aeration.

#### IV. TYPE B DROPSHAFT

##### A. Description of Model

In some prototype dropshaft locations the right-of-way for construction is limited. To stay within authorized limits it becomes necessary to turn the surface conduit 30 degrees counter-clockwise so the conduit is in a parallel line with the main tunnel. Since this could change the hydraulic operating characteristics of the structure, it was decided to test this model geometry. This variation was designated as the type B dropshaft and is shown in Photo 23; specific details are given on Chart 1. In the model, the upper elbow and the inlet conduit were conveniently turned in the O-ring junction between the elbow and vertical dropshaft so that it was parallel to the main tunnel. The inlet supply line was revised to connect to the turned conduit. The remainder of the model was left as specified under type A (Chart 1).

##### B. Model Observations

With the upper elbow and inlet conduit turned and the vertical shaft unchanged, the flow entering the dropshaft impinged on the divider at the 30 degree angle. This imparted some rotational motion to the flow, resulting in increased vorticity in the elbow and upper region of the dropshaft. Photo 24 shows a close-up view of the elbow area for the type A dropshaft and for comparison Photo 25 shows the type B dropshaft. This increased disturbance in the elbow could result in increased air entrainment at that location. The flow characteristics in the sump did not visibly seem to have changed appreciably as evidenced in comparisons of flow patterns of type A in Photo 26, and type B in Photo 27. In these photos the tailwater elevation was 0 ft. In Photos 28 and 29 the tailwater elevation was maintained at 40 ft. Photo 30 shows a close-up of the junction of the sump and exit conduit where a slight amount of air collected at the crown and spurted back into the sump. Photos 31 through 36 show views of the flow patterns in the sump, exit conduit, and junction with the main tunnel for various flow conditions. They may be compared to photos of the type A dropshaft with the corresponding flow conditions. There does not appear to be any visually significant differences when the two types are compared.



C. Piezometric Pressures

Piezometric pressures for the type B dropshaft are presented on Charts 42 through 45. Charts 42 and 43 show the pressures in the inlet pipe, dropshaft, sump, and exit conduit; and Charts 44 and 45 show the pressures at the junction and in the main tunnel. The values plot in a systematic manner and appear similar to the values obtained for type A.

D. Fluctuating Pressures

Measurements of fluctuating pressures were also made on the type B dropshaft at selected taps using the same techniques described for the type A dropshaft. Again all records made are not presented in this report, but selected, significant records are presented on the charts. Typical pressure fluctuations at the junction (taps 24 and 27) and in the sump (taps 12-14) with no main tunnel flow are presented on Charts 46 and 47, respectively, and with main tunnel flow on Charts 48 and 49, respectively. Charts 50 and 51 summarize these pressure fluctuation studies. In a comparison of records for the type A dropshaft with similar flow conditions, minor variations are noted but do not appear significant.

Typical pressure fluctuations under the dropshaft in the impact area for 300 cfs and no main tunnel flow are shown on Charts 52 through 55. It is rather interesting to note that, for all taps in this area, the fluctuations were significantly lower than those for type A. It may be speculated that these lower fluctuations were the result of increased air entrainment and vorticity in the upper elbow and dropshaft. This would tend to have a more cushioning effect when the water-air mixture impinges on the floor of the sump. With a lower flow of 200 cfs, higher fluctuations were detected at tap 8 (Chart 56), indicating that the major portion of the flow was following down the dropshaft wall and impinging directly on tap 8. Another factor was the lower vorticity for this lower flow of 200 cfs. With tunnel flow, the resulting fluctuations were similar. An example is shown on Chart 57 which shows fluctuations at tap 10 with a flow of 300 cfs. Chart 58 summarizes the study of fluctuating pressures under the dropshaft for the type B dropshaft.

## V. TYPE C DROPSHAFT

### A. Description of Model

In some specific dropshaft locations in Rochester, space is extremely limited. This necessitates the construction of the dropshaft closer to the main tunnel. To satisfy this requirement it was proposed to shorten the exit conduit, thereby moving the sump closer to the main tunnel. The top of the exit conduit remained horizontal with the slope of the floor increased from 12.5 percent (types A and B) to 25 percent, which resulted in an exit conduit one-half as long. In this situation the inlet conduit was in line with the sump and exit conduit (Chart 1). It was considered necessary to test this design variation. This design, designated as the type C dropshaft, was essentially the same as type A with the exception of the shortened exit conduit. Photo 37 shows the type C dropshaft under observation. The researcher is holding the original exit conduit next to the installed shorter exit conduit.

### B. Model Observations

Photos 38 through 40 show photos with the design flow of 300 cfs, no tunnel flow, and tailwaters of 0, 20, and 40 ft. Comparison of these with photos of types A and B dropshafts for similar flow conditions show very little visible hydraulic differences. Photos 41 and 42 show the small quantity of air that collected at the crown of the exit conduit and spurted back into the sump. This phenomenon occurred in all types and the quantity of air involved was judged quite minimal. Photo 42 of type C may be compared with Photo 30 of type B. Photos 43 through 45 show the flow patterns with main tunnel flow. Visual observations in the sump, exit conduit, and main tunnel show few noticeable differences between the three types.

### C. Piezometric Pressures

The piezometric pressures in the system for a dropshaft discharge of 300 cfs, no tunnel flow, and tailwater varied, are presented on Charts 59 and 60, and for a dropshaft discharge of 300 cfs, and tunnel flow, and tailwater varied on Charts 61 and 62. The plotted results are quite repetitious of results for types A and B.

D. Fluctuating Pressures

Measurements of fluctuating pressures were made similar to those made on the previous types of dropshafts. The resultant records were similar to those made on the previous types. Charts 63 through 66 show typical pressure fluctuations relevant to the junction and exit conduit area. The summary of pressure fluctuations, other than the impact area under the dropshaft, is presented on Charts 67 and 68.

Typical pressure fluctuations under the dropshaft for taps 8-11 are presented on Charts 69 through 73, and the summary on Chart 74. These records show fluctuations that are similar to those for the type A dropshaft and higher than those observed for the type B dropshaft.

## VI. TYPE C-1 DROPSHAFT

Although the sump was quite effective in removing the entrained air from the water-air mixture, some minute bubbles occasionally were swept into the exit conduit and in time collected and formed a larger bubble at the crown. This bubble eventually spurted back into the sump. Some concern was expressed that some of this air, although of a very small quantity, would eventually be carried into the main storage and conveyance tunnel. To reduce this possibility, it was proposed to place a cutoff plate in the crown of the exit conduit as shown in Photos 46 and 47. The plate projected downwards 1.8 ft from the crown as shown in section E-E of Chart 1. This geometry was designated as the type C-1 dropshaft and visual observations were made of its effectiveness. Photo 48 shows type C (no plate) and Photo 49, type C-1 (with plate), for comparison. The plate did effectively reduce the movement of air along the crown of the exit conduit as shown in Photo 49. Consideration was also given to the possibility that air already in the main tunnel would be prevented from escaping back through the sump by presence of the plate. As the tunnel is filling and the water level is approaching the crown of the system, the remaining air would be trapped in the tunnel by this plate. This would seem to be very undesirable and negate the use of the cutoff plate. Tests with air injected into the main tunnel flow upstream of the dropshaft showed that air was prevented from escaping back through the dropshaft.

LIST OF PHOTOS

- PHOTO 1 (Serial No. 260-1) Type A dropshaft. An overall view of the model area with the model being assembled.
- PHOTO 2 (Serial No. 260-4) Type A dropshaft. The completed model ready for testing.
- PHOTO 3 (Serial No. 260-8) Type A dropshaft. A closeup view from the left side of the 30° junction between the exit conduit and main tunnel.
- PHOTO 4 (Serial No. 260-9) Type A dropshaft. A closeup view from the right side of the 30° junction between the exit conduit and the main tunnel.
- PHOTO 5 (Serial No. 260-12) Type A dropshaft,  $Q_{DS} = 300$  cfs,  $Q_T = 0$  cfs, T.W. = 0 ft. An overall view of the model in operation.
- PHOTO 6 (Serial No. 260-19) Type A dropshaft,  $Q_{DS} = 300$  cfs,  $Q_T = 0$  cfs, T.W. = 0 ft.
- PHOTO 7 (Serial No. 260-23) Type A dropshaft,  $Q_{DS} = 300$  cfs,  $Q_T = 0$  cfs, T.W. = 0 ft. The flow pattern at the junction taken from the left side.
- PHOTO 8 (Serial No. 260-24) Type A dropshaft,  $Q_{DS} = 300$  cfs,  $Q_T = 0$  cfs, T.W. = 12 ft. The flow pattern at the junction taken from the left side.
- PHOTO 9 (Serial No. 260-26) Type A dropshaft,  $Q_{DS} = 300$  cfs,  $Q_T = 0$  cfs, T.W. = 0 ft. The flow pattern at the junction taken from the right side.
- PHOTO 10 (Serial No. 260-27) Type A dropshaft,  $Q_{DS} = 300$  cfs,  $Q_T = 0$  cfs, T.W. = 8 ft. The flow pattern at the junction taken from the right side.
- PHOTO 11 (Serial No. 260-36) Type A dropshaft,  $Q_{DS} = 300$  cfs,  $Q_T = 0$  cfs, T.W. = 0 ft. The flow pattern in the sump, exit conduit, and junction.
- PHOTO 12 (Serial No. 260-37) Type A dropshaft,  $Q_{DS} = 300$  cfs,  $Q_T = 0$  cfs, T.W. = 4 ft. The flow pattern in the sump, exit conduit, and junction.
- PHOTO 13 (Serial No. 260-38) Type A dropshaft,  $Q_{DS} = 300$  cfs,  $Q_T = 0$  cfs, T.W. = 8 ft. The flow pattern in the sump, exit conduit, and junction.
- PHOTO 14 (Serial No. 260-39) Type A dropshaft,  $Q_{DS} = 300$  cfs,  $Q_T = 0$  cfs, T.W. = 12 ft. The flow pattern in the sump, exit conduit, and junction.

LIST OF PHOTOS (Cont'd)

- PHOTO 15 (Serial No. 260-40) Type A dropshaft,  $Q_{DS} = 300$  cfs,  $Q_T = 0$  cfs, T.W. = 20 ft. The flow pattern in the sump, exit conduit, and junction.
- PHOTO 16 (Serial No. 260-41) Type A dropshaft,  $Q_{DS} = 300$  cfs,  $Q_T = 0$  cfs, T.W. = 40 ft. The flow pattern in the sump, exit conduit, and junction.
- PHOTO 17 (Serial No. 260-34) Type A dropshaft,  $Q_{DS} = 400$  cfs,  $Q_T = 0$  cfs, T.W. = 20 ft. The flow pattern in the sump, exit conduit, and junction.
- PHOTO 18 (Serial No. 260-46) Type A dropshaft,  $Q_{DS} = 200$  cfs,  $Q_T = 0$  cfs, T.W. = 20 ft. The flow pattern in the sump, exit conduit, and junction.
- PHOTO 19 (Serial No. 260-52) Type A dropshaft,  $Q_{DS} = 100$  cfs,  $Q_T = 0$  cfs, T.W. = 20 ft. The flow pattern in the sump, exit conduit, and junction.
- PHOTO 20 (Serial No. 260-171) Type A dropshaft,  $Q_{DS} = 300$  cfs,  $Q_T = 800$  cfs, T.W. = 8 ft. The flow pattern in the sump, exit conduit, and junction.
- PHOTO 21 (Serial No. 260-172) Type A dropshaft,  $Q_{DS} = 300$  cfs,  $Q_T = 2400$  cfs, T.W. = 11 ft. The flow pattern in the sump, exit conduit, and junction.
- PHOTO 22 (Serial No. 260-173) Type A dropshaft,  $Q_{DS} = 300$  cfs,  $Q_T = 4000$  cfs, T.W. = 40 ft. The flow pattern in the sump, exit conduit, and junction.
- PHOTO 23 (Serial No. 260-196) Type B dropshaft,  $Q_{DS} = 300$  cfs,  $Q_T = 0$  cfs, T.W. = 0 ft.
- PHOTO 24 (Serial No. 260-20) Type A dropshaft,  $Q_{DS} = 300$  cfs,  $Q_T = 0$  cfs, T.W. = 0 ft. The flow pattern in the elbow.
- PHOTO 25 (Serial No. 260-197) Type B dropshaft,  $Q_{DS} = 300$  cfs,  $Q_T = 0$  cfs, T.W. = 0 ft. The flow pattern in the elbow.
- PHOTO 26 (Serial No. 260-21) Type A dropshaft,  $Q_{DS} = 300$  cfs,  $Q_T = 0$  cfs, T.W. = 0 ft. The flow pattern in the sump.
- PHOTO 27 (Serial No. 260-199) Type B dropshaft,  $Q_{DS} = 300$  cfs,  $Q_T = 0$  cfs, T.W. = 0 ft. The flow pattern in the sump.
- PHOTO 28 (Serial No. 260-22) Type A dropshaft,  $Q_{DS} = 300$  cfs,  $Q_T = 0$  cfs, T.W. = 40 ft. The flow pattern in the sump.

LIST OF PHOTOS (Cont'd)

- PHOTO 29 (Serial No. 260-201) Type B dropshaft,  $Q_{DS} = 300$  cfs,  $Q_T = 0$  cfs, T.W. = 40 ft. The flow pattern in the sump.
- PHOTO 30 (Serial No. 260-204) Type B dropshaft,  $Q_{DS} = 300$  cfs,  $Q_T = 0$  cfs, T.W. = 40 ft. The air collecting at the junction of the sump and exit conduit.
- PHOTO 31 (Serial No. 260-206) Type B dropshaft,  $Q_{DS} = 300$  cfs,  $Q_T = 0$  cfs, T.W. = 0 ft. The flow pattern in the sump, exit conduit, and junction.
- PHOTO 32 (Serial No. 260-207) Type B dropshaft,  $Q_{DS} = 300$  cfs,  $Q_T = 0$  cfs, T.W. = 20 ft. The flow pattern in the sump, exit conduit, and junction.
- PHOTO 33 (Serial No. 260-208) Type B dropshaft,  $Q_{DS} = 300$  cfs,  $Q_T = 0$  cfs, T.W. = 40 ft. The flow pattern in the sump, exit conduit, and junction.
- PHOTO 34 (Serial No. 260-215) Type B dropshaft,  $Q_{DS} = 300$  cfs,  $Q_T = 800$  cfs, T.W. = 8 ft. The flow pattern in the sump, exit conduit, and junction.
- PHOTO 35 (Serial No. 260-216) Type B dropshaft,  $Q_{DS} = 300$  cfs,  $Q_T = 2400$  cfs, T.W. = 11 ft. The flow pattern in the sump, exit conduit, and junction.
- PHOTO 36 (Serial No. 260-217) Type B dropshaft,  $Q_{DS} = 300$  cfs,  $Q_T = 4000$  cfs, T.W. = 40 ft. The flow pattern in the sump, exit conduit, and junction.
- PHOTO 37 (Serial No. 260-289) Type C dropshaft,  $Q_{DS} = 300$  cfs,  $Q_T = 0$  cfs, T.W. = 0 ft. The exit conduit (slope 12.5%) used in Types A and B dropshafts is shown along side of the exit conduit (slope 25%) for Type C dropshaft.
- PHOTO 38 (Serial No. 260-302) Type C dropshaft,  $Q_{DS} = 300$  cfs,  $Q_T = 0$  cfs, T.W. = 0 ft. The flow pattern in the sump, exit conduit, and junction.
- PHOTO 39 (Serial No. 260-303) Type C dropshaft,  $Q_{DS} = 300$  cfs,  $Q_T = 0$  cfs, T.W. = 20 ft. The flow pattern in the sump, exit conduit, and junction.
- PHOTO 40 (Serial No. 260-304) Type C dropshaft,  $Q_{DS} = 300$  cfs,  $Q_T = 0$  cfs, T.W. = 40 ft. The flow pattern in the sump, exit conduit, and junction.
- PHOTO 41 (Serial No. 260-293) Type C dropshaft,  $Q_{DS} = 300$  cfs,  $Q_T = 0$  cfs, T.W. = 20 ft. The flow pattern at the junction of the sump and exit conduit.

LIST OF PHOTOS (Cont'd)

- PHOTO 42 (Serial No. 260-295) Type C dropshaft,  $Q_{DS} = 300$  cfs,  $Q_T = 0$  cfs, T.W. = 40 ft. The flow pattern at the junction of the sump and exit conduit.
- PHOTO 43 (Serial No. 260-311) Type C dropshaft,  $Q_{DS} = 300$  cfs,  $Q_T = 800$  cfs, T.W. = 8 ft. The flow pattern in the sump, exit conduit, and junction.
- PHOTO 44 (Serial No. 260-312) Type C dropshaft,  $Q_{DS} = 300$  cfs,  $Q_T = 2400$  cfs, T.W. = 11 ft. The flow pattern in the sump, exit conduit, and junction.
- PHOTO 45 (Serial No. 260-313) Type C dropshaft,  $Q_{DS} = 300$  cfs,  $Q_T = 4000$  cfs, T.W. = 40 ft. The flow pattern in the sump, exit conduit, and junction.
- PHOTO 46 (Serial No. 260-392) Type C-1 dropshaft. The plate being installed in the top of the exit conduit.
- PHOTO 47 (Serial No. 260-393) Type C-1 dropshaft. The plate being installed in the top of the exit conduit.
- PHOTO 48 (Serial No. 260-397) Type C dropshaft,  $Q_{DS} = 300$  cfs,  $Q_T = 0$  cfs, T.W. = 20 ft. The flow pattern in the exit conduit.
- PHOTO 49 (Serial No. 260-399) Type C-1 dropshaft,  $Q_{DS} = 300$  cfs,  $Q_T = 0$  cfs, T.W. = 20 ft. The flow pattern in the exit conduit.



Photo 1 (Serial No. 260-1) Type A dropshaft,  
An overall view of the model area  
with the model being assembled.

Photo 2 (Serial No. 260-4) Type A dropshaft,  
The completed model ready for  
testing.

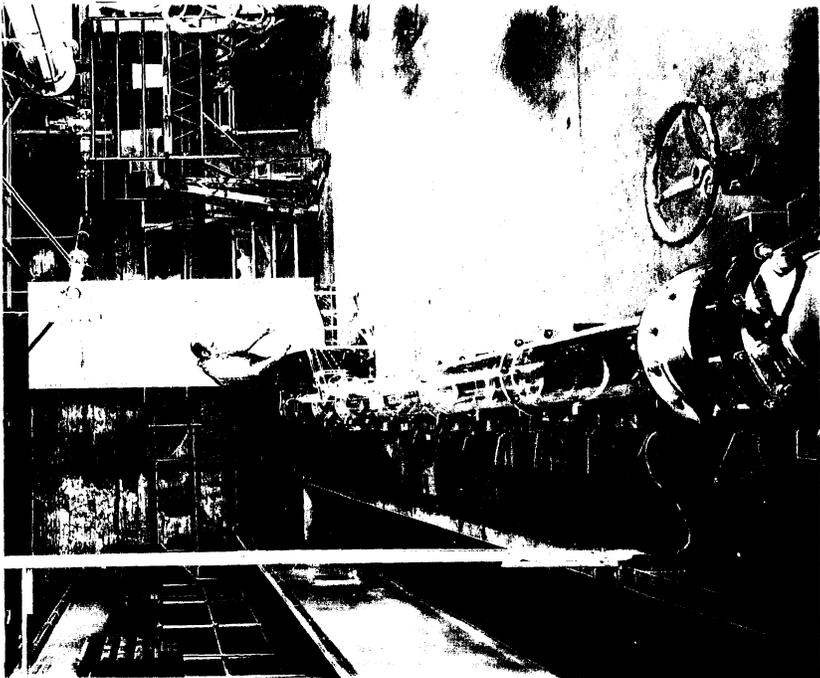
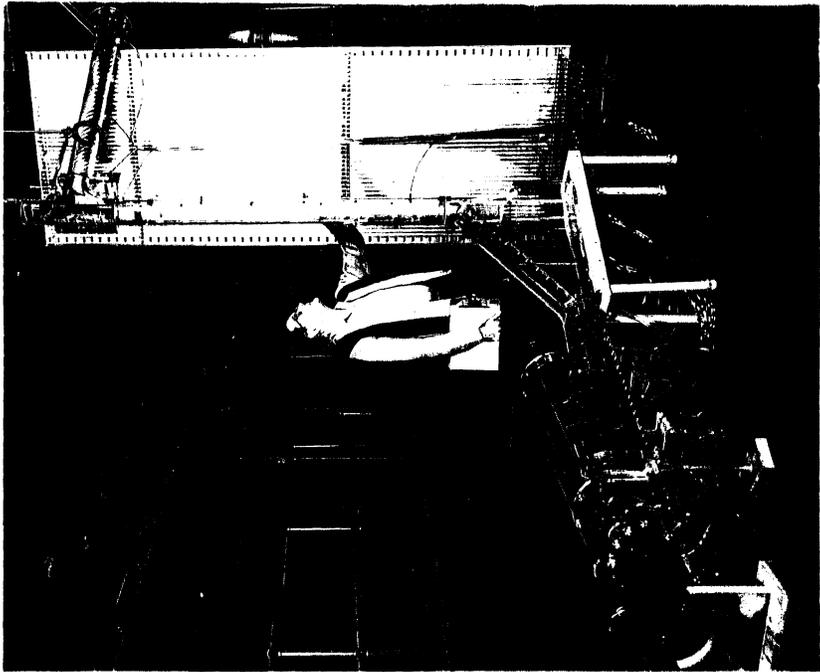


Photo 3 (Serial No. 260-8) Type A dropshaft,  
A close up view from the left side  
of the 30° junction between the exit  
conduit and main tunnel.

Photo 4 (Serial No. 260-9) Type A dropshaft,  
A close up view from the right side  
of the 30° junction between the exit  
conduit and the main tunnel.

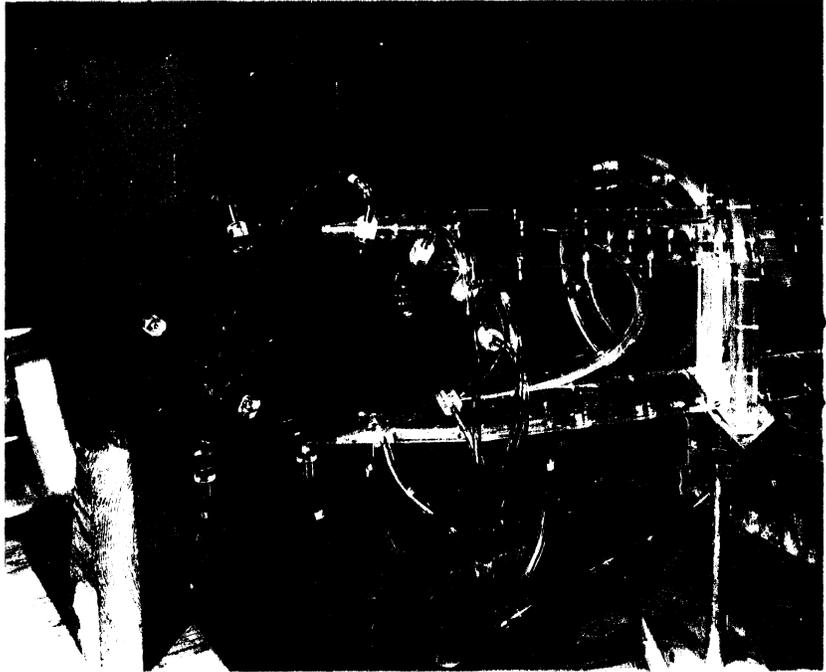


Photo 5 (Serial No. 260-12) Type A dropshaft,  
 $Q_{DS} = 300$  cfs,  $Q_T = 0$  cfs, T.W. = 0 ft.  
An overall view of the model in  
operation.

Photo 6 (Serial No. 260-19) Type A dropshaft,  
 $Q_{DS} = 300$  cfs,  $Q_T = 0$  cfs, T.W. = 0 ft.

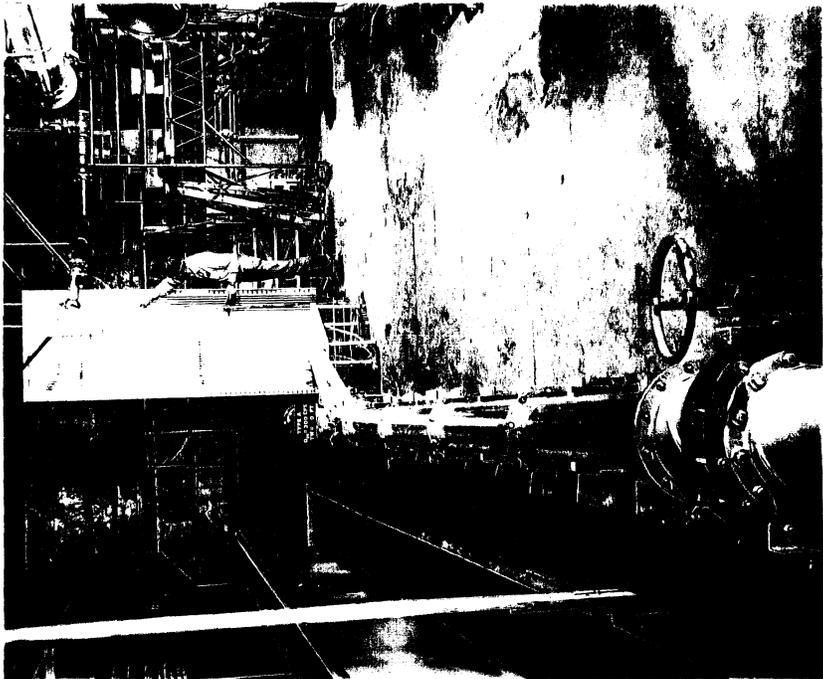
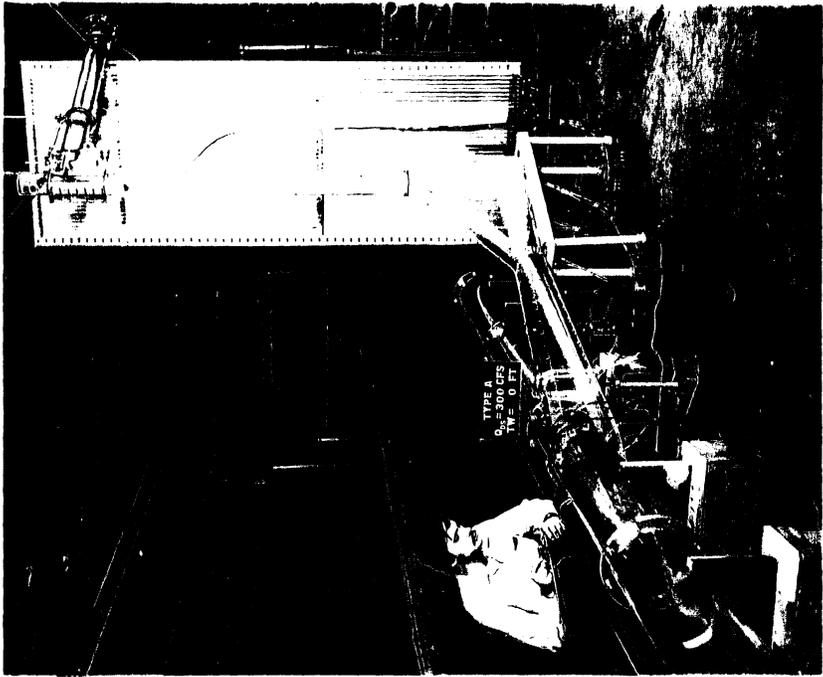


Photo 7 (Serial No. 260-23) Type A dropshaft,  
 $Q_{DS} = 300$  cfs,  $Q_T = 0$  cfs, T.W. = 0 ft.  
The flow pattern at the junction taken  
from the left side.

Photo 8 (Serial No. 260-24) Type A dropshaft,  
 $Q_{DS} = 300$  cfs,  $Q_T = 0$  cfs, T.W. = 12 ft.  
The flow pattern at the junction taken  
from the left side.

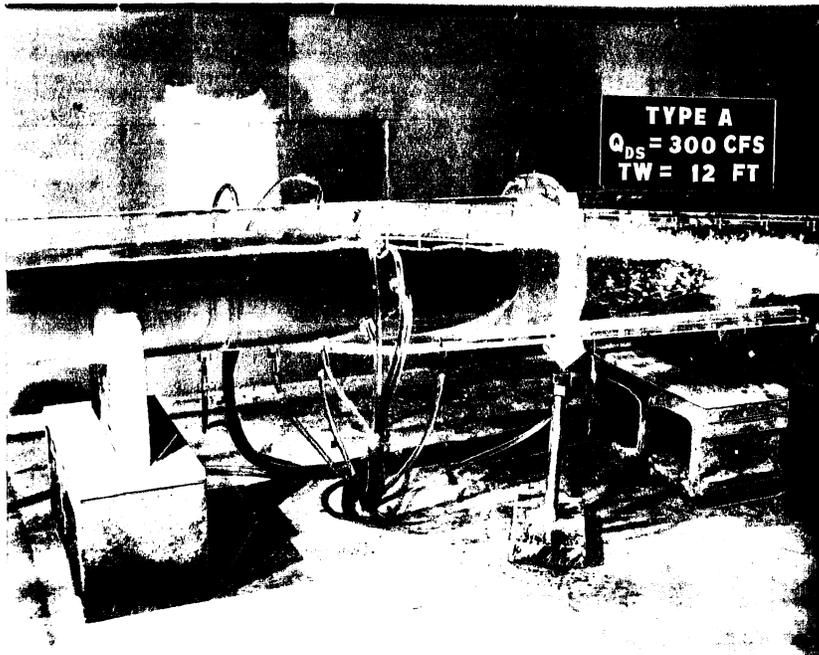
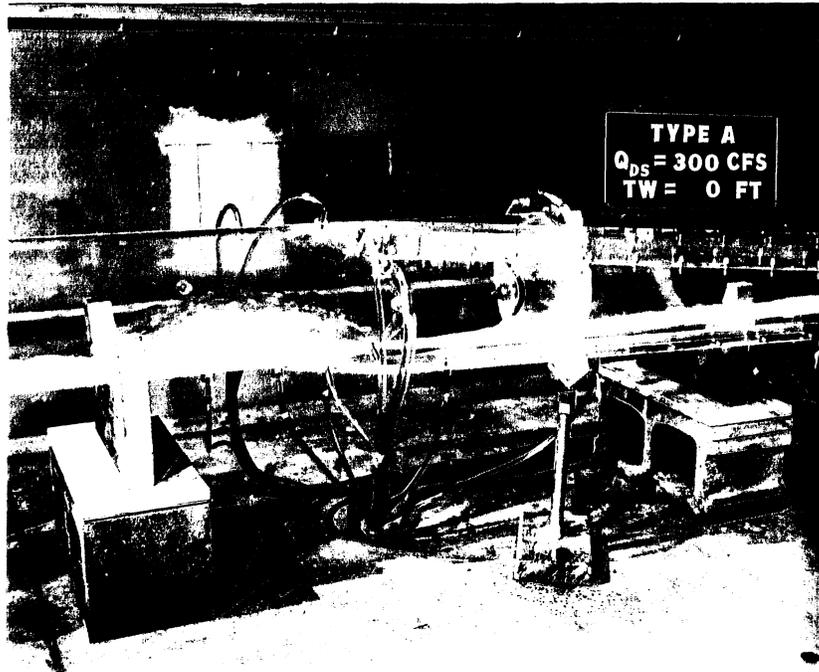




Photo 9 (Serial No. 260-26) Type A dropshaft,  
 $Q_{DS} = 300$  cfs,  $Q_T = 0$  cfs, T.W. = 0 ft.  
The flow pattern at the junction taken  
from the right side.

Photo 10 (Serial No. 260-27) Type A dropshaft,  
 $Q_{DS} = 300$  cfs,  $Q_T = 0$  cfs, T.W. = 8 ft.  
The flow pattern at the junction taken  
from the right side.

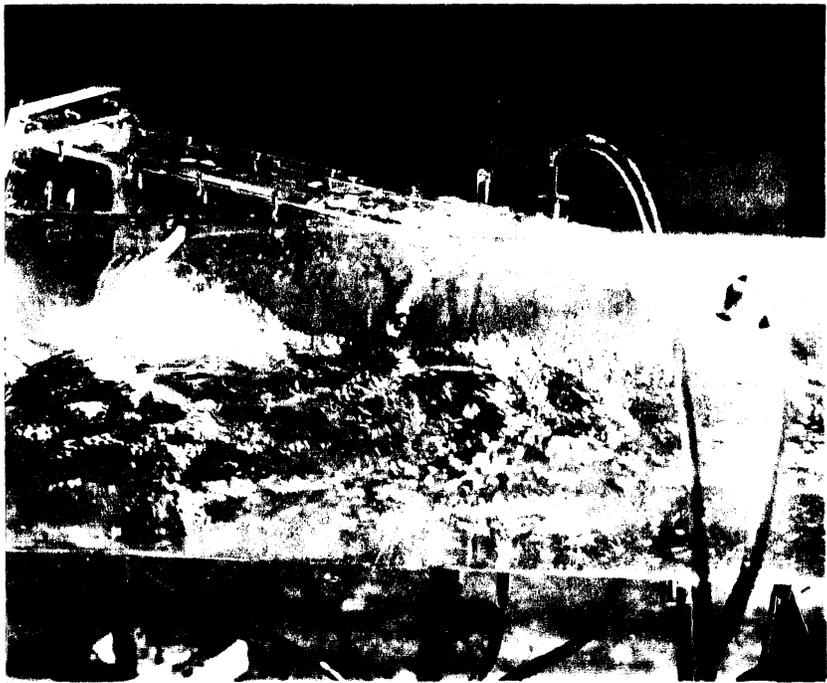
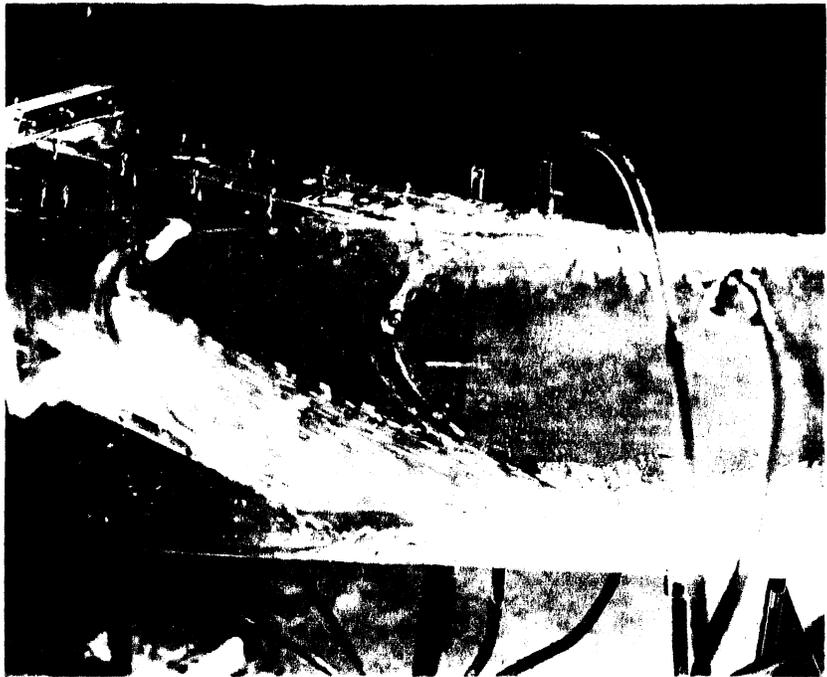


Photo 11 (Serial No. 260-36) Type A dropshaft,  
 $Q_{DS} = 300$  cfs,  $Q_T = 0$  cfs, T.W. = 0 ft.  
The flow pattern in the sump, exit conduit,  
and junction.

Photo 12 (Serial No. 260-37) Type A dropshaft,  
 $Q_{DS} = 300$  cfs,  $Q_T = 0$  cfs, T.W. = 4 ft.  
The flow pattern in the sump, exit conduit,  
and junction.

Photo 13 (Serial No. 260-38) Type A dropshaft,  
 $Q_{DS} = 300$  cfs,  $Q_T = 0$  cfs, T.W. = 8 ft.  
The flow pattern in the sump, exit conduit,  
and junction.

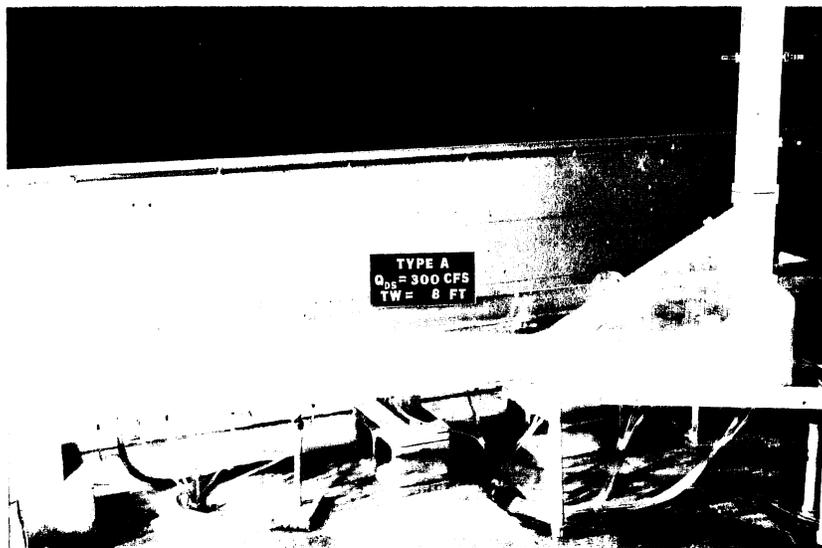
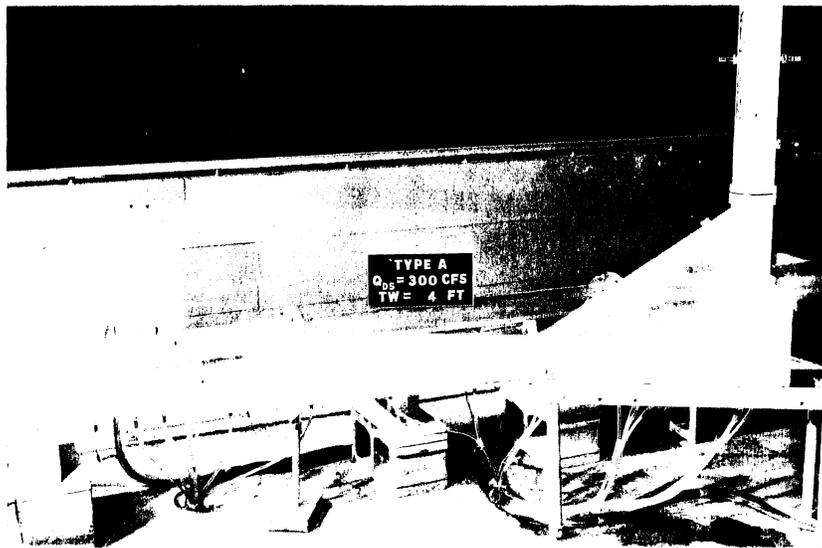
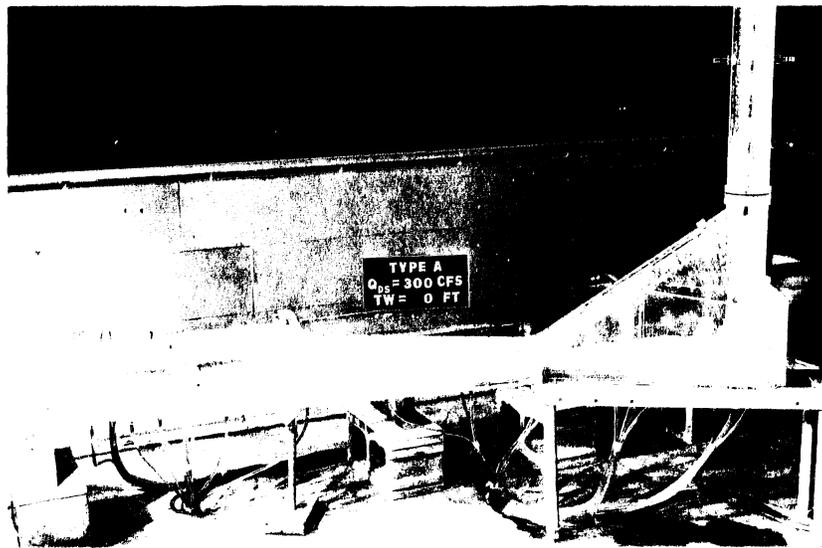


Photo 14 (Serial No. 260-39) Type A dropshaft,  
 $Q_{DS} = 300$  cfs,  $Q_T = 0$  cfs, T.W. = 12 ft.  
The flow pattern in the sump, exit conduit,  
and junction.

Photo 15 (Serial No. 260-40) Type A dropshaft,  
 $Q_{DS} = 300$  cfs,  $Q_T = 0$  cfs, T.W. = 20 ft.  
The flow pattern in the sump, exit conduit,  
and junction.

Photo 16 (Serial No. 260-41) Type A dropshaft,  
 $Q_{DS} = 300$  cfs,  $Q_T = 0$  cfs, T.W. = 40 ft.  
The flow pattern in the sump, exit conduit,  
and junction.

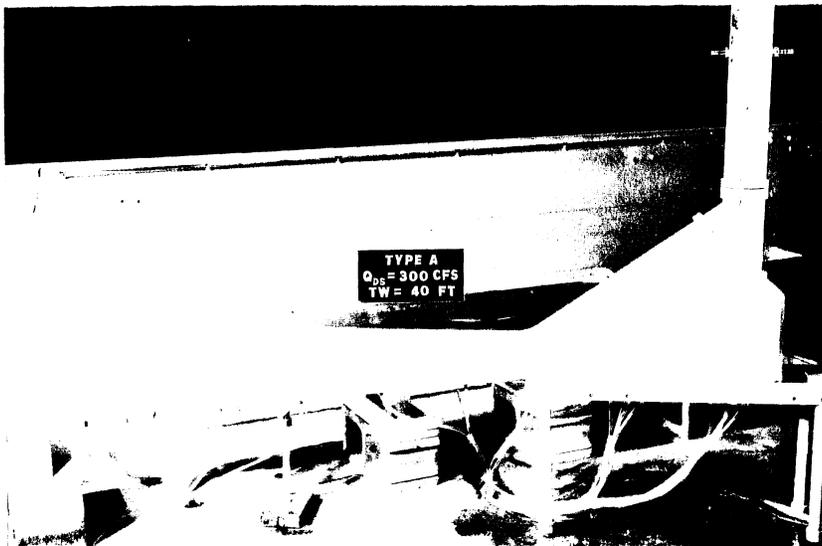
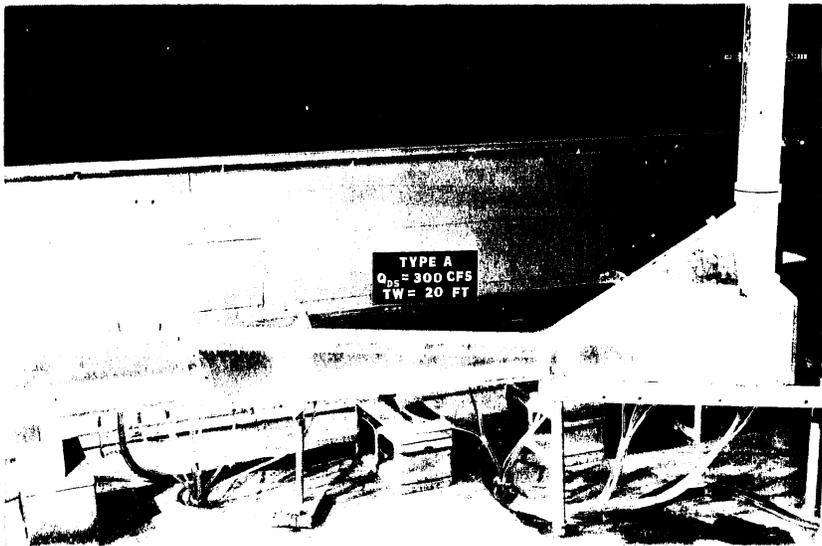
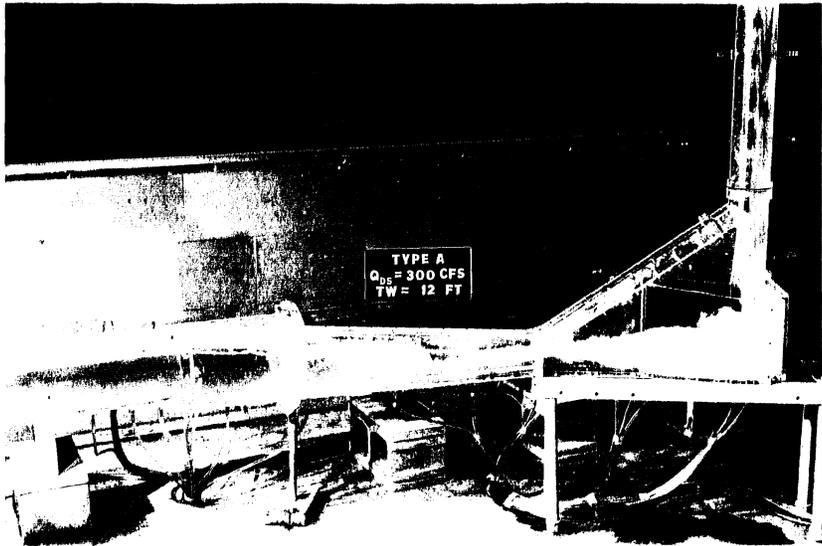


Photo 17 (Serial No. 260-34) Type A dropshaft,  
 $Q_{DS} = 400$  cfs,  $Q_T = 0$  cfs, T.W. = 20 ft.  
The flow pattern in the sump, exit conduit,  
and junction.

Photo 18 (Serial No. 260-46) Type A dropshaft,  
 $Q_{DS} = 200$  cfs,  $Q_T = 0$  cfs, T.W. = 20 ft.  
The flow pattern in the sump, exit conduit,  
and junction.

Photo 19 (Serial No. 260-52) Type A dropshaft,  
 $Q_{DS} = 100$  cfs,  $Q_T = 0$  cfs, T.W. = 20 ft.  
The flow pattern in the sump, exit conduit,  
and junction.

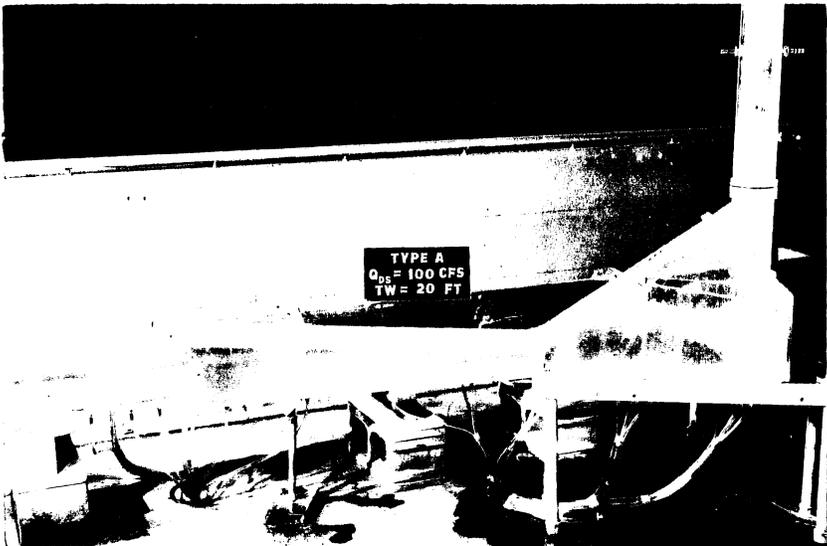
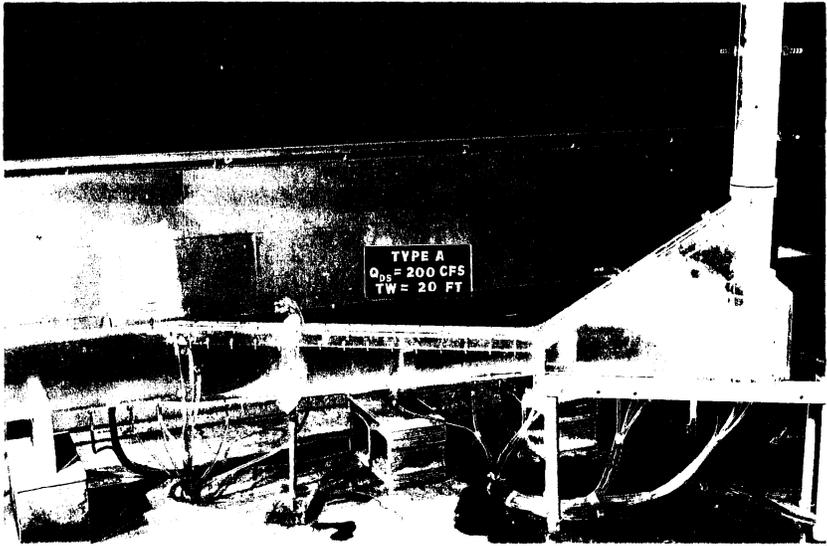
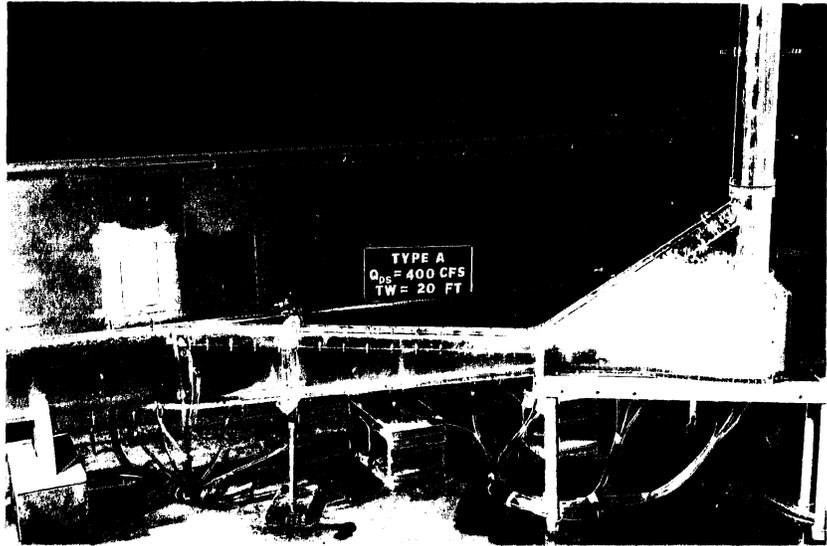




Photo 20 (Serial No. 260-171) Type A dropshaft,  
 $Q_{DS} = 300$  cfs,  $Q_T = 800$  cfs, T.W. = 8 ft.  
The flow pattern in the sump, exit conduit,  
and junction.

Photo 21 (Serial No. 260-172) Type A dropshaft,  
 $Q_{DS} = 300$  cfs,  $Q_T = 2,400$  cfs, T.W. = 11 ft.  
The flow pattern in the sump, exit conduit,  
and junction.

Photo 22 (Serial No. 260-173) Type A dropshaft,  
 $Q_{DS} = 300$  cfs,  $Q_T = 4,000$  cfs, T.W. = 40 ft.  
The flow pattern in the sump, exit conduit,  
and junction.

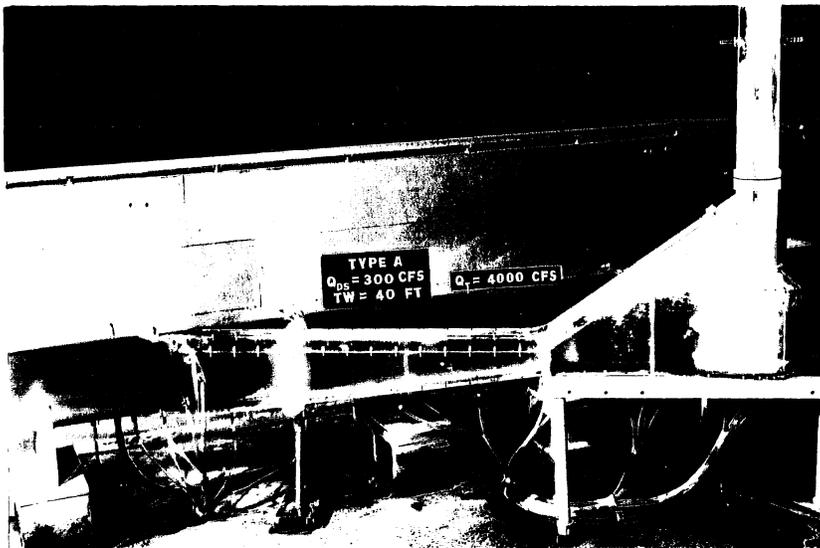
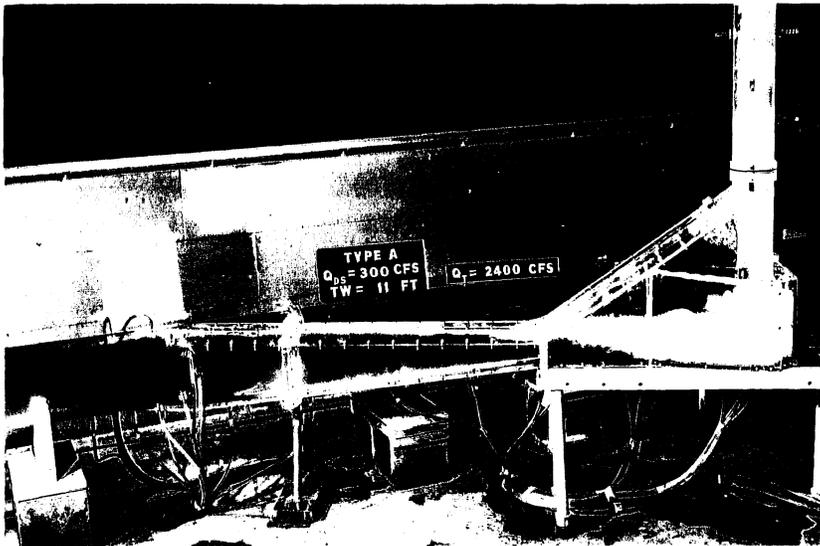
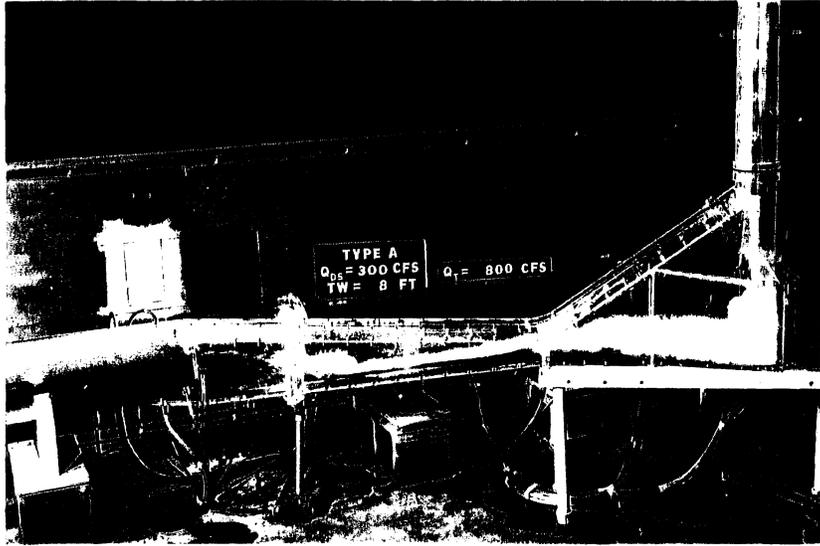


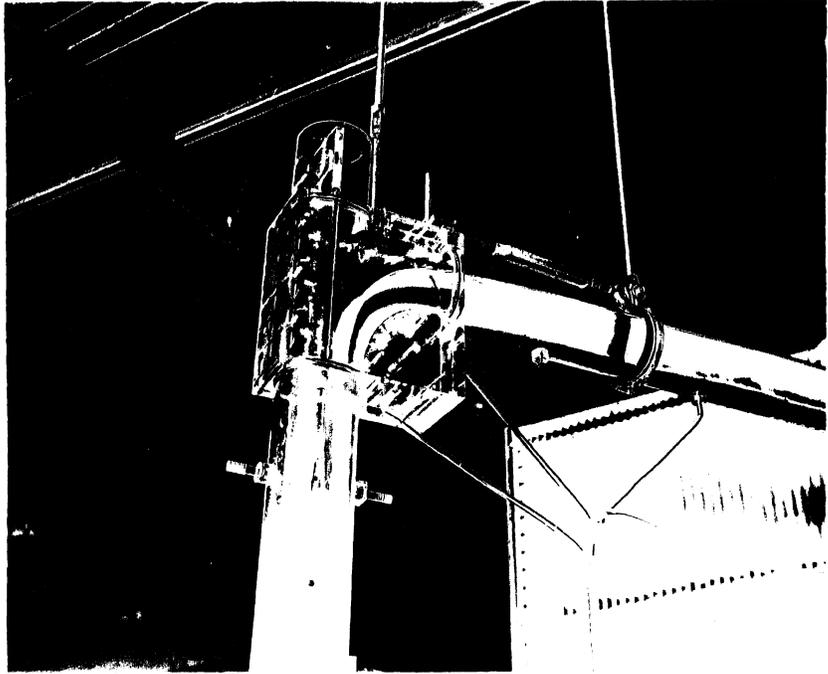
Photo 23 (Serial No. 260-196) Type B dropshaft,  $Q_{DS} = 300$  cfs,  
 $Q_T = 0$  cfs, T.W. = 0 ft.



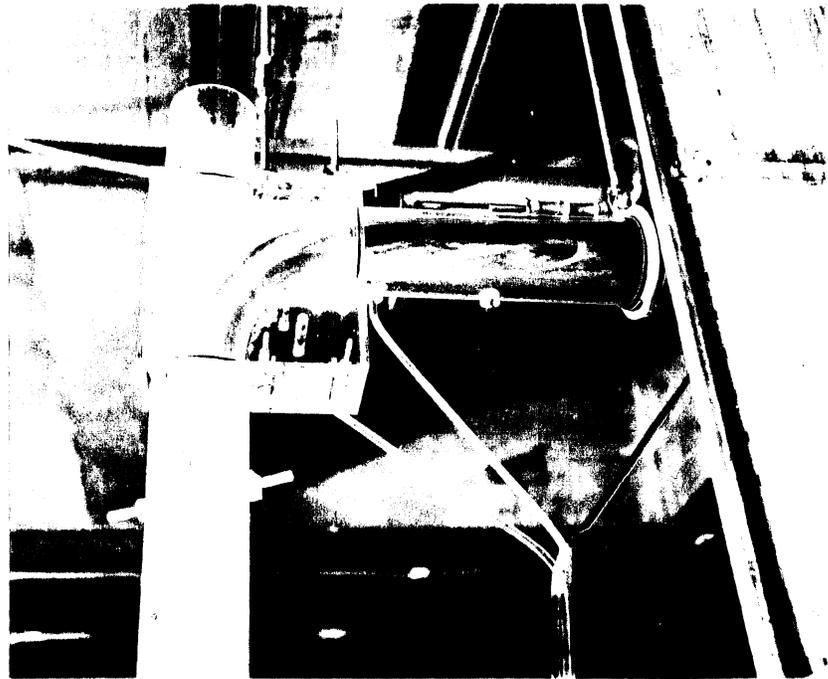
Photo 24 (Serial No. 260-20) Type A dropshaft,  $Q_{DS} = 300$  cfs,  
 $Q_T = 0$  cfs, T.W. = 0 ft, The flow pattern in the elbow.

Photo 25 (Serial No. 260-197) Type B dropshaft,  $Q_{DS} = 300$  cfs,  
 $Q_T = 0$  cfs, T.W. = 0 ft. The flow pattern in the elbow.

100



101



102

Photo 26 (Serial No. 260-21) Type A dropshaft,  $Q_{DS} = 300$  cfs,  
 $Q_T = 0$  cfs, T.W. 0 ft. The flow pattern in the sump.

Photo 27 (Serial No. 260-199) Type B dropshaft,  $Q_{DS} = 300$  cfs,  
 $Q_T = 0$  cfs, T.W. 0 ft. The flow pattern in the sump.

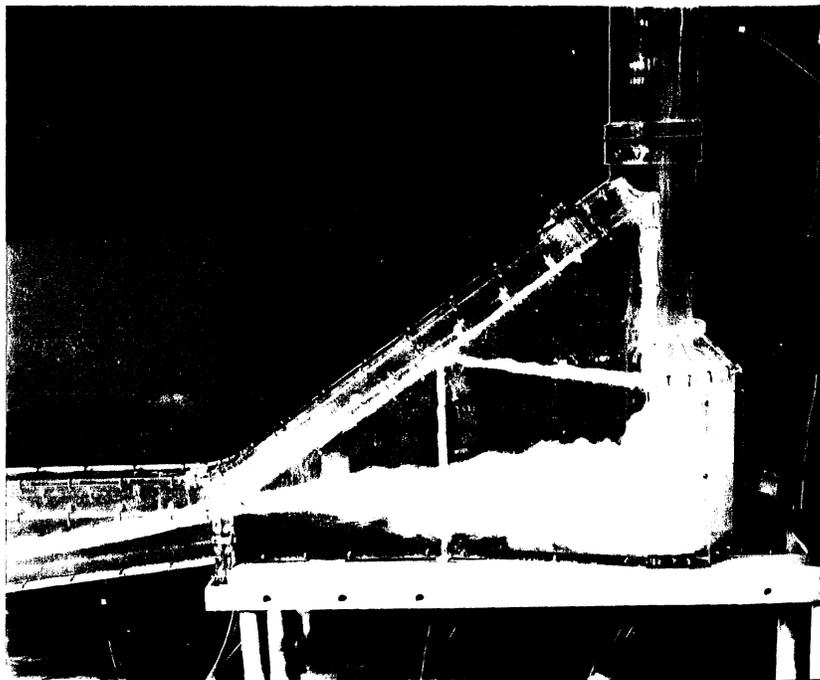
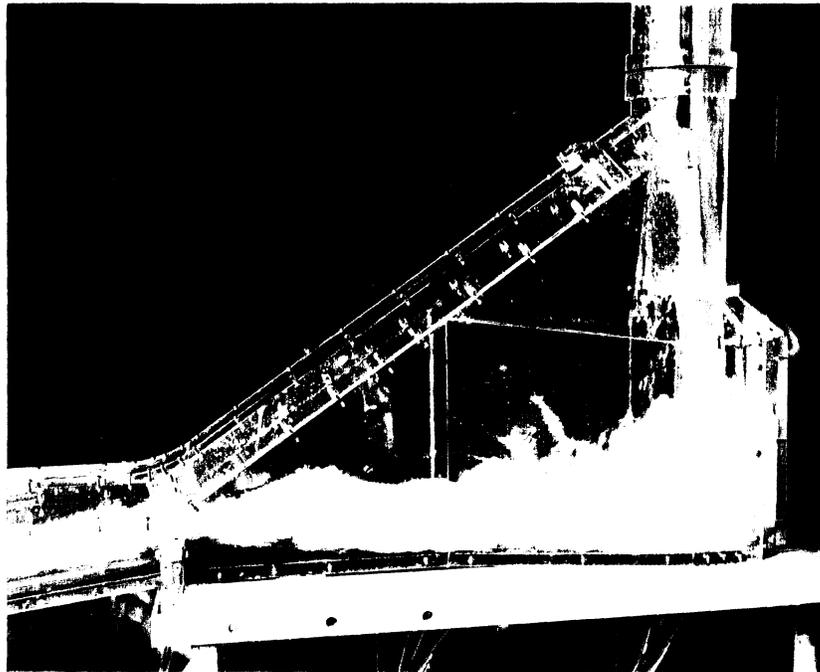


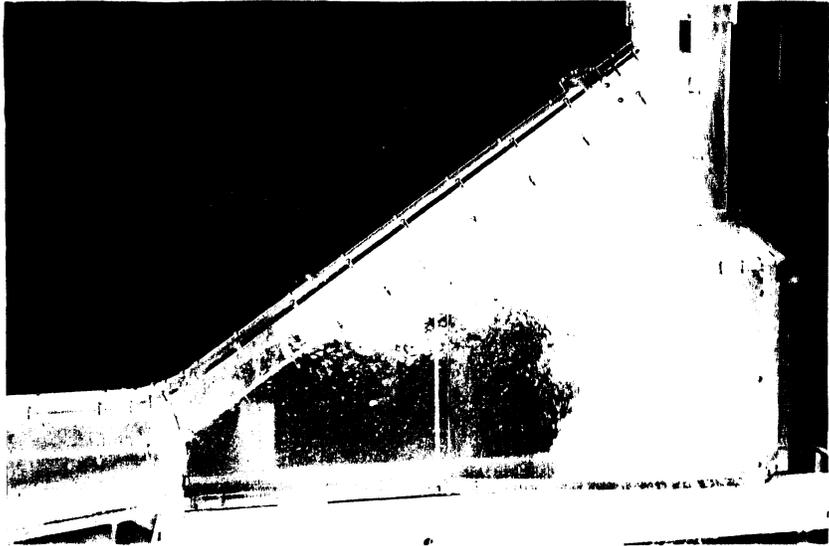


Photo 28 (Serial No. 260-22) Type A dropshaft,  $Q_{DS} = 300$  cfs,  
 $Q_T = 0$  cfs, T.W. = 40 ft. The flow pattern in the sump.

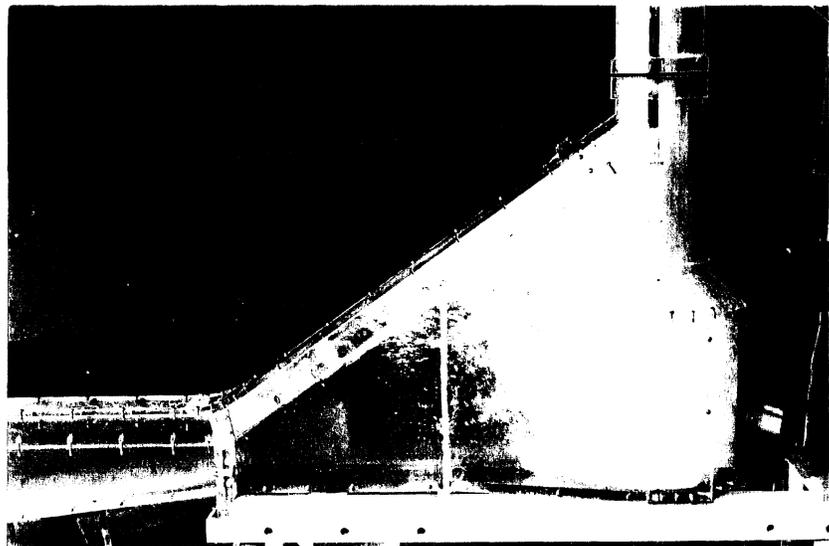
Photo 29 (Serial No. 260-201) Type B dropshaft,  $Q_{DS} = 300$  cfs,  
 $Q_T = 0$  cfs, T.W. = 40 ft. The flow pattern in the sump.

Photo 30 (Serial No. 260-204) Type B dropshaft,  $Q_{DS} = 300$  cfs,  
 $Q_T = 0$  cfs, T.W. = 40 ft. The air collecting at the junction  
of the sump and exit conduit.

100



101



102

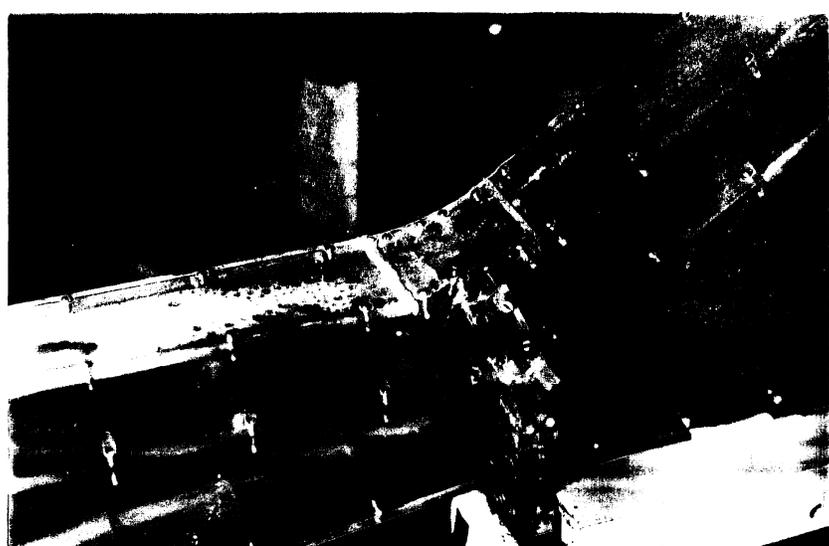


Photo 31 (Serial No. 260-206) Type B dropshaft,  $Q_{DS} = 300$  cfs,  
 $Q_{\pi} = 0$  cfs, T.W. = 0 ft. The flow pattern in the sump, exit  
conduit, and junction.

Photo 32 (Serial No. 260-207) Type B dropshaft,  $Q_{DS} = 300$  cfs,  
 $Q_{\pi} = 0$  cfs, T.W. = 20 ft. The flow pattern in the sump, exit  
conduit, and junction.

Photo 33 (Serial No. 260-208) Type B dropshaft,  $Q_{DS} = 300$  cfs,  
 $Q_{\pi} = 0$  cfs, T.W. = 40 ft. The flow pattern in the sump, exit  
conduit, and junction.

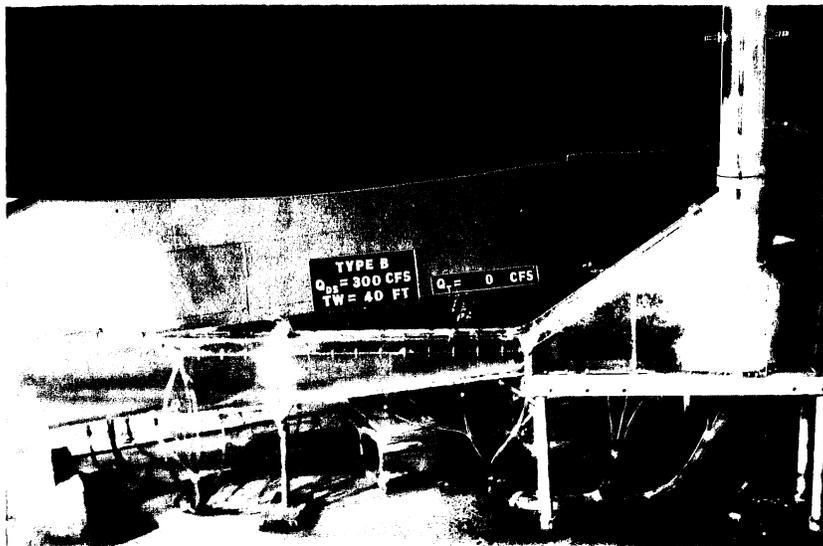
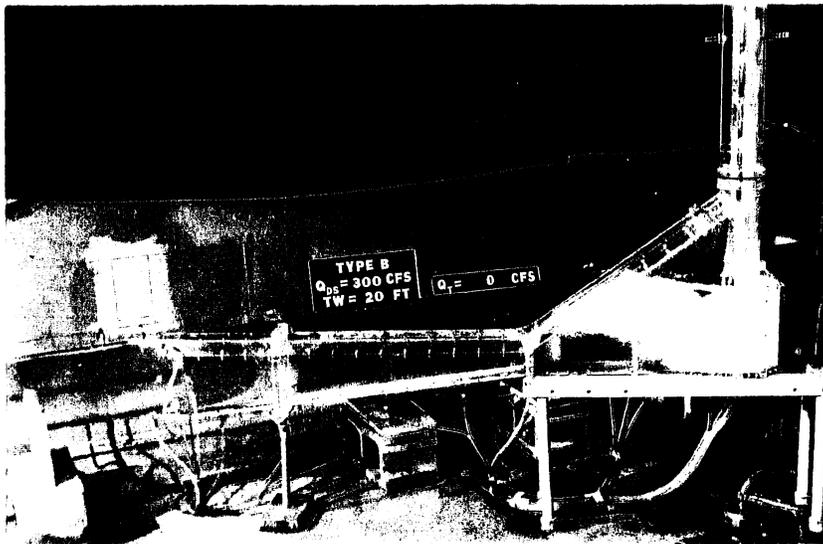
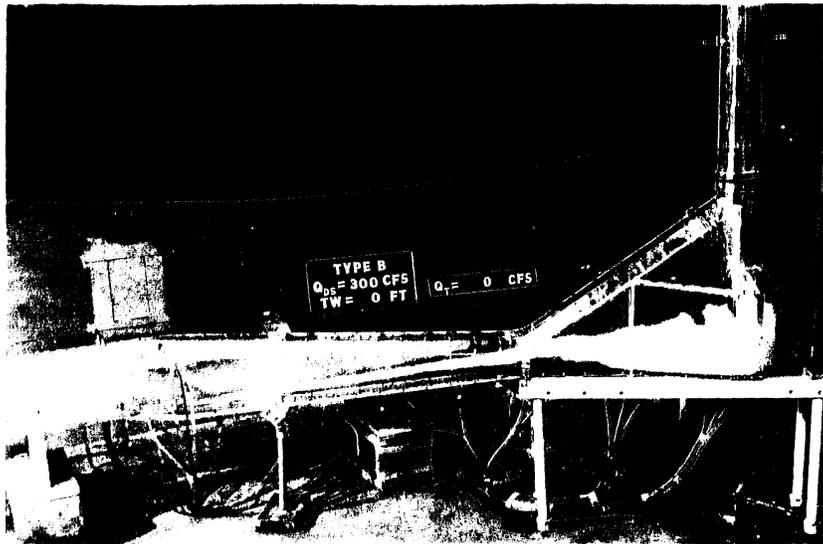


Photo 34 (Serial No. 260-215) Type B dropshaft,  $Q_{DS} = 300$  cfs,  
 $Q_T = 800$  cfs, T.W. = 8 ft. The flow pattern in the sump, exit  
conduit, and junction.

Photo 35 (Serial No. 260-216) Type B dropshaft,  $Q_{DS} = 300$  cfs,  
 $Q_T = 2,400$  cfs. T.W. = 11 ft. The flow pattern in the sump,  
exit conduit, and junction.

Photo 36 (Serial No. 260-217) Type B dropshaft,  $Q_{DS} = 300$  cfs,  
 $Q_T = 4,000$  cfs, T.W. = 40 ft. The flow pattern in the sump,  
exit conduit, and junction.

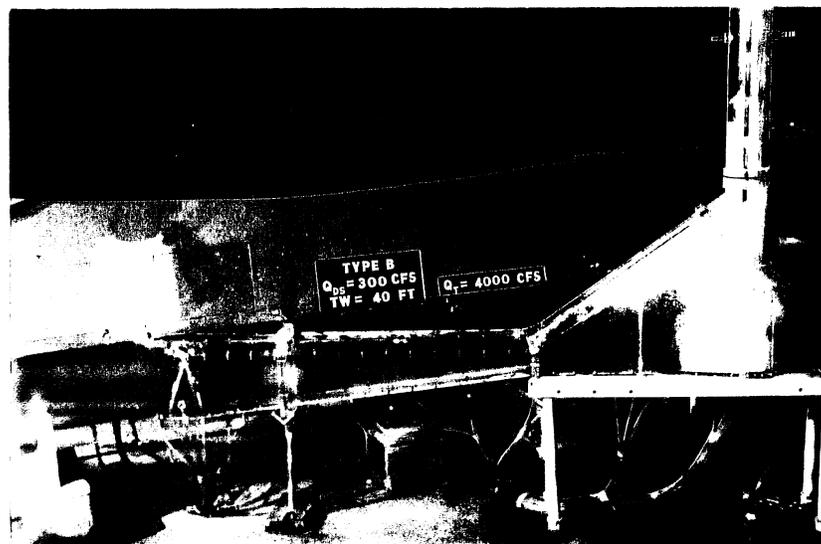
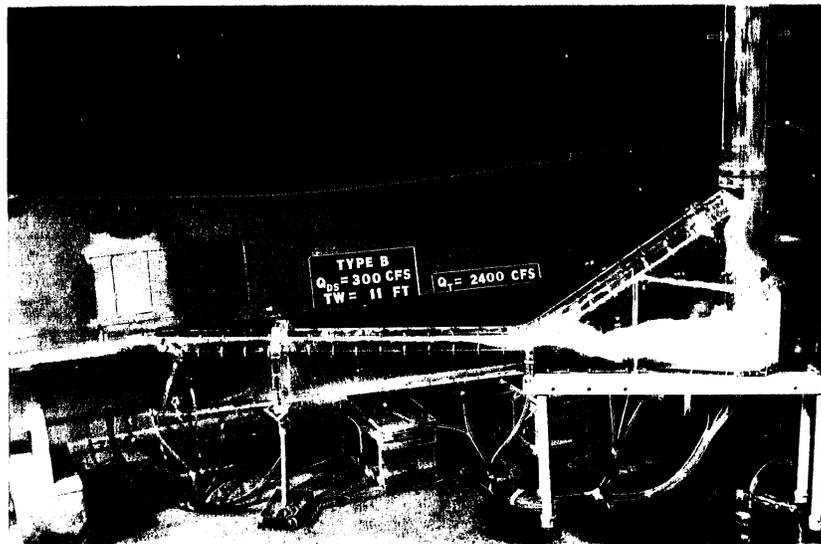


Photo 37 (Serial No. 260-289) Type C dropshaft,  $Q_{DS} = 300$  cfs,  
 $Q_T = 0$  cfs, T.W. = 0 ft. The exit conduit (slope 12.5%)  
used in Types A and B dropshafts is shown along side of  
the exit conduit (slope 25%) for Type C dropshaft.

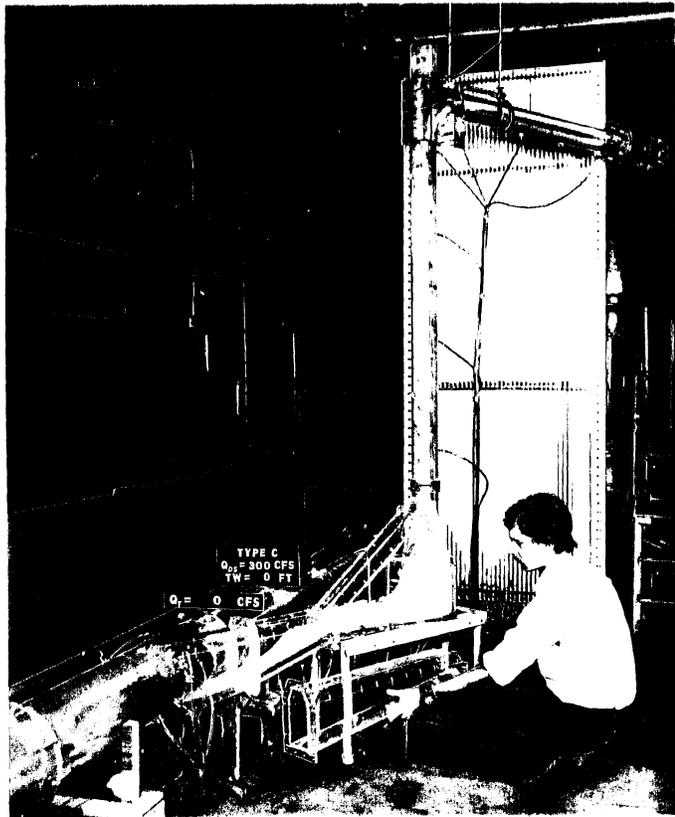




Photo 38 (Serial No. 260-302) Type C dropshaft,  $Q_{DS} = 300$  cfs,  
 $Q_T = 0$  cfs, T.W. = 0 ft. The flow pattern in the sump,  
exit conduit, and junction.

Photo 39 (Serial No. 260-303) Type C dropshaft,  $Q_{DS} = 300$  cfs,  
 $Q_T = 0$  cfs, T.W. = 20 ft. The flow pattern in the sump,  
exit conduit, and junction.

Photo 40 (Serial No. 260-304) Type C dropshaft,  $Q_{DS} = 300$  cfs,  
 $Q_T = 0$  cfs, T.W. = 40 ft. The flow pattern in the sump,  
exit conduit, and junction.

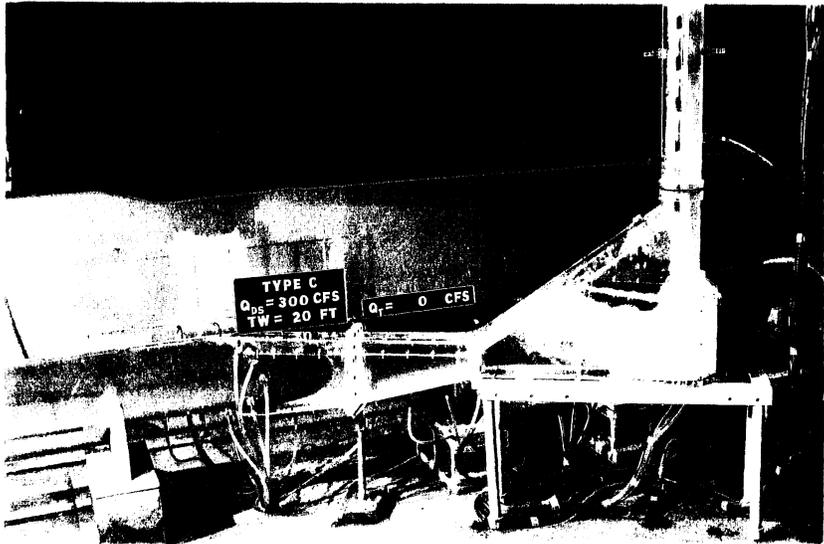
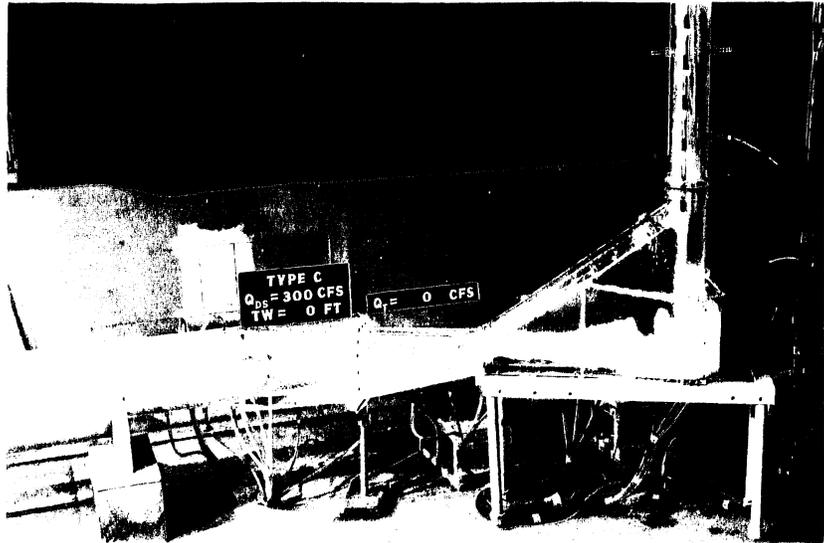


Photo 41 (Serial No. 260-293) Type C dropshaft,  $Q_{DS} = 300$  cfs,  
 $Q_T = 0$  cfs, T.W. = 20 ft. The flow pattern at the junction  
of the sump and exit conduit.

Photo 42 (Serial No. 260-295) Type C dropshaft,  $Q_{DS} = 300$  cfs,  
 $Q_T = 0$  cfs, T.W. = 40 ft. The flow pattern at the junction  
of the sump and exit conduit.

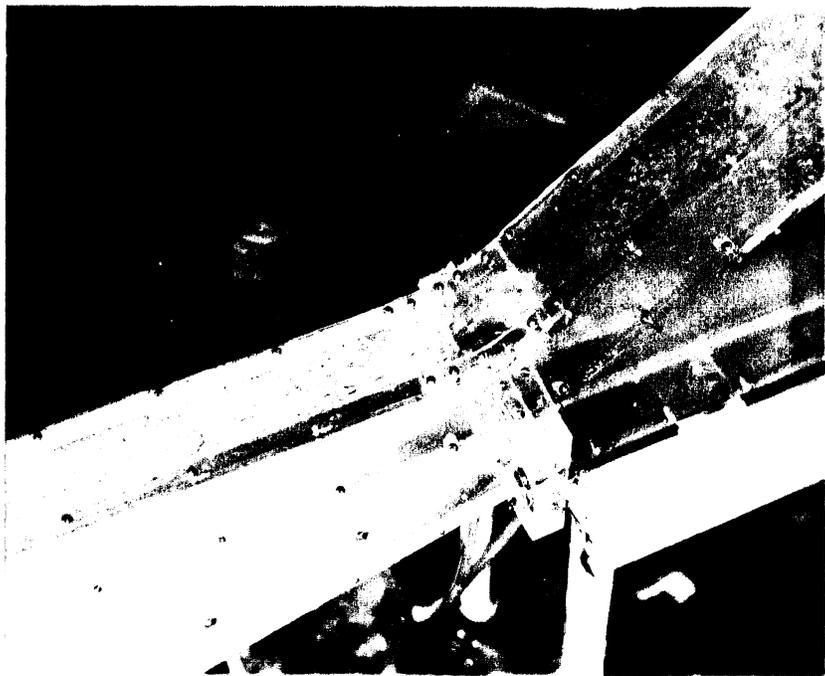
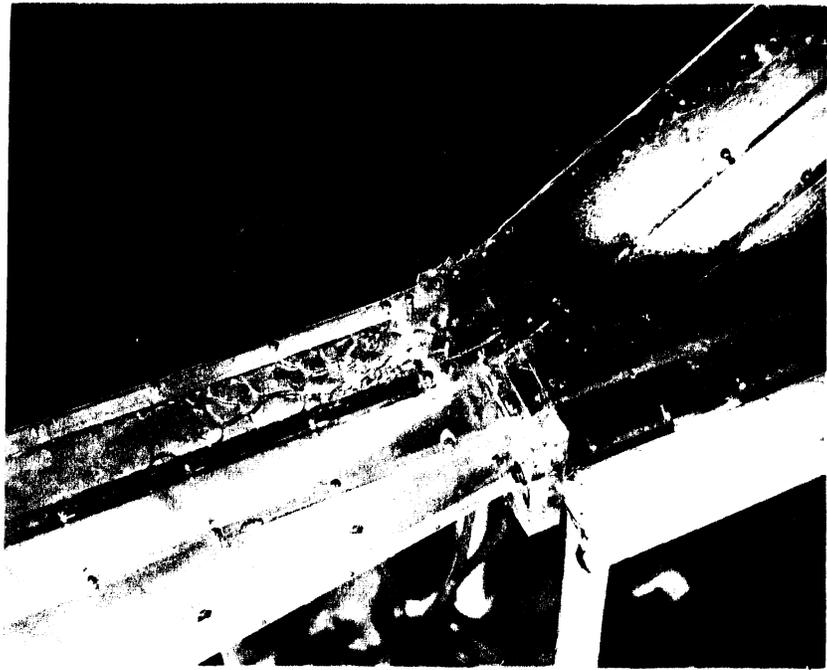


Photo 43 (Serial No. 260-311) Type C dropshaft,  $Q_{DS} = 300$  cfs,  
 $Q_T = 800$  cfs, T.W. = 8 ft. The flow pattern in the sump,  
exit conduit, and junction.

Photo 44 (Serial No. 260-312) Type C dropshaft,  $Q_{DS} = 300$  cfs,  
 $Q_T = 2400$  cfs, T.W. = 11 ft. The flow pattern in the  
sump, exit conduit, and junction.

Photo 45 (Serial No. 260-313) Type C dropshaft,  $Q_{DS} = 300$  cfs  
 $Q_T = 4000$  cfs, T.W. = 40 ft. The flow pattern in the  
sump, exit conduit, and junction.

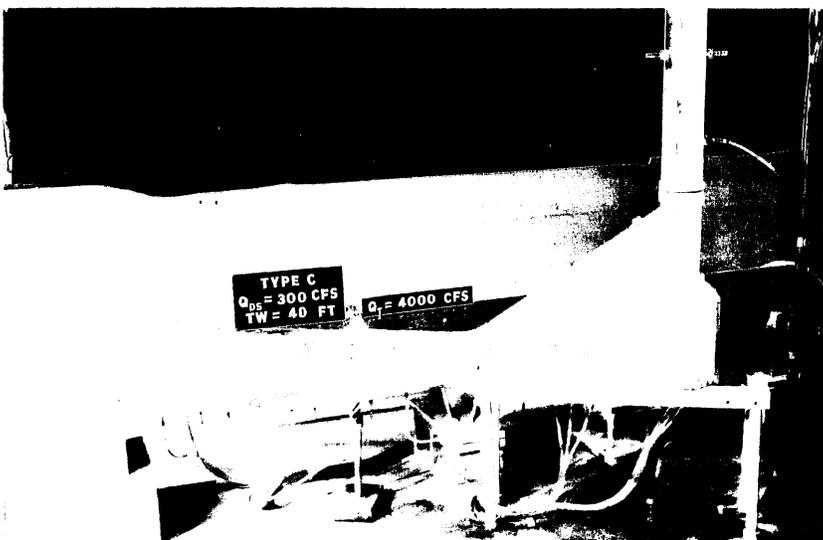
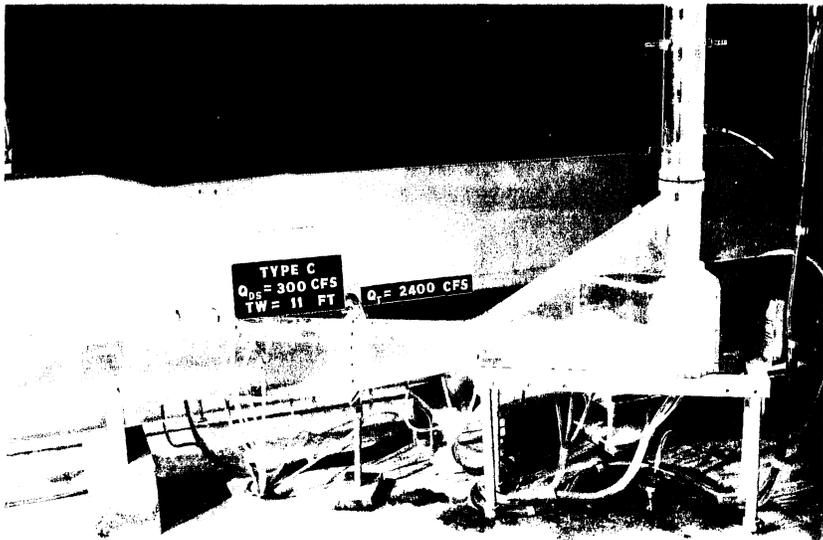
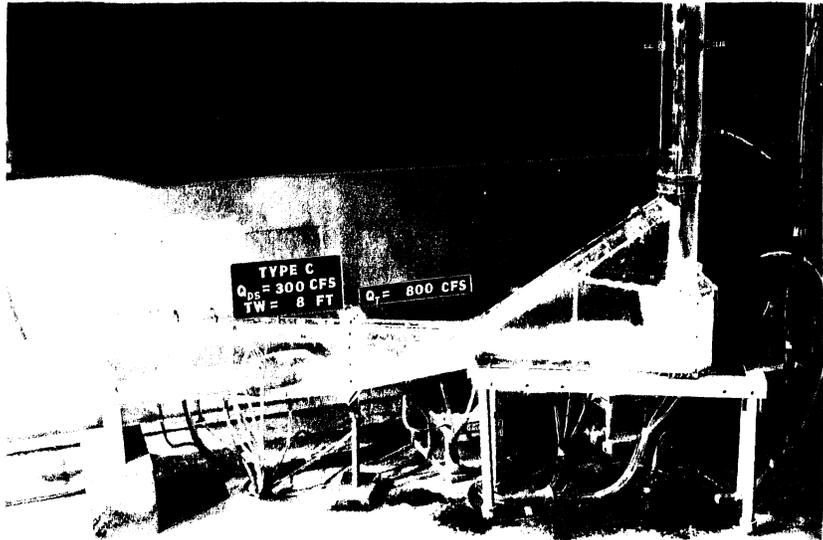


Photo 46 (Serial No. 260-392) Type C-1 dropshaft, the plate being installed in the top of the exit conduit.

Photo 47 (Serial No. 260-393) Type C-1 dropshaft, the plate being installed in the top of the exit conduit.

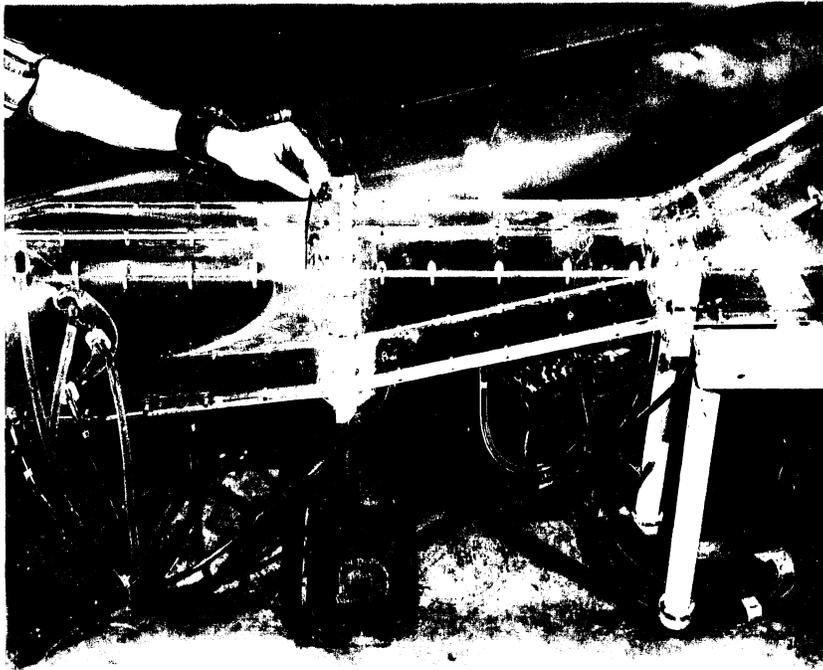
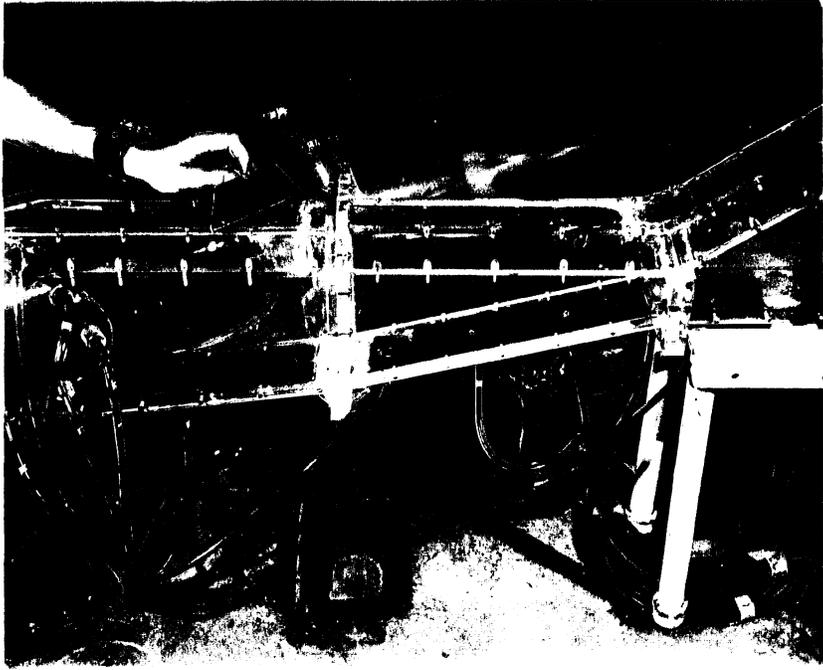
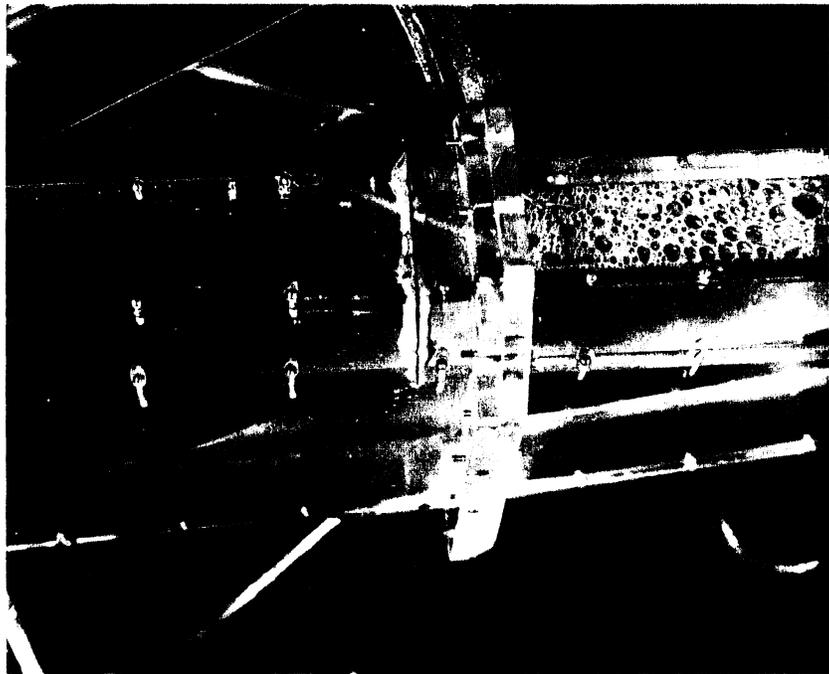
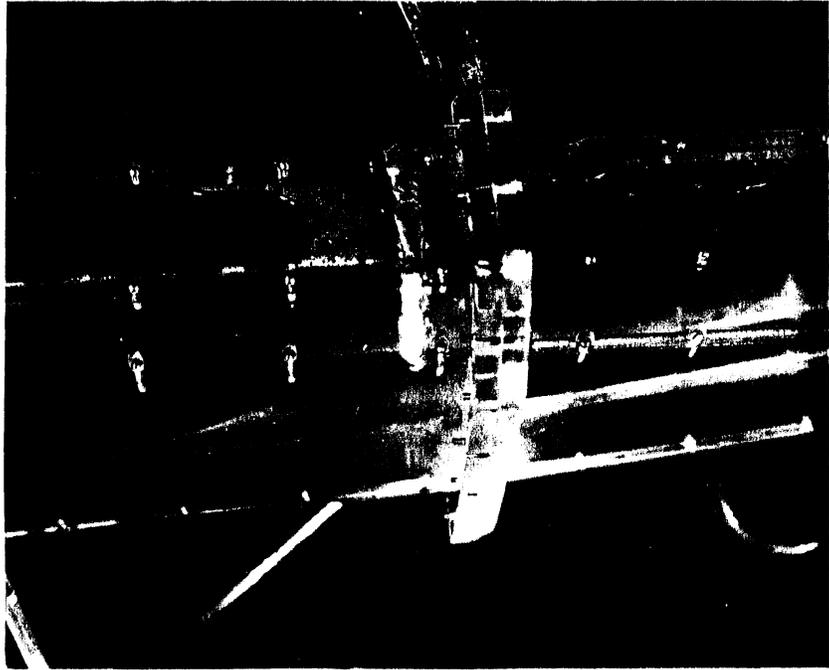




Photo 48 (Serial No. 260-397) Type C dropshaft,  $Q_{DS} = 300$  cfs,  
 $Q_T = 0$  cfs, T.W. = 20 ft. The flow pattern in the exit  
conduit.

Photo 49 (Serial No. 260-399) Type C-1 dropshaft,  $Q_{DS} = 300$  cfs,  
 $Q_T = 0$  cfs, T.W. = 20 ft. The flow pattern in the exit  
conduit.



LIST OF CHARTS

- CHART 1 (260B503-5) Types A, B, and C dropshafts, dropshaft types tested.
- CHART 2 (260A2313-33) Type A dropshaft,  $Q_{DS} = 300$  cfs,  $Q_T = 0$  cfs, T.W. elevation varied. Piezometric pressures in the dropshaft and exit conduit.
- CHART 3 (260A2313-37) Type A dropshaft,  $Q_{DS} = 300$  cfs,  $Q_T = 0$  cfs, T.W. elevation varied. Piezometric pressures in the tunnel.
- CHART 4 (260A2313-32) Type A dropshaft,  $Q_{DS} = 400$  cfs,  $Q_T = 0$  cfs, T.W. elevation varied. Piezometric pressures in the dropshaft and exit conduit.
- CHART 5 (260A2313-36) Type A dropshaft,  $Q_{DS} = 400$  cfs,  $Q_T = 0$  cfs, T.W. elevation varied. Piezometric pressures in the tunnel.
- CHART 6 (260A2313-75) Type A dropshaft,  $Q_{DS} = 300$  cfs,  $Q_T$  and T.W. elevation varied. Piezometric pressures in the dropshaft and exit conduit.
- CHART 7 (260A2313-78) Type A dropshaft,  $Q_{DS} = 300$  cfs,  $Q_T$  and T.W. elevation varied. Piezometric pressures in the tunnel.
- CHART 8 (260A2313-74) Type A dropshaft,  $Q_{DS} = 400$  cfs,  $Q_T$  and T.W. elevation varied. Piezometric pressures in the dropshaft and exit conduit.
- CHART 9 (260A2313-77) Type A dropshaft,  $Q_{DS} = 400$  cfs,  $Q_T$  and T.W. elevation varied. Piezometric pressures in the tunnel.
- CHART 10 (260A2313-12) Type A dropshaft,  $Q_{DS} = 300$  cfs,  $Q_T = 0$  cfs, T.W. elevation varied. Typical pressure fluctuations at tap 24.
- CHART 11 (260A2313-16) Type A dropshaft,  $Q_{DS} = 300$  cfs,  $Q_T = 0$  cfs, T.W. elevation varied. Typical pressure fluctuations at tap 27.
- CHART 12 (260A2313-46) Type A dropshaft,  $Q_{DS} = 300$  cfs,  $Q_T = 0$  cfs, T.W. elevation varied. Typical pressure fluctuations at taps 12, 13, and 14.
- CHART 13 (260A2313-28) Type A dropshaft,  $Q_{DS} = 300$  cfs,  $Q_T = 0$  cfs, T.W. elevation varied. Typical pressure fluctuations at taps 21, 22, and 23.
- CHART 14 (260A2313-30) Type A dropshaft,  $Q_{DS} = 300$  cfs,  $Q_T = 0$  cfs, T.W. elevation varied. Typical pressure fluctuations at taps 28, 29, and 30.
- CHART 15 (260A2313-31) Type A dropshaft,  $Q_{DS} = 300$  cfs,  $Q_T = 0$  cfs, T.W. elevation varied. Typical pressure fluctuations at taps 31, 32, and 33.

LIST OF CHARTS (Cont'd)

- CHART 16 (260A2313-11) Type A dropshaft,  $Q_{DS} = 400$  cfs,  $Q_T = 0$  cfs, T.W. elevation varied. Typical pressure fluctuations at tap 24.
- CHART 17 (260A2313-15) Type A dropshaft,  $Q_{DS} = 400$  cfs,  $Q_T = 0$  cfs, T.W. elevation varied. Typical pressure fluctuations at tap 27.
- CHART 18 (260A2313-63) Type A dropshaft,  $Q_{DS}$ ,  $Q_T$ , and T.W. elevation varied. Typical pressure fluctuations at tap 24.
- CHART 19 (260A2313-64) Type A dropshaft,  $Q_{DS}$ ,  $Q_T$ , and T.W. elevation varied. Typical pressure fluctuations at tap 27.
- CHART 20 (260A2313-65) Type A dropshaft,  $Q_{DS} = 300$  cfs,  $Q_T$  and T.W. elevation varied. Typical pressure fluctuations at taps 12, 13, and 14.
- CHART 21 (260A2313-68) Type A dropshaft,  $Q_{DS} = 300$  cfs,  $Q_T$  and T.W. elevation varied. Typical pressure fluctuations at taps 21, 22, and 23.
- CHART 22 (260A2313-70) Type A dropshaft,  $Q_{DS} = 300$  cfs,  $Q_T$  and T.W. elevation varied. Typical pressure fluctuations at taps 29, 30, and 31.
- CHART 23 (260A2313-80) Type A dropshaft. Summary of pressure fluctuations for various flow conditions.
- CHART 24 (260A2313-81) Type A dropshaft. Summary of pressure fluctuations for various flow conditions.
- CHART 25 (260A2313-82) Type A dropshaft. Summary of pressure fluctuations for various flow conditions.
- CHART 26 (260A2313-83) Type A dropshaft. Summary of pressure fluctuations for various flow conditions.
- CHART 27 (260A2313-84) Type A dropshaft. Summary of pressure fluctuations for various flow conditions.
- CHART 28 (260A2313-85) Type A dropshaft. Summary of pressure fluctuations for various flow conditions.
- CHART 29 (260A2313-86) Type A dropshaft. Summary of pressure fluctuations for various flow conditions.
- CHART 30 (260A2313-87) Type A dropshaft. Summary of pressure fluctuations for various flow conditions.
- CHART 31 (260A2313-51) Type A dropshaft,  $Q_{DS} = 300$  cfs,  $Q_T = 0$  cfs, T.W. elevation varied. Typical pressure fluctuations at tap 10.

LIST OF CHARTS (Cont'd)

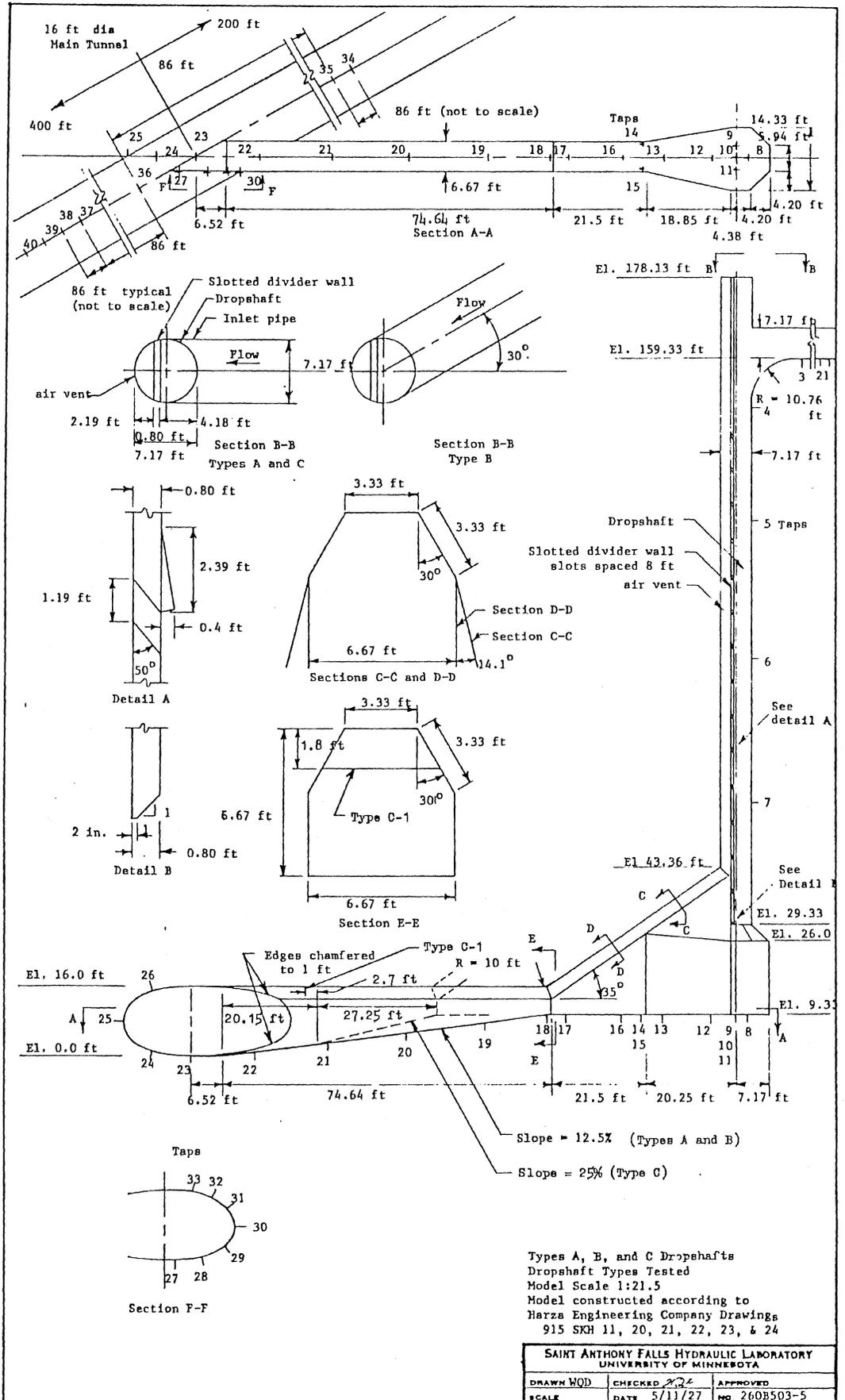
- CHART 32 (260A2313-52) Type A dropshaft,  $Q_{DS} = 300$  cfs,  $Q_T = 0$  cfs, T.W. elevation varied. Typical pressure fluctuations at tap 10.
- CHART 33 (260A2313-54) Type A dropshaft,  $Q_{DS} = 300$  cfs,  $Q_T = 0$  cfs, T.W. elevation varied. Typical pressure fluctuations at tap 8.
- CHART 34 (260A2313-55) Type A dropshaft,  $Q_{DS} = 300$  cfs,  $Q_T = 0$  cfs, T.W. elevation varied. Typical pressure fluctuations at tap 9.
- CHART 35 (260A2313-56) Type A dropshaft,  $Q_{DS} = 300$  cfs,  $Q_T = 0$  cfs, T.W. elevation varied. Typical pressure fluctuations at tap 11.
- CHART 36 (260A2313-53) Type A dropshaft,  $Q_{DS} = 400$  cfs,  $Q_T = 0$  cfs, T.W. elevation varied. Typical pressure fluctuations at tap 10.
- CHART 37 (260A2313-50) Type A dropshaft,  $Q_{DS} = 200$  cfs,  $Q_T = 0$  cfs, T.W. elevation varied. Typical pressure fluctuations at tap 10.
- CHART 38 (260A2313-58) Type A dropshaft,  $Q_{DS} = 300$  cfs,  $Q_T$  and T.W. elevation varied. Typical pressure fluctuations at tap 10.
- CHART 39 (260A2313-119) Type A dropshaft. Summary of pressure fluctuations for various flow conditions.
- CHART 40 (260A2313-120) Type A dropshaft. Summary of pressure fluctuations for various flow conditions.
- CHART 41 (260A2313-121) Type A dropshaft. Summary of pressure fluctuations for various flow conditions.
- CHART 42 (260A2313-88) Type B dropshaft,  $Q_{DS} = 300$  cfs,  $Q_T = 0$  cfs, T.W. elevation varied. Piezometric pressures in the dropshaft and exit conduit.
- CHART 43 (260A2313-90) Type B dropshaft,  $Q_{DS} = 300$  cfs,  $Q_T$  and T.W. elevation varied. Piezometric pressures in the dropshaft and exit conduit.
- CHART 44 (260A2313-89) Type B dropshaft,  $Q_{DS} = 300$  cfs,  $Q_T = 0$  cfs, T.W. elevation varied. Piezometric pressures in the tunnel.
- CHART 45 (260A2313-91) Type B dropshaft,  $Q_{DS} = 300$  cfs,  $Q_T$  and T.W. elevation varied. Piezometric pressures in the tunnel.
- CHART 46 (260A2313-92) Type B dropshaft,  $Q_{DS} = 300$  cfs,  $Q_T = 0$  cfs, T.W. elevation varied. Typical pressure fluctuations at taps 24 and 27.
- CHART 47 (260A2313-93) Type B dropshaft,  $Q_{DS} = 300$  cfs,  $Q_T = 0$  cfs, T.W. elevation varied. Typical pressure fluctuations at taps 12, 13, and 14.

LIST OF CHARTS (Cont'd)

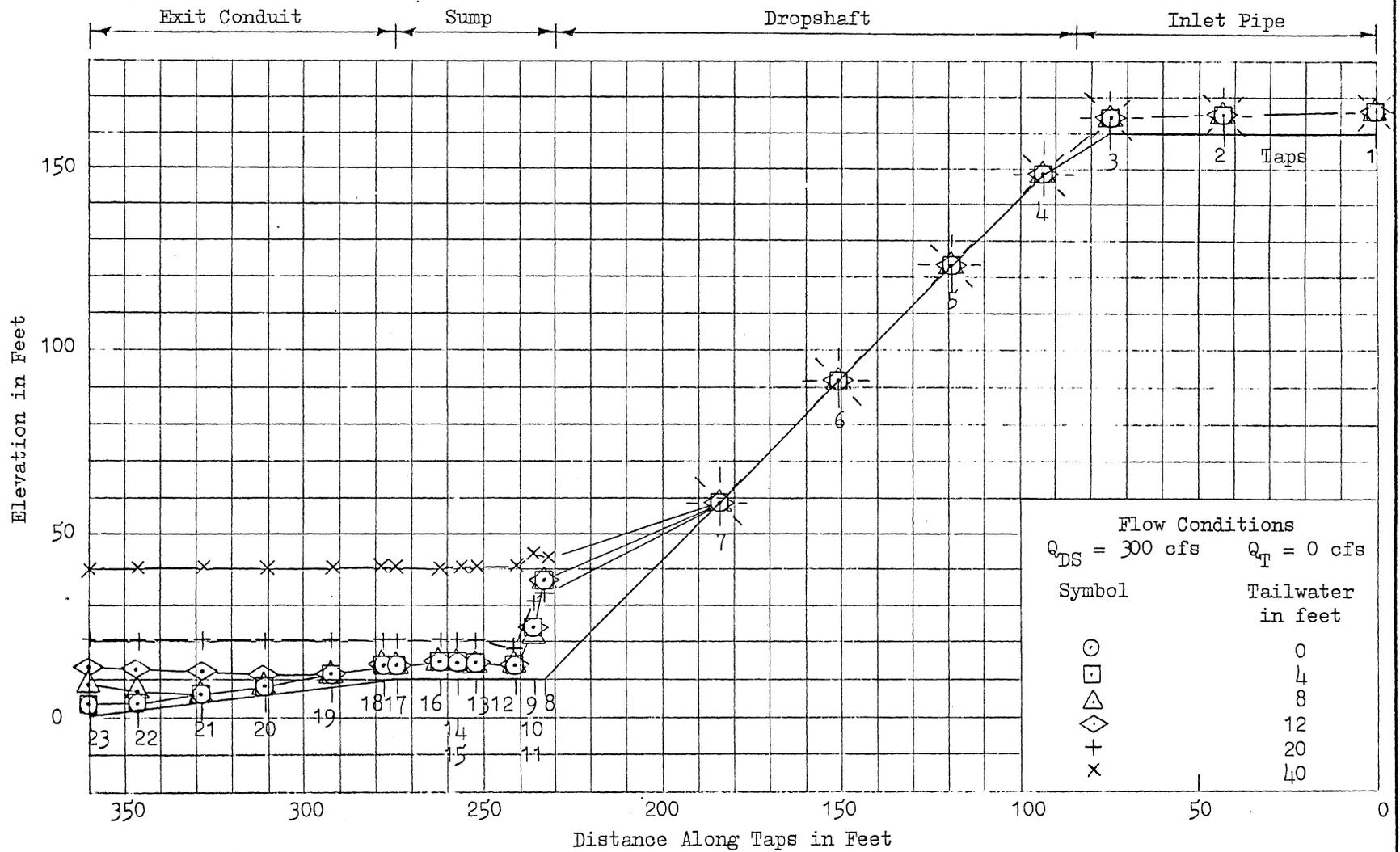
- CHART 48 (260A2313-99) Type B dropshaft,  $Q_{DS} = 300$  cfs,  $Q_T$  and T.W. elevation varied. Typical pressure fluctuations at taps 24 and 27.
- CHART 49 (260A2313-96) Type B dropshaft,  $Q_{DS} = 300$  cfs,  $Q_T$  and T.W. elevation varied. Typical pressure fluctuations at taps 12, 13, and 14.
- CHART 50 (260A2313-116) Type B dropshaft. Summary of pressure fluctuations for various flow conditions.
- CHART 51 (260A2313-117) Type B dropshaft. Summary of pressure fluctuations for various flow conditions.
- CHART 52 (260A2313-102) Type B dropshaft,  $Q_{DS} = 300$  cfs,  $Q_T = 0$  cfs, T.W. elevation varied. Typical pressure fluctuations at tap 10.
- CHART 53 (260A2313-100) Type B dropshaft,  $Q_{DS} = 300$  cfs,  $Q_T = 0$  cfs, T.W. elevation varied. Typical pressure fluctuations at tap 8.
- CHART 54 (260A2313-101) Type B dropshaft,  $Q_{DS} = 300$  cfs,  $Q_T = 0$  cfs, T.W. elevation varied. Typical pressure fluctuations at tap 9.
- CHART 55 (260A2313-103) Type B dropshaft,  $Q_{DS} = 300$  cfs,  $Q_T = 0$  cfs, T.W. elevation varied. Typical pressure fluctuations at tap 11.
- CHART 56 (260A2313-108) Type B dropshaft,  $Q_{DS} = 200$  cfs,  $Q_T = 0$  cfs, T.W. elevation varied. Typical pressure fluctuations at tap 8.
- CHART 57 (260A2313-106) Type B dropshaft,  $Q_{DS} = 300$  cfs,  $Q_T$  and T.W. elevation varied. Typical pressure fluctuations at tap 10.
- CHART 58 (260A2313-118) Type B dropshaft. Summary of pressure fluctuations for various flow conditions.
- CHART 59 (260A2313-151) Type C dropshaft,  $Q_{DS} = 300$  cfs,  $Q_T = 0$  cfs, T.W. elevation varied. Piezometric pressures in the dropshaft and exit conduit.
- CHART 60 (260A2313-153) Type C dropshaft,  $Q_{DS} = 300$  cfs,  $Q_T = 0$  cfs, T.W. elevation varied. Piezometric pressures in the tunnel.
- CHART 61 (260A2313-152) Type C dropshaft,  $Q_{DS} = 300$  cfs,  $Q_T$  and T.W. elevation varied. Piezometric pressures in the dropshaft and exit conduit.
- CHART 62 (260A2313-154) Type C dropshaft,  $Q_{DS} = 300$  cfs,  $Q_T$  and T.W. elevation varied. Piezometric pressures in the tunnel.
- CHART 63 (260A2313-122) Type C dropshaft,  $Q_{DS} = 300$  cfs,  $Q_T = 0$  cfs, T.W. elevation varied. Typical pressure fluctuations at taps 24 and 27.

LIST OF CHARTS (Cont'd)

- CHART 64 (260A2313-125) Type C dropshaft,  $Q_{DS} = 300$  cfs,  $Q_T = 0$  cfs, T.W. elevation varied. Typical pressure fluctuations at taps 18, 20, and 22.
- CHART 65 (260A2313-126) Type C dropshaft,  $Q_{DS} = 300$  cfs,  $Q_T$  and T.W. elevation varied. Typical pressure fluctuations at taps 24 and 27.
- CHART 66 (260A2313-129) Type C dropshaft,  $Q_{DS} = 300$  cfs,  $Q_T$  and T.W. elevation varied. Typical pressure fluctuations at taps 18, 20, and 22.
- CHART 67 (260A2313-148) Type C dropshaft. Summary of pressure fluctuations for various flow conditions.
- CHART 68 (260A2313-149) Type C dropshaft. Summary of pressure fluctuations for various flow conditions.
- CHART 69 (260A2313-132) Type C dropshaft,  $Q_{DS} = 300$  cfs,  $Q_T = 0$  cfs, T.W. elevation varied. Typical pressure fluctuations at tap 10.
- CHART 70 (260A2313-130) Type C dropshaft,  $Q_{DS} = 300$  cfs,  $Q_T = 0$  cfs, T.W. elevation varied. Typical pressure fluctuations at tap 8.
- CHART 71 (260A2313-131) Type C dropshaft,  $Q_{DS} = 300$  cfs,  $Q_T = 0$  cfs, T.W. elevation varied. Typical pressure fluctuations at tap 9.
- CHART 72 (260A2313-133) Type C dropshaft,  $Q_{DS} = 300$  cfs,  $Q_T = 0$  cfs, T.W. elevation varied. Typical pressure fluctuations at tap 11.
- CHART 73 (260A2313-144) Type C dropshaft,  $Q_{DS} = 300$  cfs,  $Q_T$  and T.W. elevation varied. Typical pressure fluctuations at tap 10.
- CHART 74 (260A2313-150) Type C dropshaft. Summary of pressure fluctuations for various flow conditions.



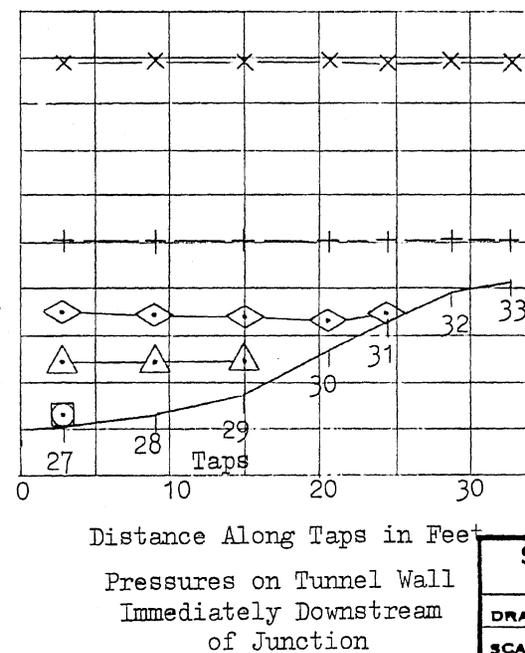
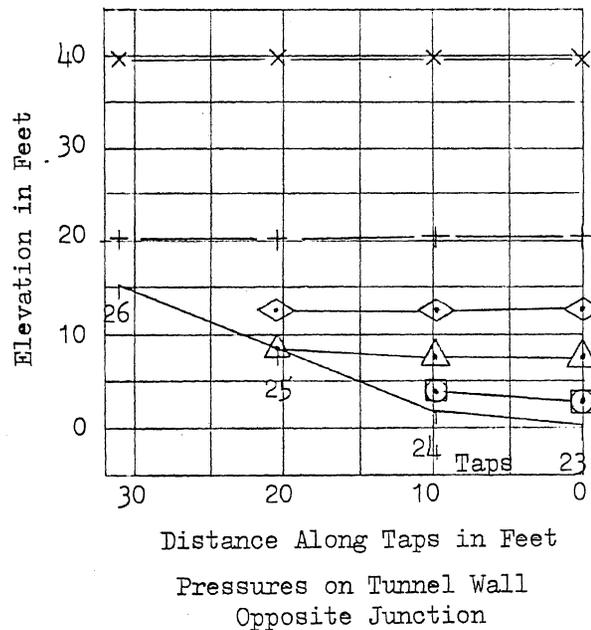
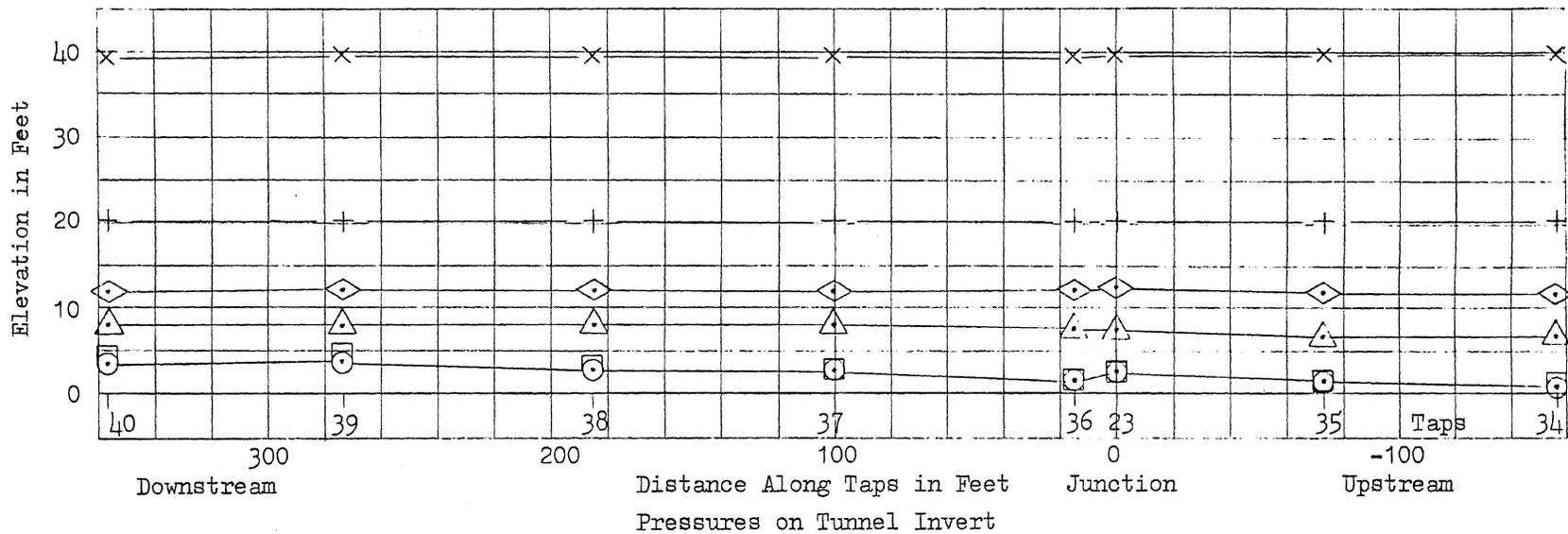




Flow Conditions	
$Q_{DS} = 300$ cfs	$Q_T = 0$ cfs
Symbol	Tailwater in feet
○	0
□	4
△	8
◇	12
+	20
x	40

CULVER-GOODMAN MODEL STUDIES  
 Type A Dropshaft Scale 1:21.5  
 Piezometric Pressures

SAINT ANTHONY FALLS HYDRAULIC LABORATORY UNIVERSITY OF MINNESOTA		
DRAWN DA	CHECKED <i>WLB</i>	APPROVED
SCALE	DATE 3/29/77	NO. 260A2313-33

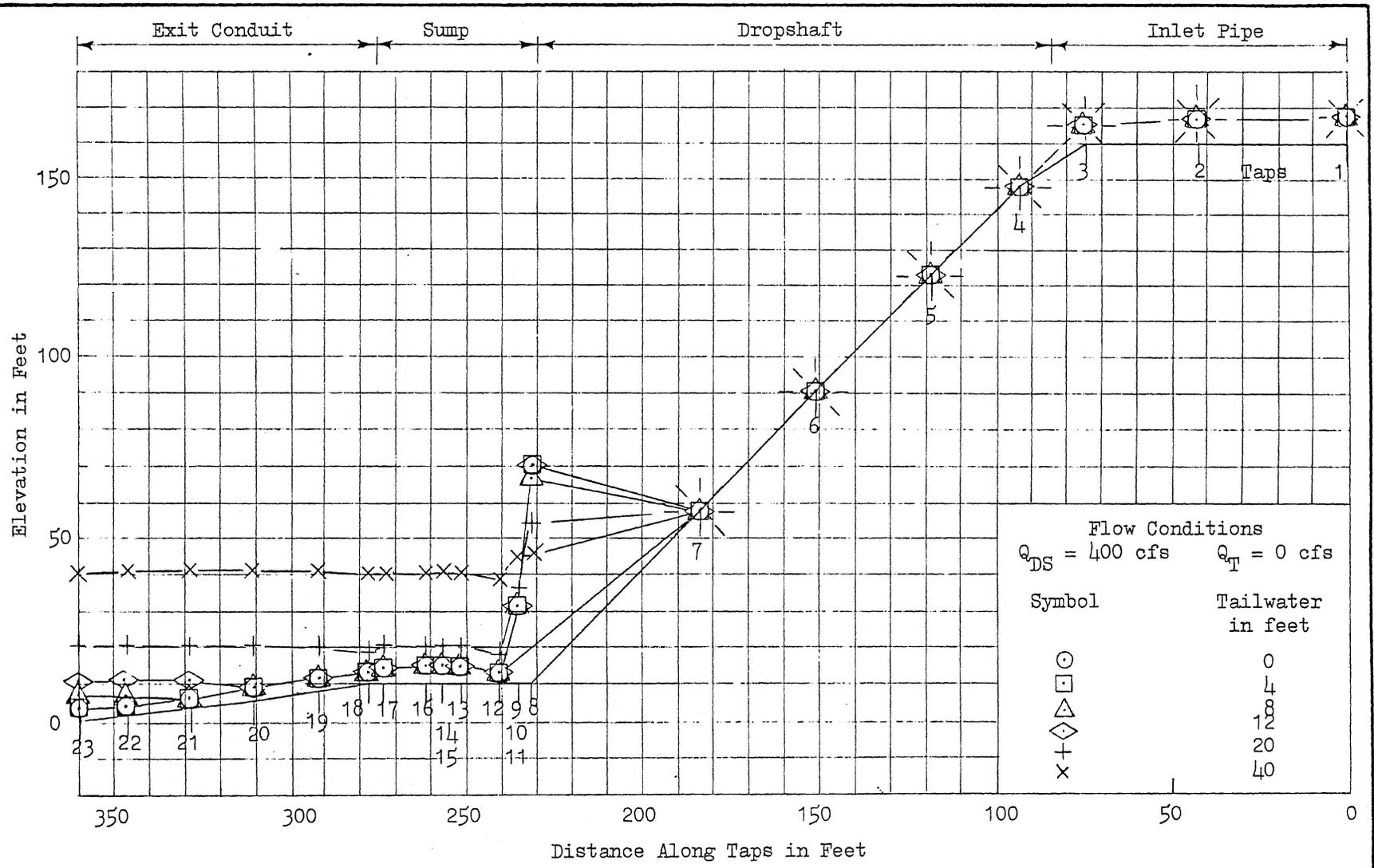


Flow Conditions  
 $Q_{DS} = 300$  cfs     $Q_T = 0$  cfs

Symbol	Tailwater in Feet
○	0
□	4
△	8
◇	12
+	20
x	40

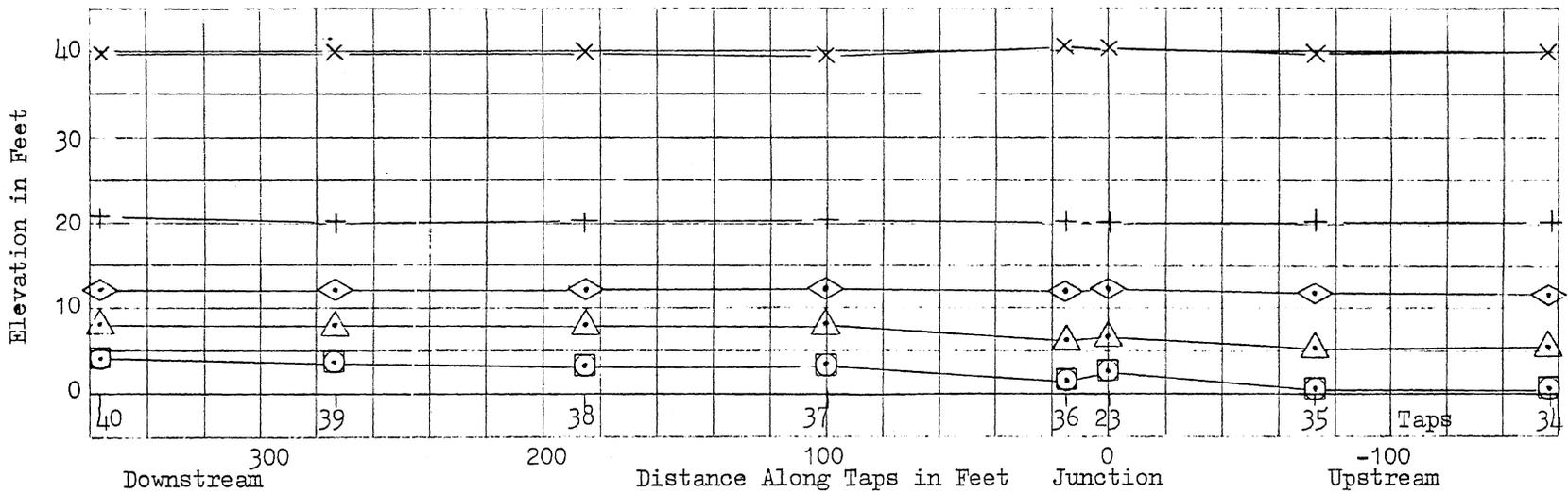
CULVER-GOODMAN MODEL STUDIES  
 Type A Dropshaft    Scale 1:21.5  
 Piezometric Pressures

SAINT ANTHONY FALLS HYDRAULIC LABORATORY UNIVERSITY OF MINNESOTA		
DRAWN DA	CHECKED <i>DA</i>	APPROVED
SCALE	DATE 3/30/77	NO. 260A2313-37

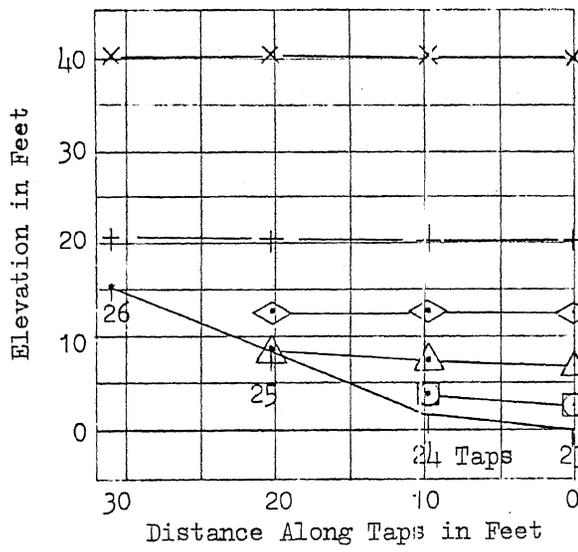


CULVER-GOODMAN MODEL STUDIES  
 Type A Dropshaft Scale 1:21.5  
 Piezometric Pressures

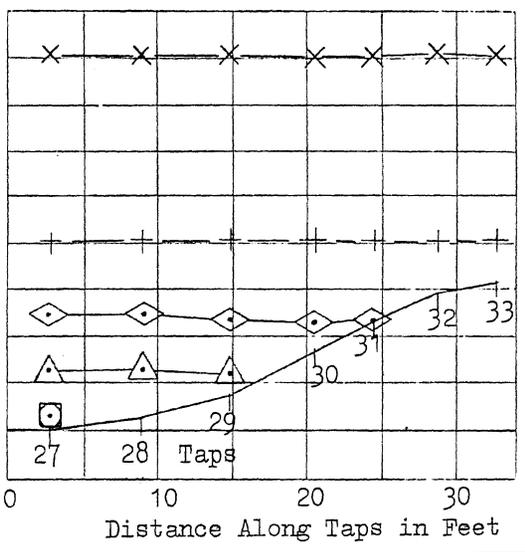
SAINT ANTHONY FALLS HYDRAULIC LABORATORY UNIVERSITY OF MINNESOTA		
DRAWN DA	CHECKED <i>WJ</i>	APPROVED
SCALE	DATE 3/29/77	NO. 260A2313-32



Pressures on Tunnel Invert



Pressures on Tunnel Wall  
Opposite Junction



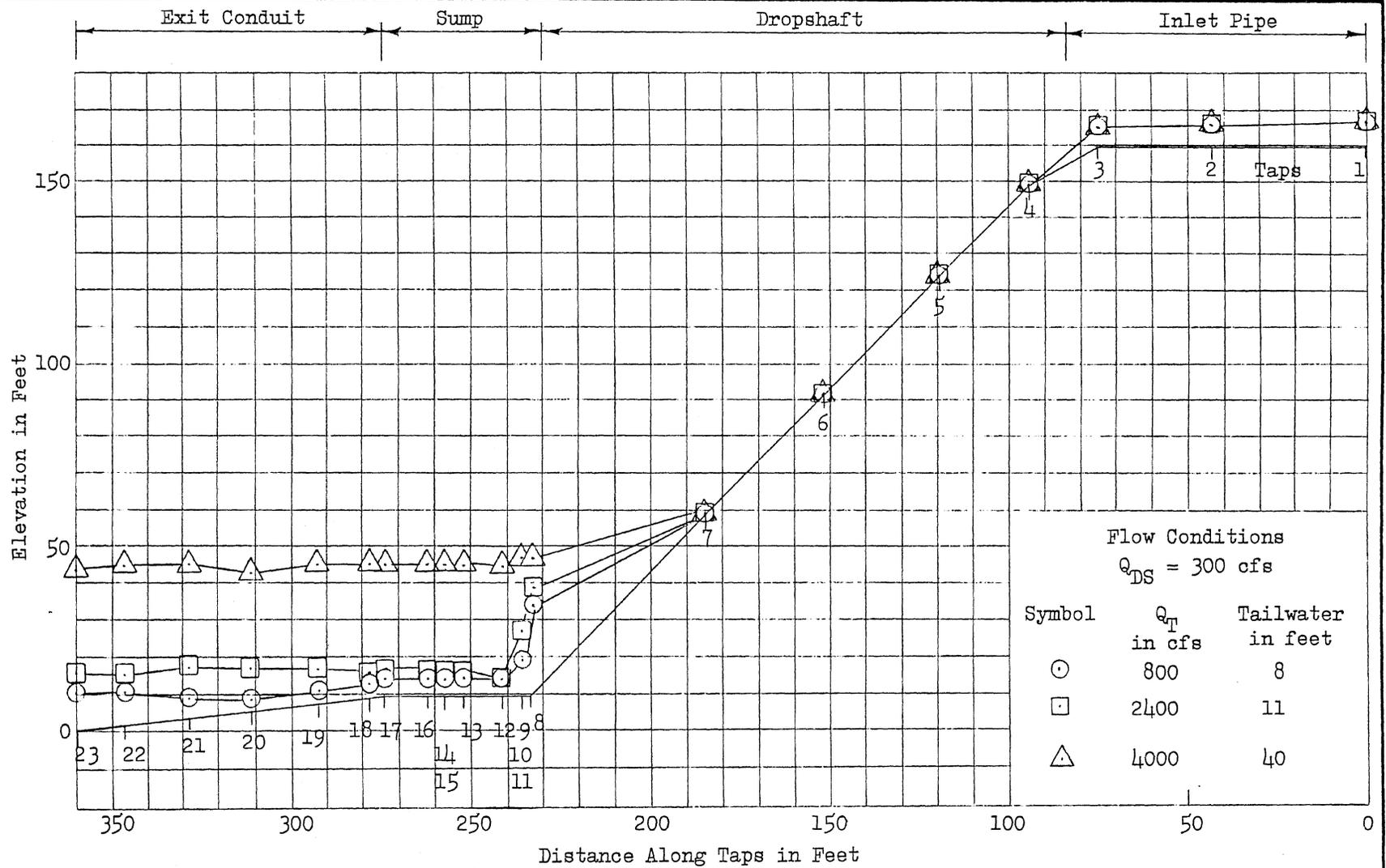
Pressures on Tunnel Wall  
Immediately Downstream  
of Junction

Flow Conditions  
 $Q_{DS} = 400$  cfs     $Q_T = 0$  cfs

Symbol	Tailwater in Feet
○	0
□	4
△	8
◇	12
+	20
x	40

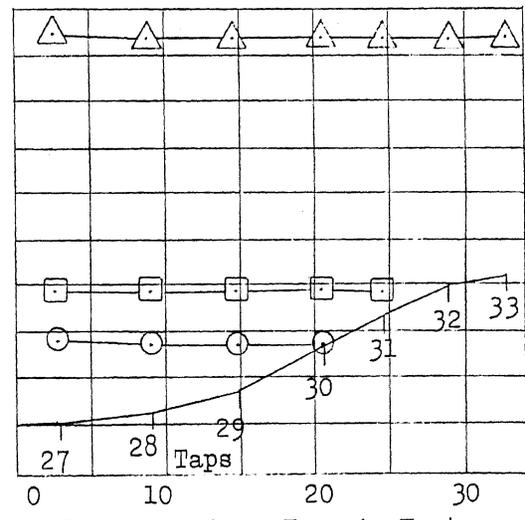
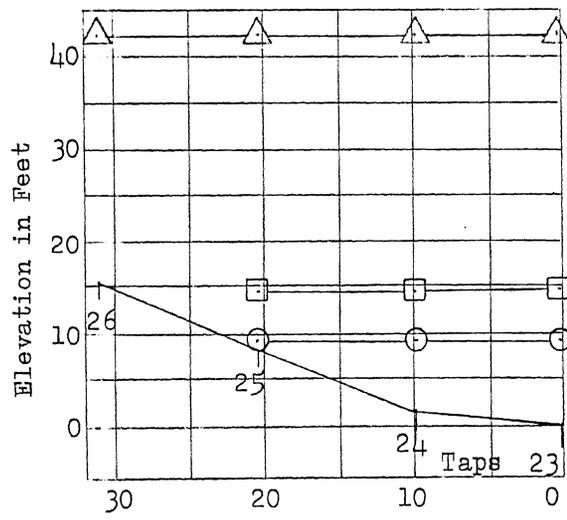
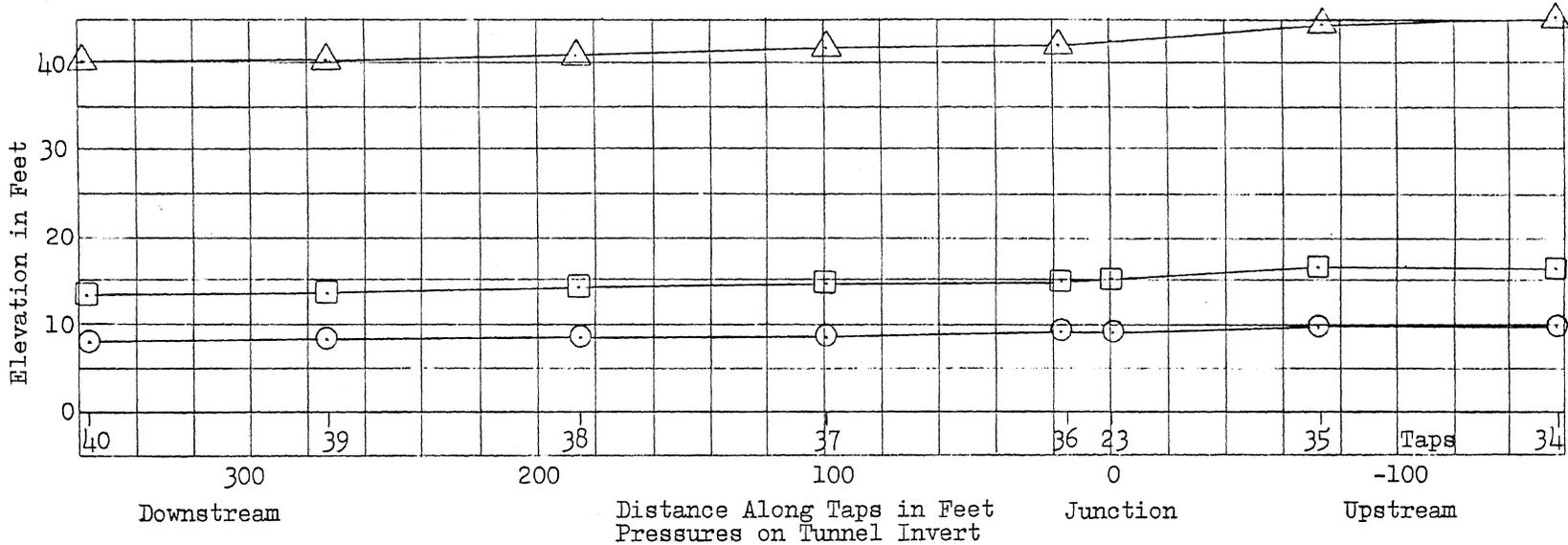
CULVER-GOODMAN MODEL STUDIES  
 Type A Dropshaft    Scale 1:21.5  
 Piezometric Pressures

SAINT ANTHONY FALLS HYDRAULIC LABORATORY			
UNIVERSITY OF MINNESOTA			
DRAWN	DA	CHECKED <i>WZ</i>	APPROVED
SCALE		DATE 3/30/77	NO. 260A2313-36



CULVER-GOODMAN MODEL STUDIES  
 Type A Dropshaft Scale 1:21.5  
 Piezometric Pressures

SAINT ANTHONY FALLS HYDRAULIC LABORATORY UNIVERSITY OF MINNESOTA			
DRAWN	DA	CHECKED	APPROVED
SCALE		DATE 5/6/77	NO. 260A2313-75

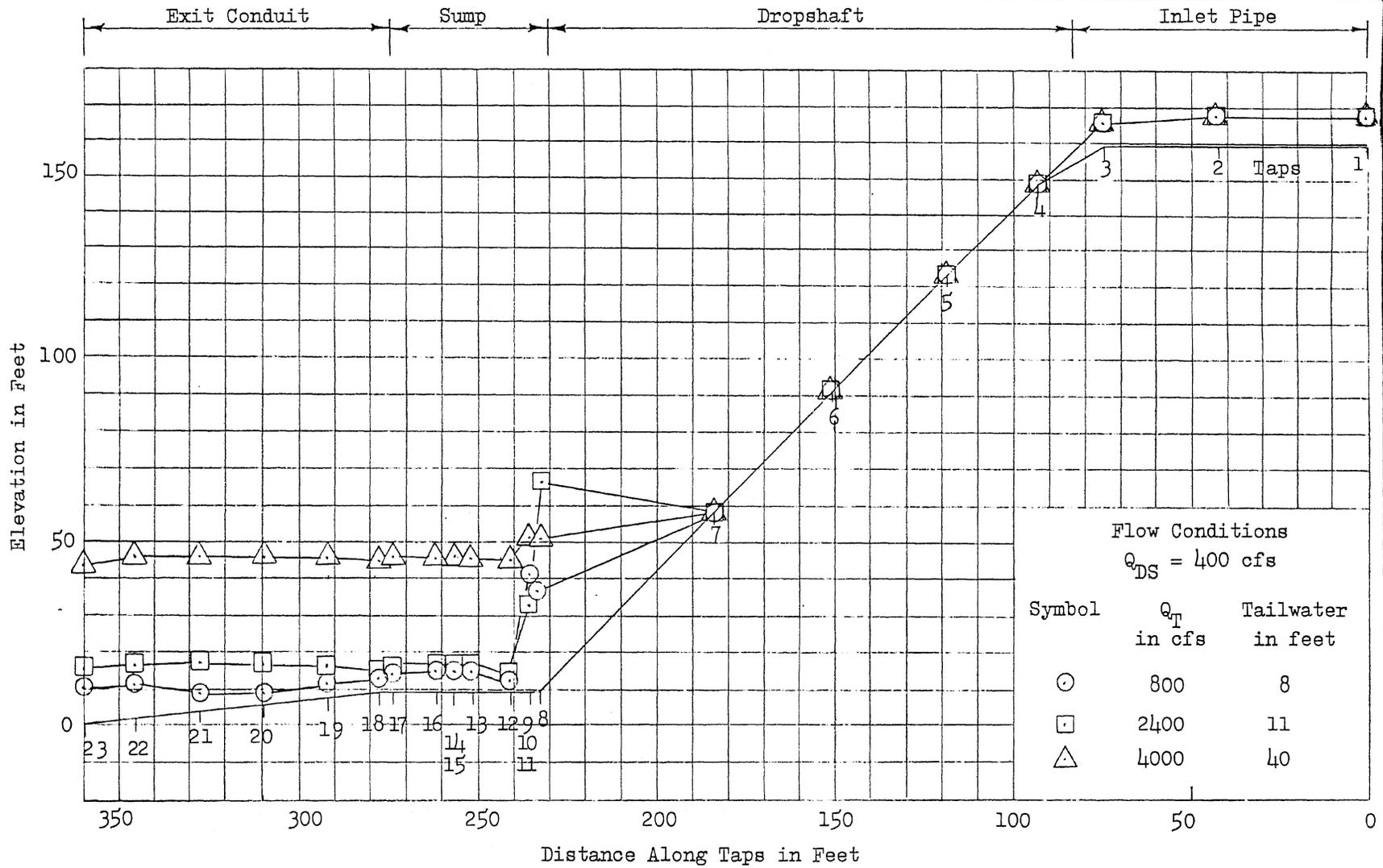


Flow Conditions  
 $Q_{DS} = 300$  cfs

Symbol	$Q_T$ in cfs	Tailwater in feet
○	800	8
□	2400	11
△	4000	40

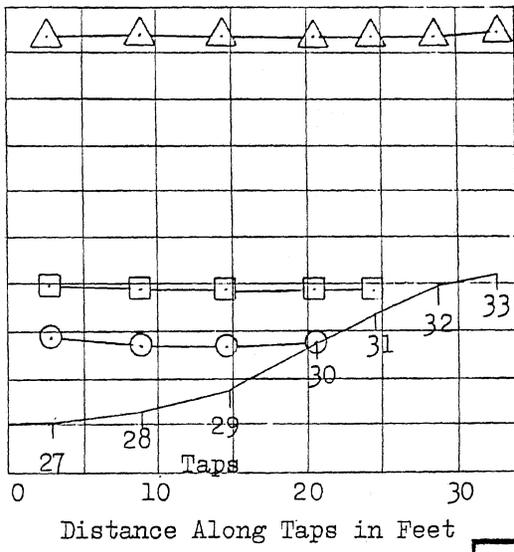
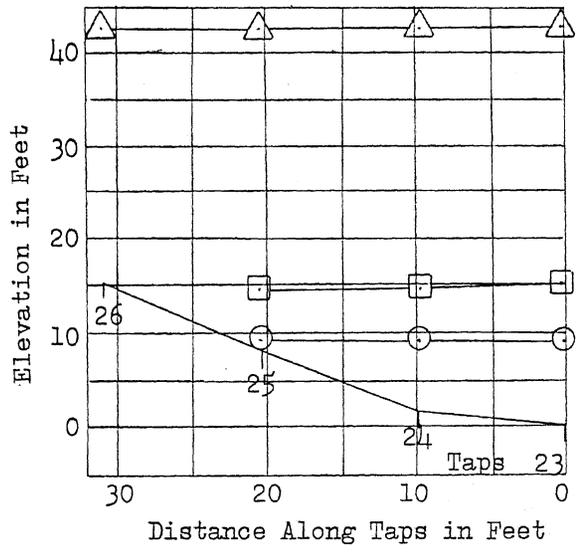
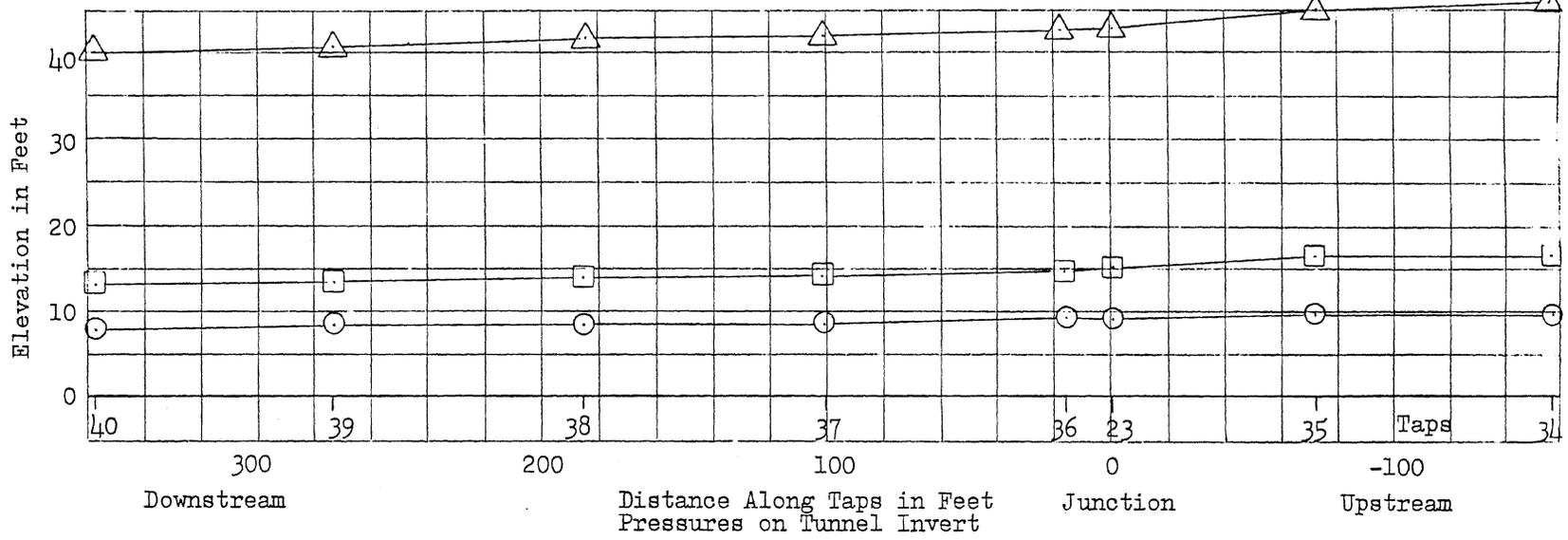
CULVER-GOODMAN MODEL STUDIES  
 Type A Dropshaft Scale 1:21.5  
 Piezometric Pressures

SAINT ANTHONY FALLS HYDRAULIC LABORATORY UNIVERSITY OF MINNESOTA		
DRAWN DA	CHECKED <i>WDS</i>	APPROVED
SCALE	DATE 5/6/77	NO. 260A2313-78



CULVER-GOODMAN MODEL STUDIES  
 Type A Dropshaft Scale 1:21.5  
 Piezometric Pressures

SAINT ANTHONY FALLS HYDRAULIC LABORATORY UNIVERSITY OF MINNESOTA			
DRAWN	DA	CHECKED <i>2/08</i>	APPROVED
SCALE		DATE 5/6/77	NO. 260A2313-74



Flow Conditions  
 $Q_{DS} = 400$  cfs

Symbol	$Q_T$ in cfs	Tailwater in feet
○	800	8
□	2400	11
△	4000	40

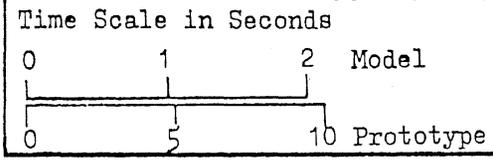
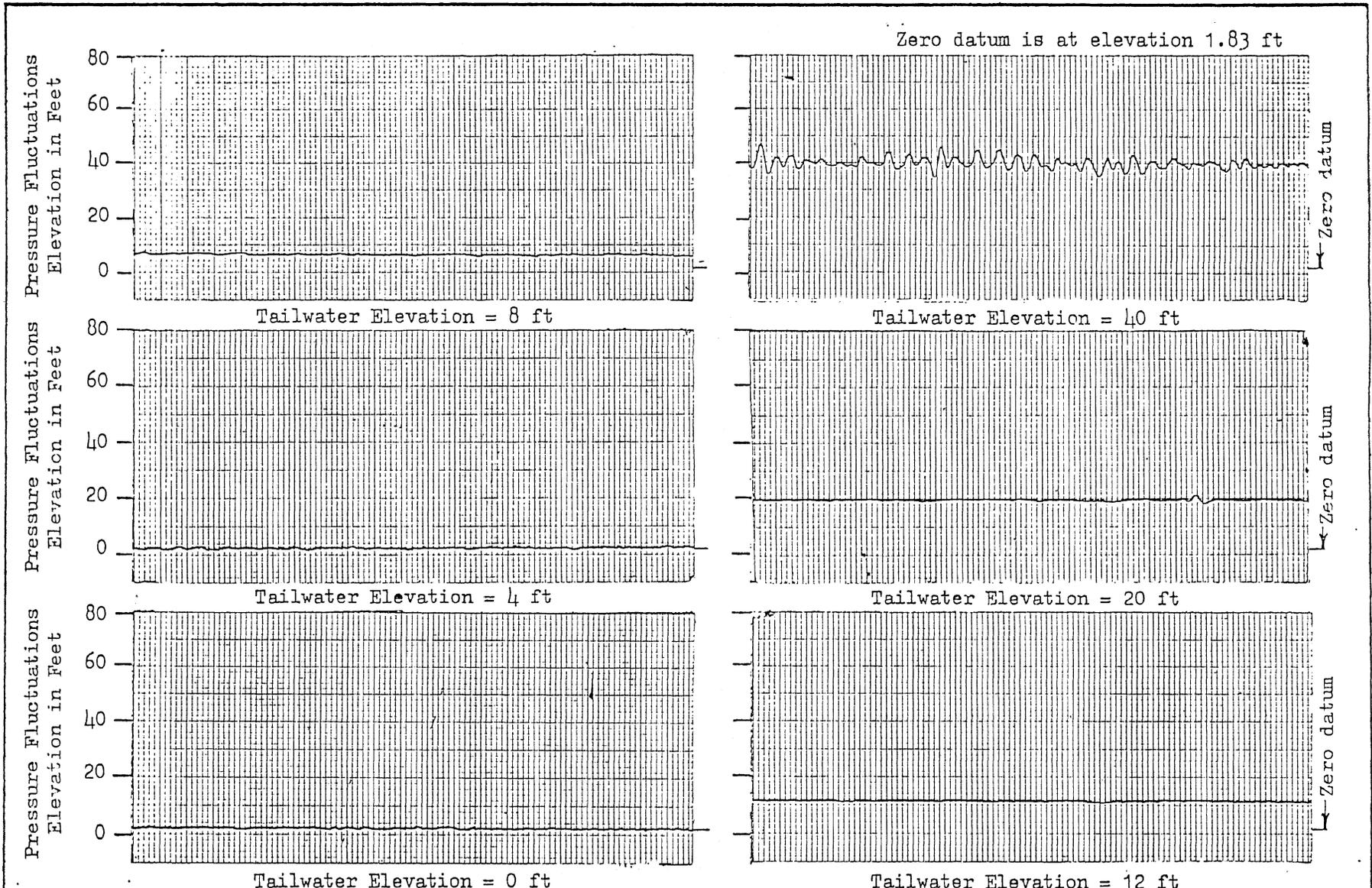
CULVER-GOODMAN MODEL STUDIES  
 Type A Dropshaft Scale 1:21.5  
 Piezometric Pressures

Distances Along Taps in Feet  
 Pressures on Tunnel Wall  
 Opposite Junction

Distances Along Taps in Feet  
 Pressures on Tunnel Wall  
 Immediately Downstream  
 of Junction

SAINT ANTHONY FALLS HYDRAULIC LABORATORY			
UNIVERSITY OF MINNESOTA			
DRAWN	DA	CHECKED <i>WDE</i>	APPROVED
SCALE		DATE 5/6/77	NO. 260A2313-77

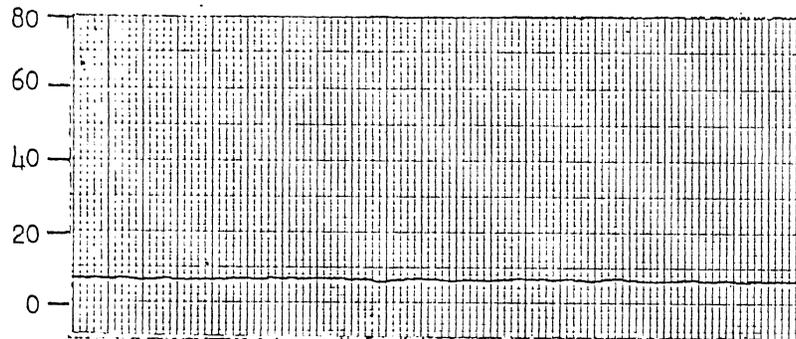




CULVER-GOODMAN MODEL STUDIES  
 Type A Dropshaft Scale 1:21.5  
 Typical Pressure Fluctuations - Tap 24  
 $Q_{DS} = 300$  cfs,  $Q_T = 0$  cfs

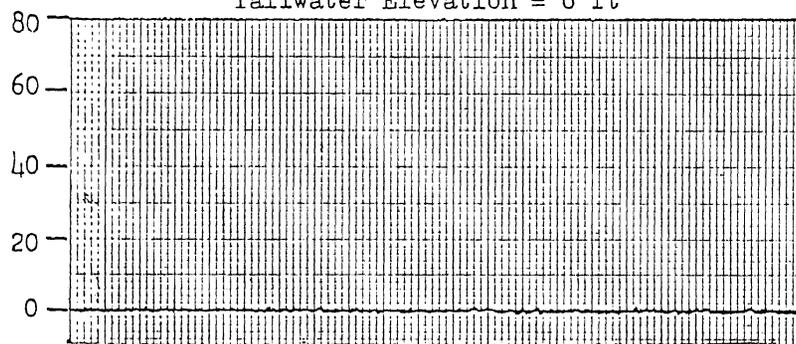
SAINT ANTHONY FALLS HYDRAULIC LABORATORY UNIVERSITY OF MINNESOTA		
DRAWN WQD	CHECKED <i>WJA</i>	APPROVED
SCALE	DATE 3/24/77	NO. 260A2313-12

Pressure Fluctuations  
Elevation in Feet



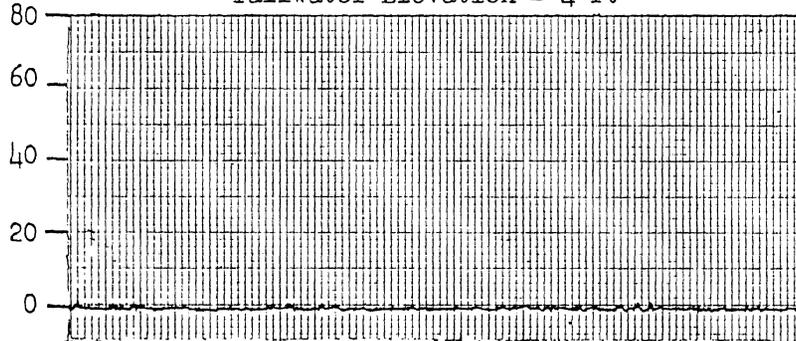
Tailwater Elevation = 8 ft

Pressure Fluctuations  
Elevation in Feet



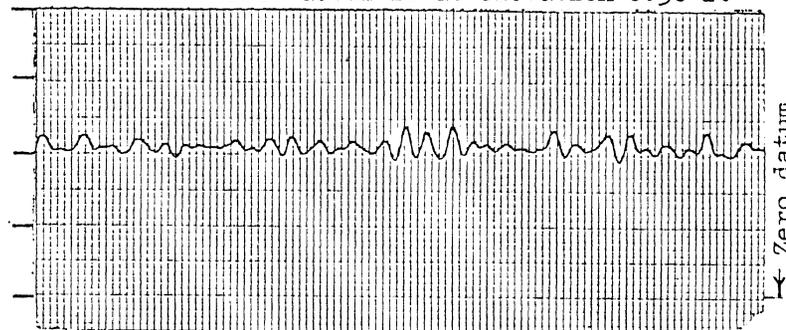
Tailwater Elevation = 4 ft

Pressure Fluctuations  
Elevation in Feet

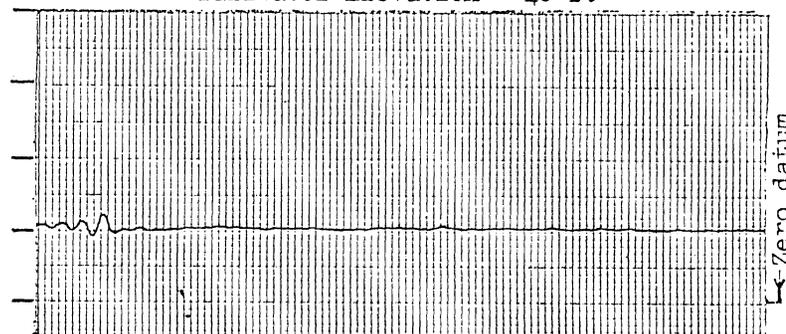


Tailwater Elevation = 0 ft

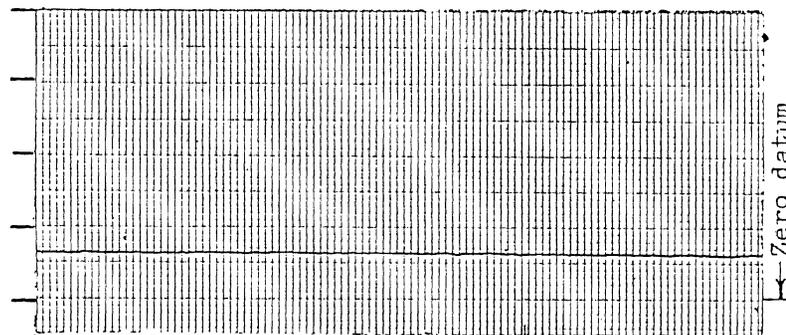
Zero datum is at elevation 0.38 ft



Tailwater Elevation = 40 ft



Tailwater Elevation = 20 ft



Tailwater Elevation = 12 ft

Time Scale in Seconds

0 1 2 Model

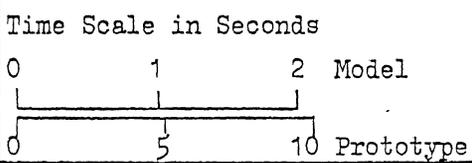
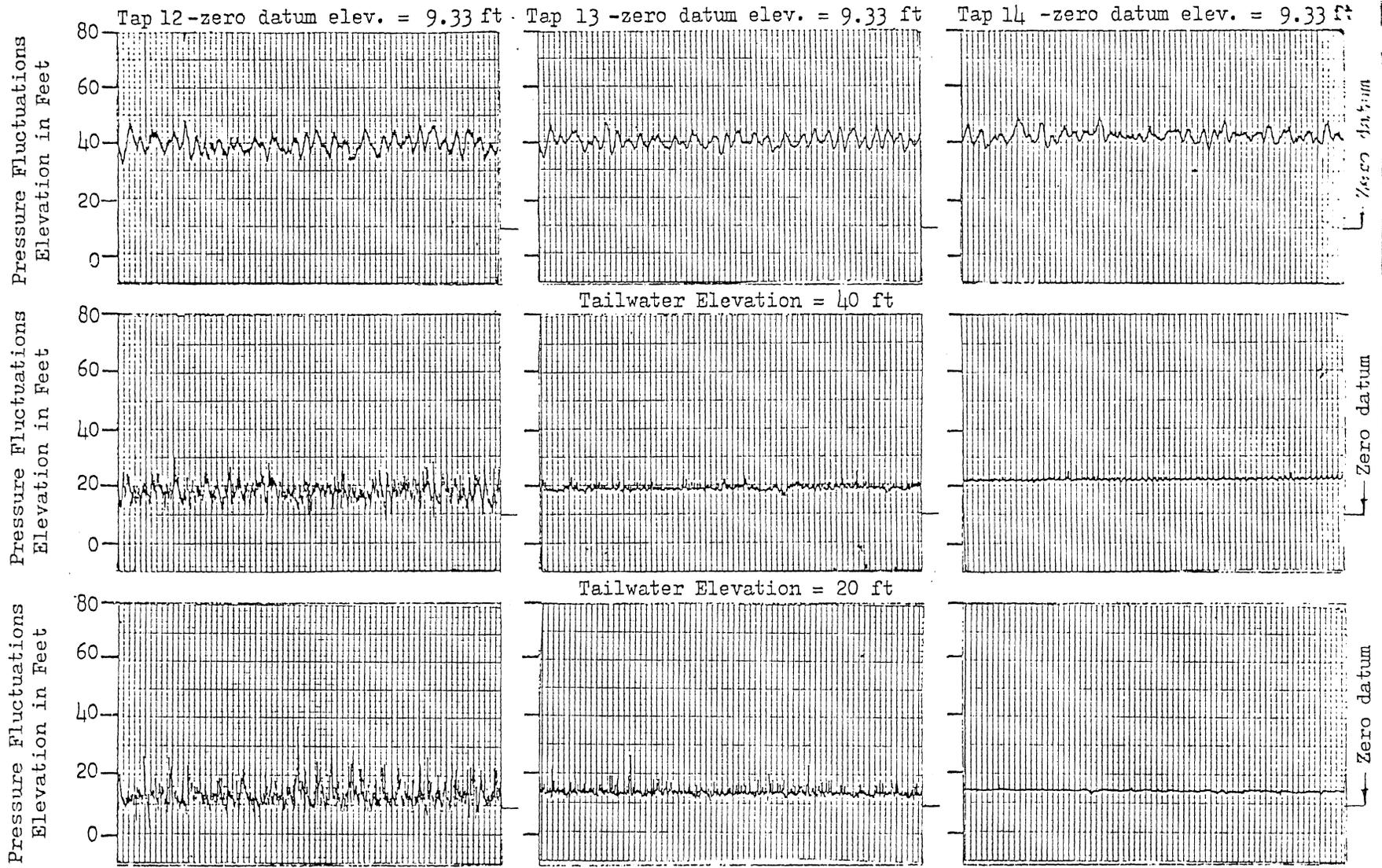
0 5 10 Prototype

CULVER-GOODMAN MODEL STUDIES  
Type A Dropshaft Scale 1:21.5  
Typical Pressure Fluctuations - Tap 27  
 $Q_{DS} = 300$  cfs,  $Q_T = 0$  cfs

SAINT ANTHONY FALLS HYDRAULIC LABORATORY  
UNIVERSITY OF MINNESOTA

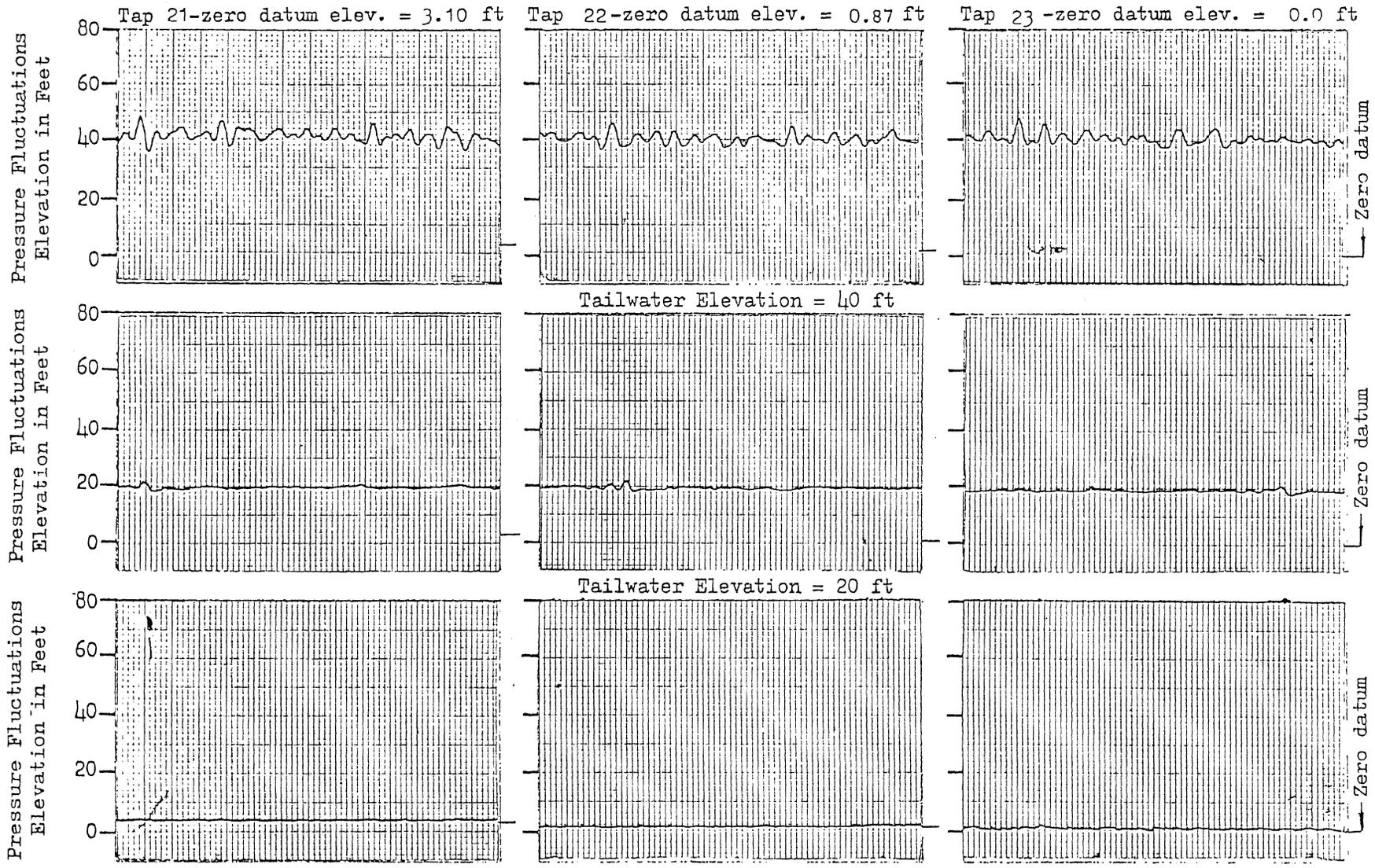
DRAWN WQD	CHECKED <i>WQD</i>	APPROVED
SCALE	DATE 3/24/77	NO. 260A2313-16

CHART 11



CULVER-GOODMAN MODEL STUDIES  
 Type A Dropshaft Scale 1:21.5  
 Typical Pressure Fluctuations  
 $Q_{DS} = 300 \text{ cfs}, Q_T = 0 \text{ cfs}$

SAINT ANTHONY FALLS HYDRAULIC LABORATORY UNIVERSITY OF MINNESOTA		
DRAWN WQD	CHECKED <i>J. J. [Signature]</i>	APPROVED
SCALE	DATE 3/28/77	NO. 260A2313-46



Time Scale in Seconds

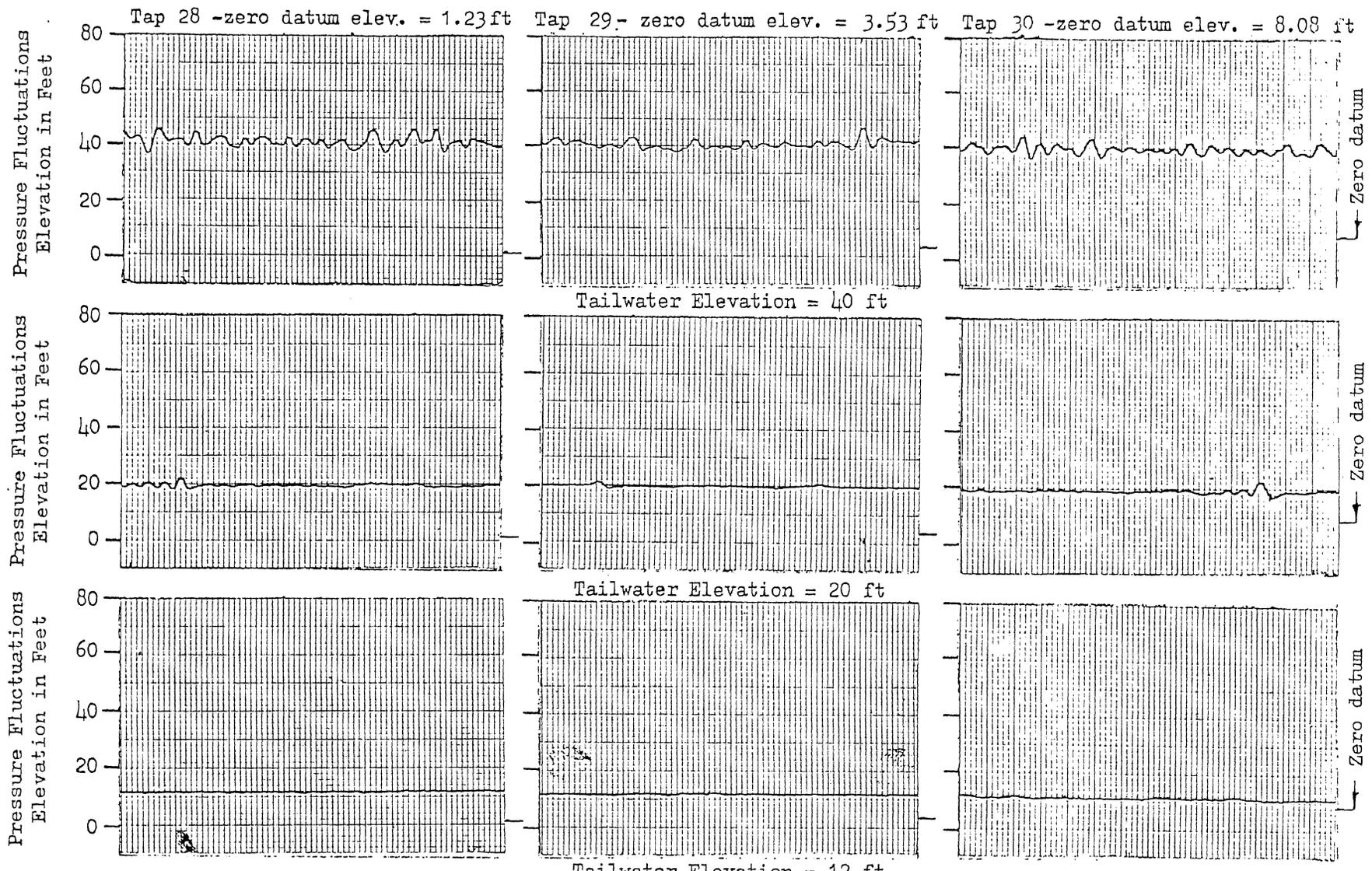
0      1      2 Model

0      5      10 Prototype

CULVER-GOODMAN MODEL STUDIES  
 Type A Dropshaft    Scale 1:21.5  
 Typical Pressure Fluctuations  
 $Q_{DS} = 300$  cfs,  $Q_T = 0$  cfs

SAINT ANTHONY FALLS HYDRAULIC LABORATORY UNIVERSITY OF MINNESOTA		
DRAWN WQD	CHECKED <i>[Signature]</i>	APPROVED
SCALE	DATE 3/28/77	NO. 260A2313-28

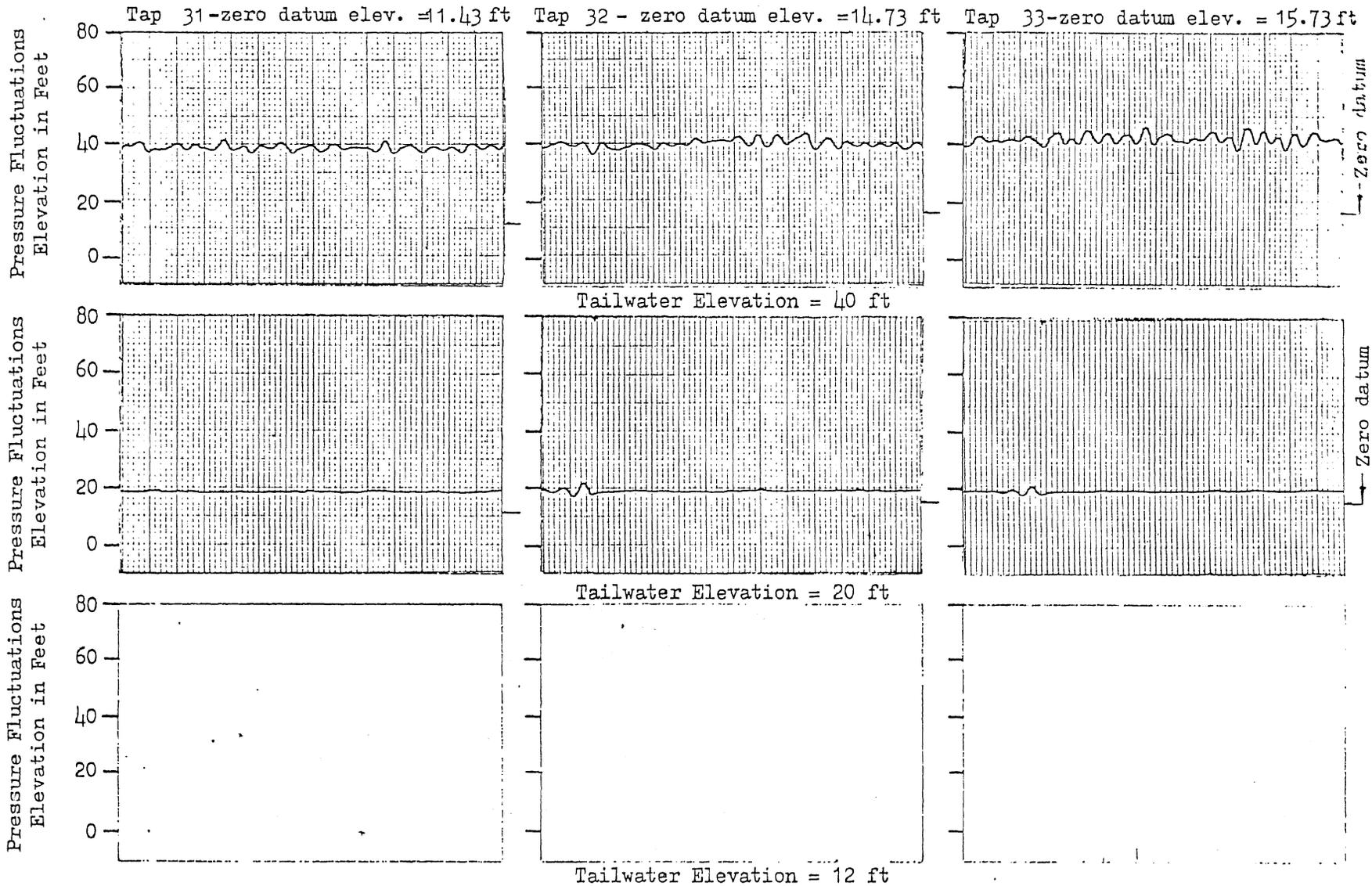
CHART 13



Time Scale in Seconds  
 0 1 2 Model  
 0 5 10 Prototype

CULVER-GOODMAN MODEL STUDIES  
 Type A Dropshaft Scale 1:21.5  
 Typical Pressure Fluctuations  
 $Q_{DS} = 300$  cfs,  $Q_T = 0$  cfs

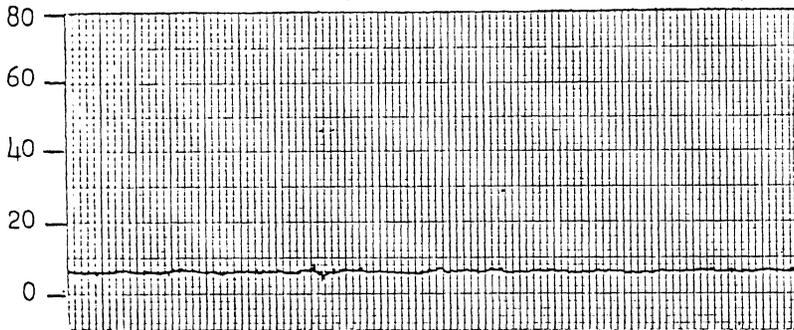
SAINT ANTHONY FALLS HYDRAULIC LABORATORY UNIVERSITY OF MINNESOTA		
DRAWN WQD	CHECKED <i>JTG</i>	APPROVED
SCALE	DATE 3/28/77	NO. 260A2313-30



CULVER-GOODMAN MODEL STUDIES  
 Type A Dropshaft    Scale 1:21.5  
 Typical Pressure Fluctuations  
 $Q_{DS} = 300$  cfs,  $Q_T = 0$  cfs

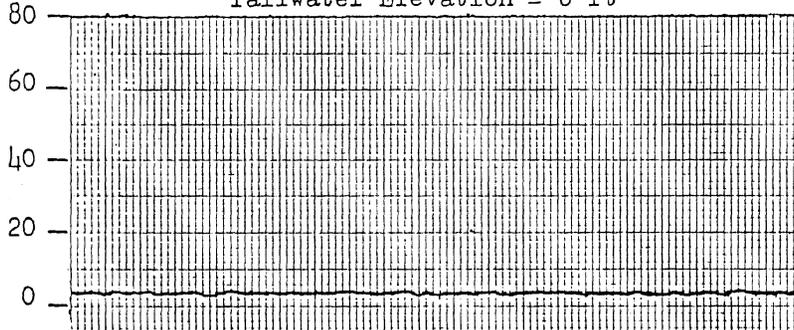
SAINT ANTHONY FALLS HYDRAULIC LABORATORY UNIVERSITY OF MINNESOTA		
DRAWN WGD	CHECKED <i>WGD</i>	APPROVED
SCALE	DATE 3/28/77	NO.260A2313- 31

Pressure Fluctuations  
Elevation in Feet



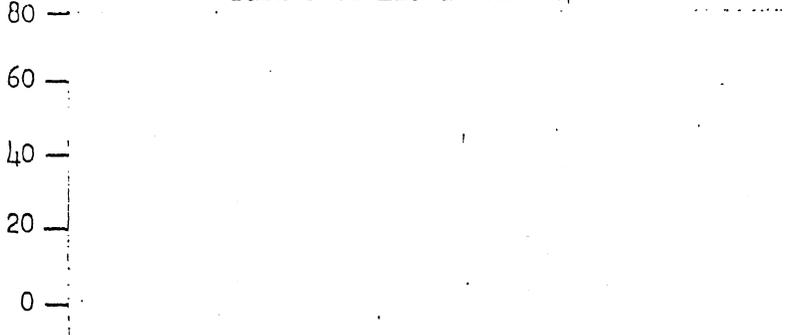
Tailwater Elevation = 8 ft

Pressure Fluctuations  
Elevation in Feet



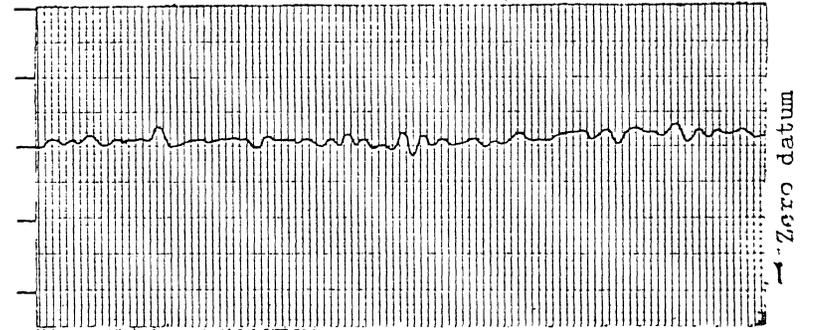
Tailwater Elevation = 4 ft

Pressure Fluctuations  
Elevation in Feet

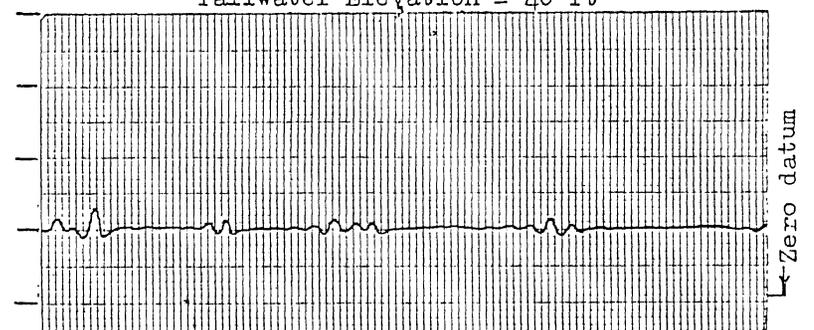


Tailwater Elevation = 0 ft

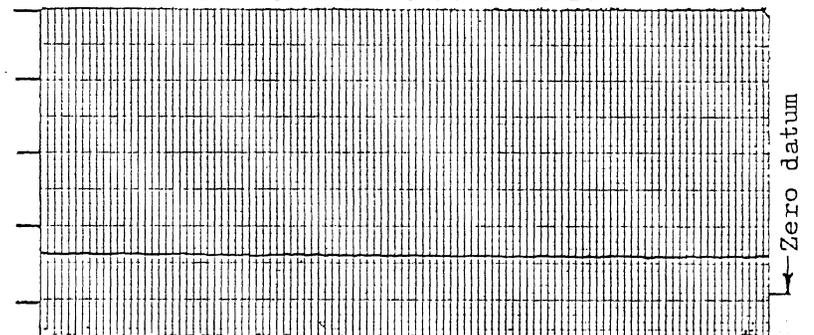
Zero datum is at elevation 1.83 ft



Tailwater Elevation = 40 ft



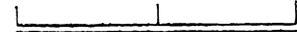
Tailwater Elevation = 20 ft



Tailwater Elevation = 12 ft

Time Scale in Seconds

0 1 2 Model



0 5 10 Prototype

CULVER-GOODMAN MODEL STUDIES

Type A Dropshaft Scale 1:21.5

Typical Pressure Fluctuations - Tap 24

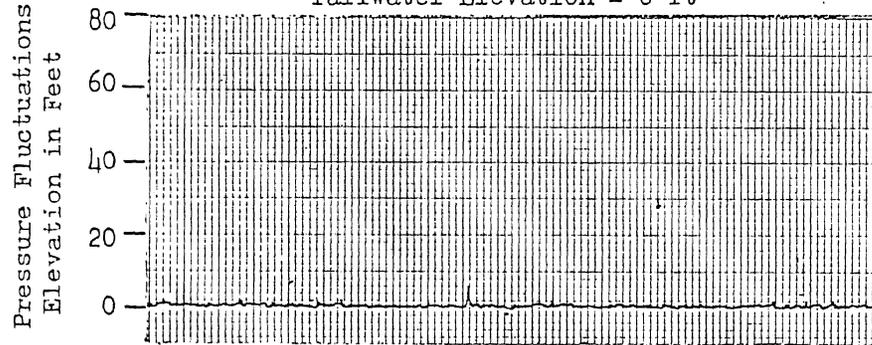
$Q_{DS} = 400$  cfs,  $Q_T = 0$  cfs

SAINT ANTHONY FALLS HYDRAULIC LABORATORY  
UNIVERSITY OF MINNESOTA

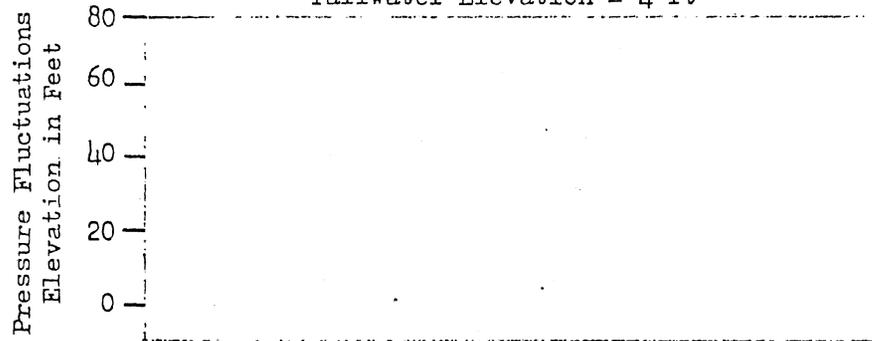
DRAWN WQD	CHECKED <i>WQD</i>	APPROVED
SCALE	DATE 3/24/77	NO. 260A2313-11



Tailwater Elevation = 8 ft

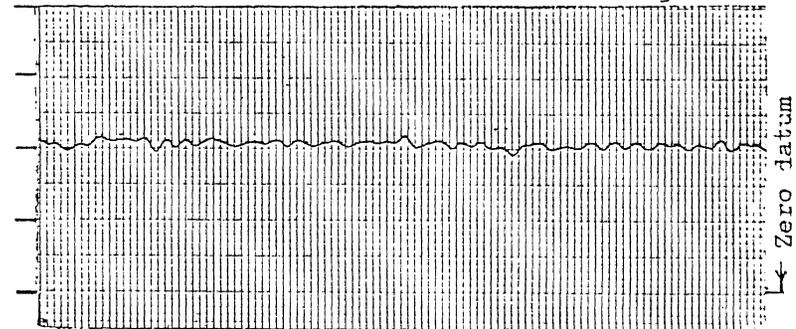


Tailwater Elevation = 4 ft

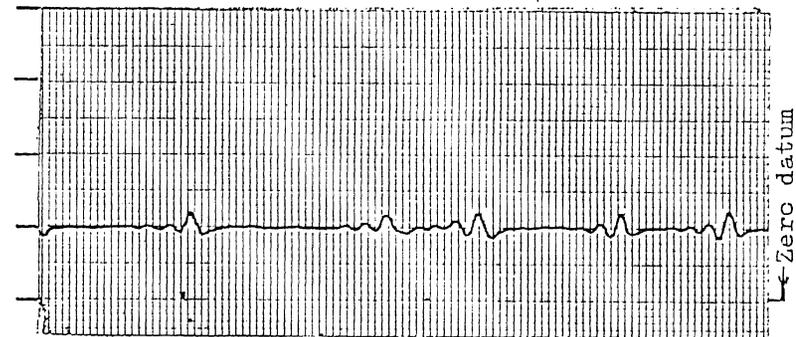


Tailwater Elevation = 0 ft

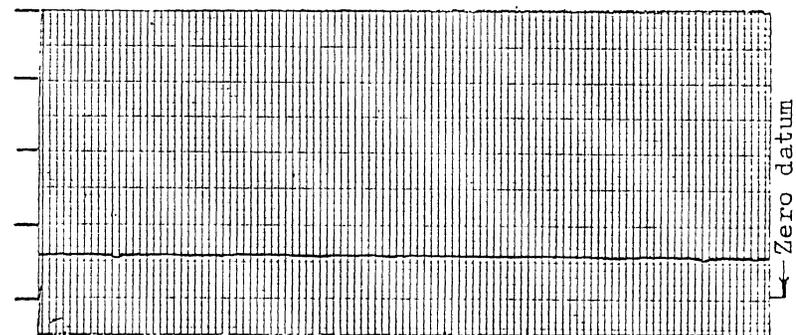
Zero datum is at elevation 0.38 ft



Tailwater Elevation = 40 ft



Tailwater Elevation = 20 ft



Tailwater Elevation = 12 ft

Time Scale in Seconds

0 1 2 Model

0 5 10 Prototype

CULVER-GOODMAN MODEL STUDIES

Type A Dropshaft Scale 1:21.5

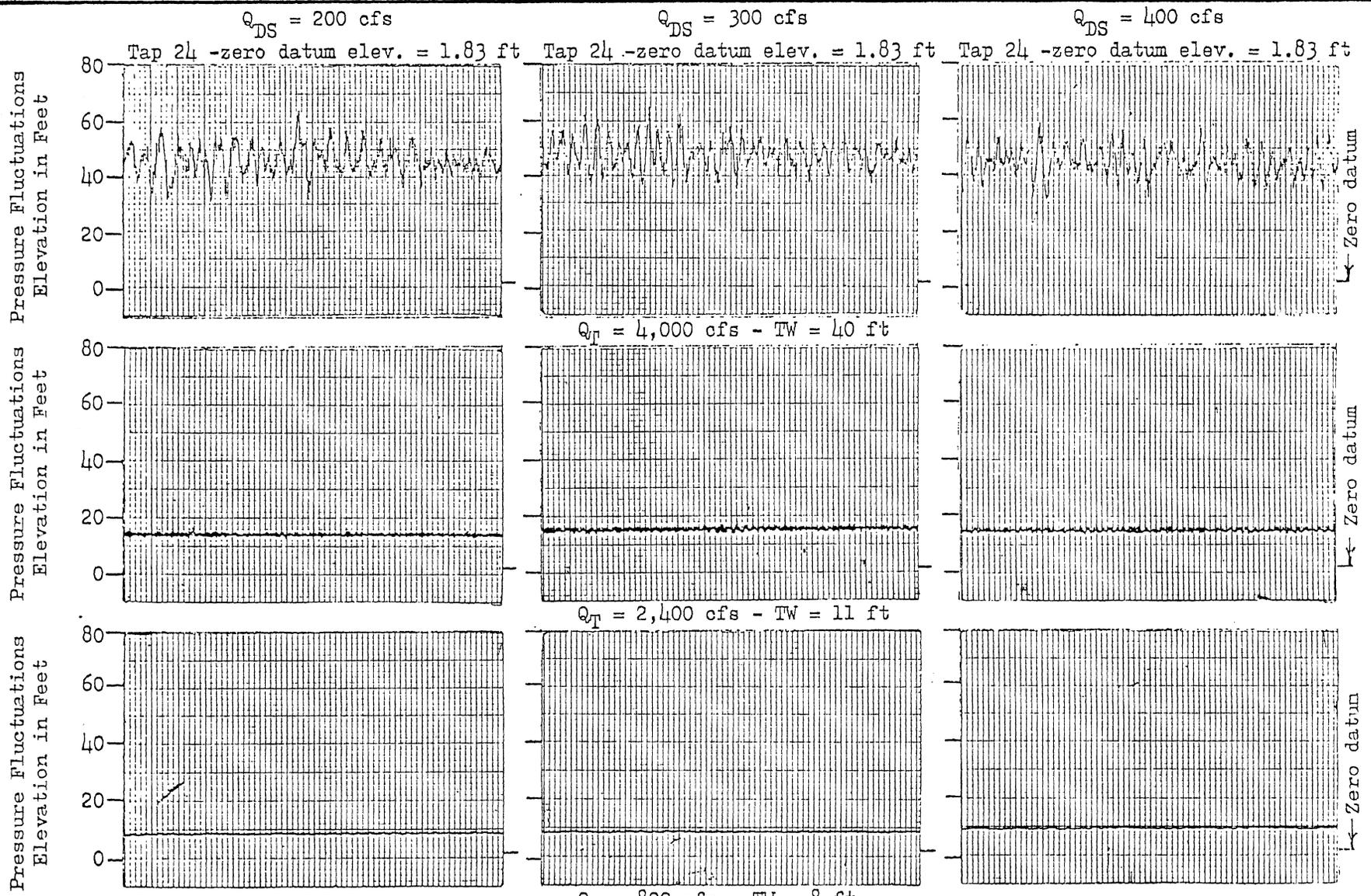
Typical Pressure Fluctuations - Tap 27

$Q_{DS} = 400$  cfs,  $Q_T = 0$  cfs

SAINT ANTHONY FALLS HYDRAULIC LABORATORY  
UNIVERSITY OF MINNESOTA

DRAWN WQD	CHECKED <i>WQD</i>	APPROVED
SCALE	DATE 3/24/77	NO. 260A2313-15





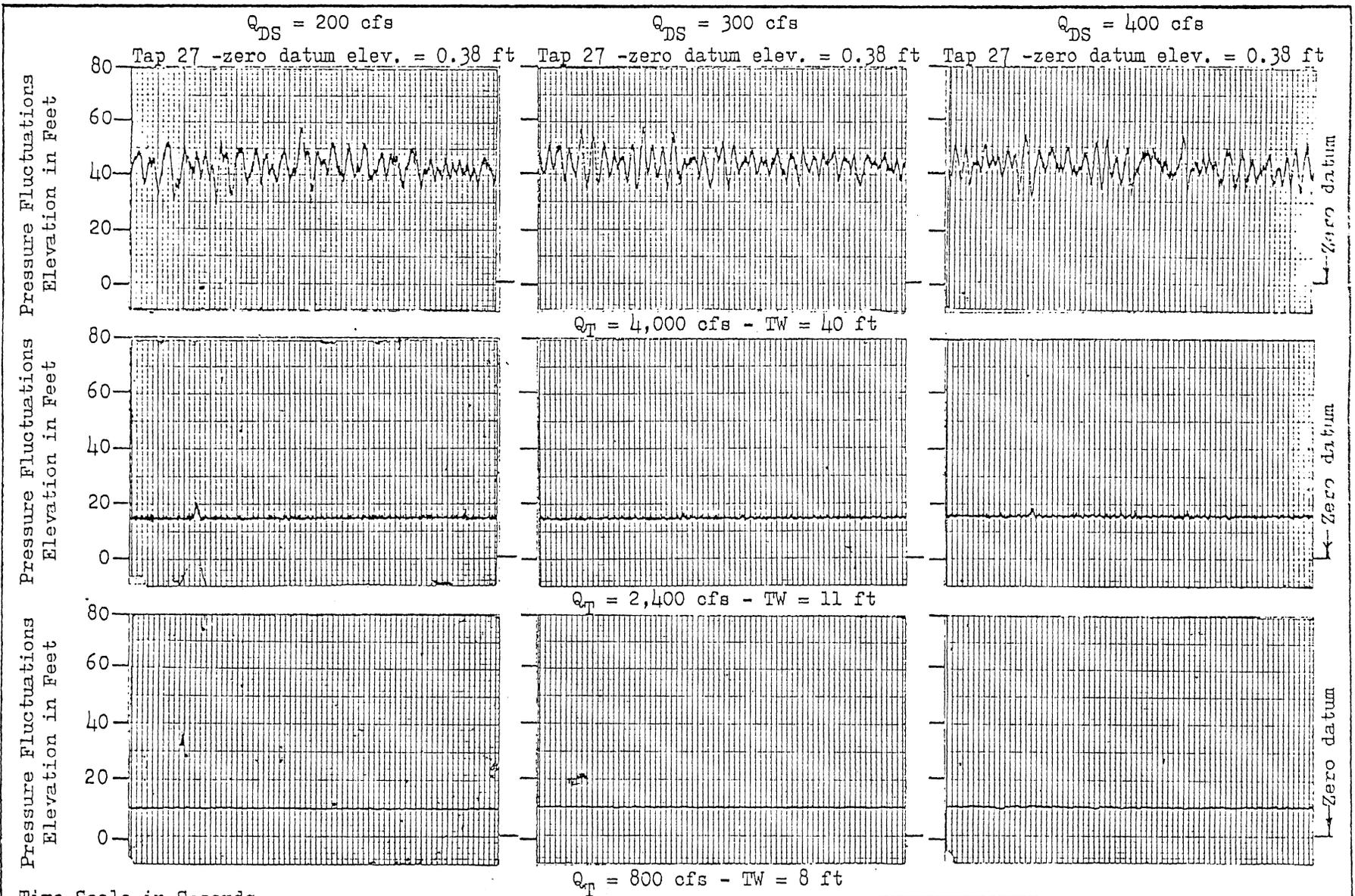
Time Scale in Seconds

0      1      2      Model

0      5      10      Prototype

CULVER-GOODMAN MODEL STUDIES  
 Type A Dropshaft      Scale 1:21.5  
 Typical Pressure Fluctuations

SAINT ANTHONY FALLS HYDRAULIC LABORATORY		
UNIVERSITY OF MINNESOTA		
DRAWN -KJA	CHECKED <i>[Signature]</i>	APPROVED
SCALE	DATE 5/2/77	NO. 260A2313-63



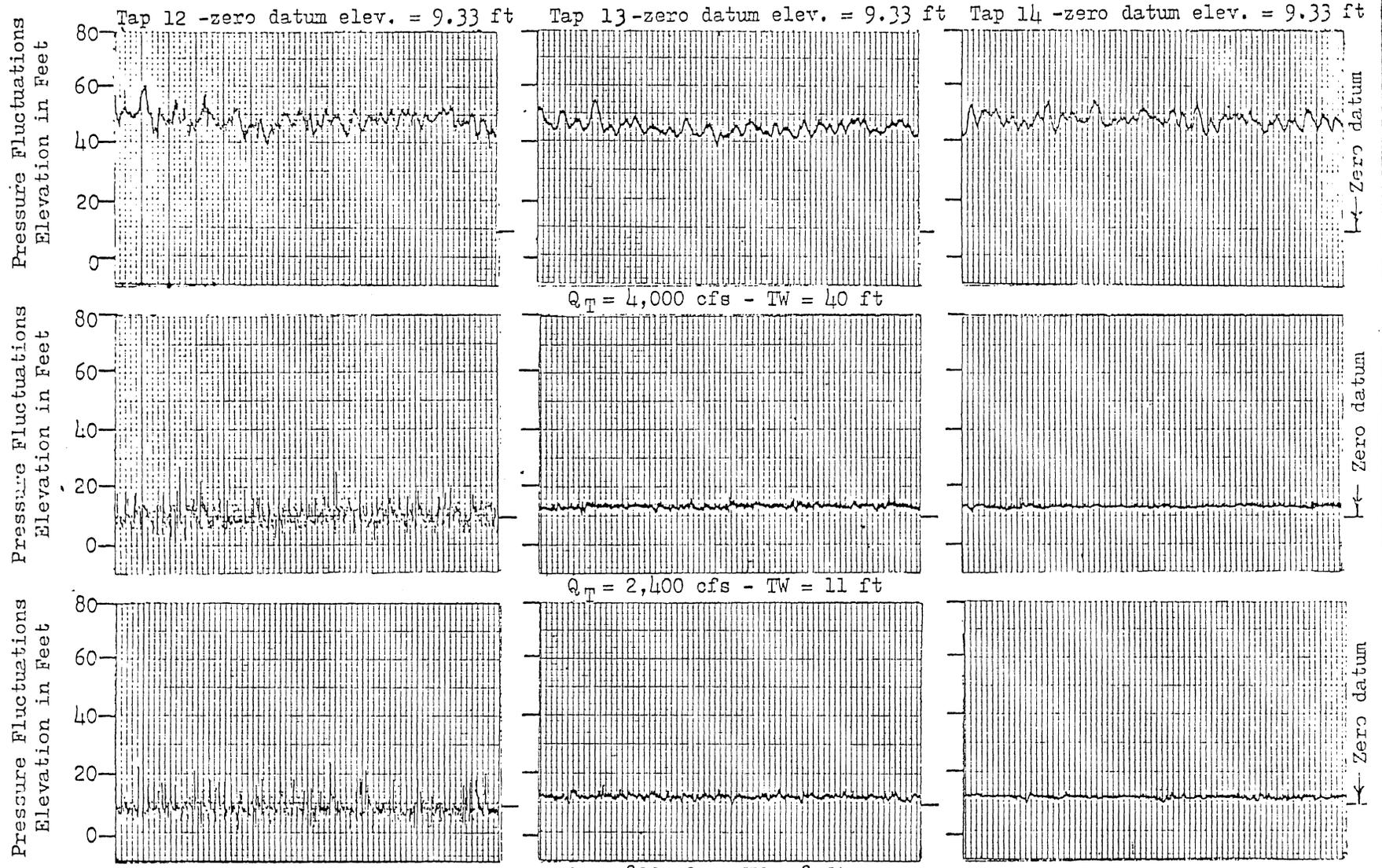
Time Scale in Seconds

0      1      2      Model

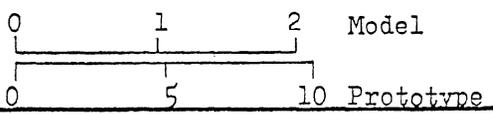
0      5      10      Prototype

CULVER-GOODMAN MODEL STUDIES  
 Type A Dropshaft    Scale 1:21.5 .  
 Typical Pressure Fluctuations

SAINT ANTHONY FALLS HYDRAULIC LABORATORY			
UNIVERSITY OF MINNESOTA			
DRAWN	KJA	CHECKED <i>[Signature]</i>	APPROVED
SCALE		DATE 5/2/77	NO. 260A2313-64

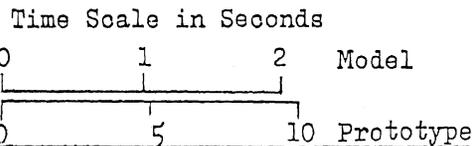
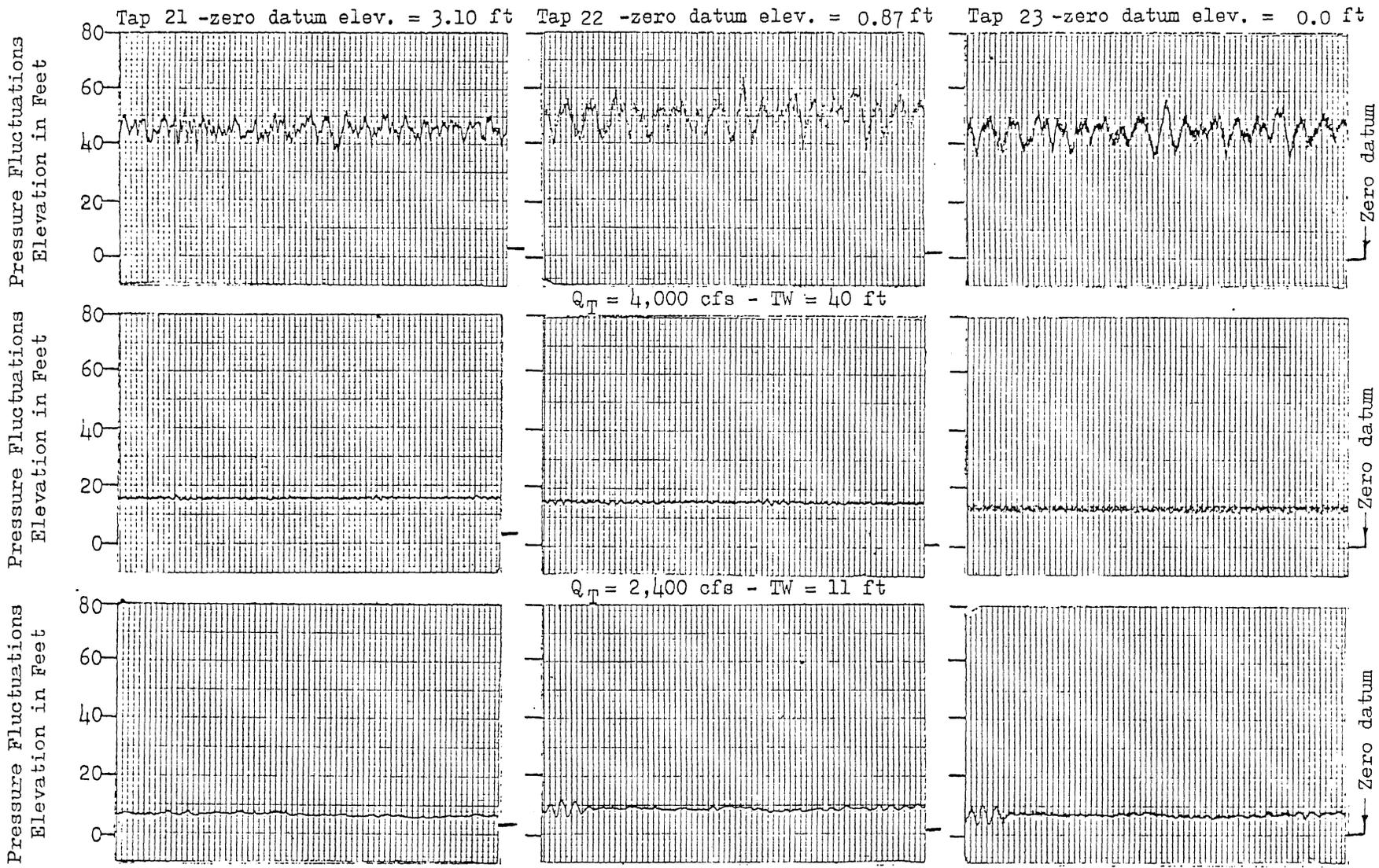


Time Scale in Seconds



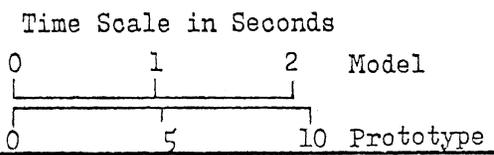
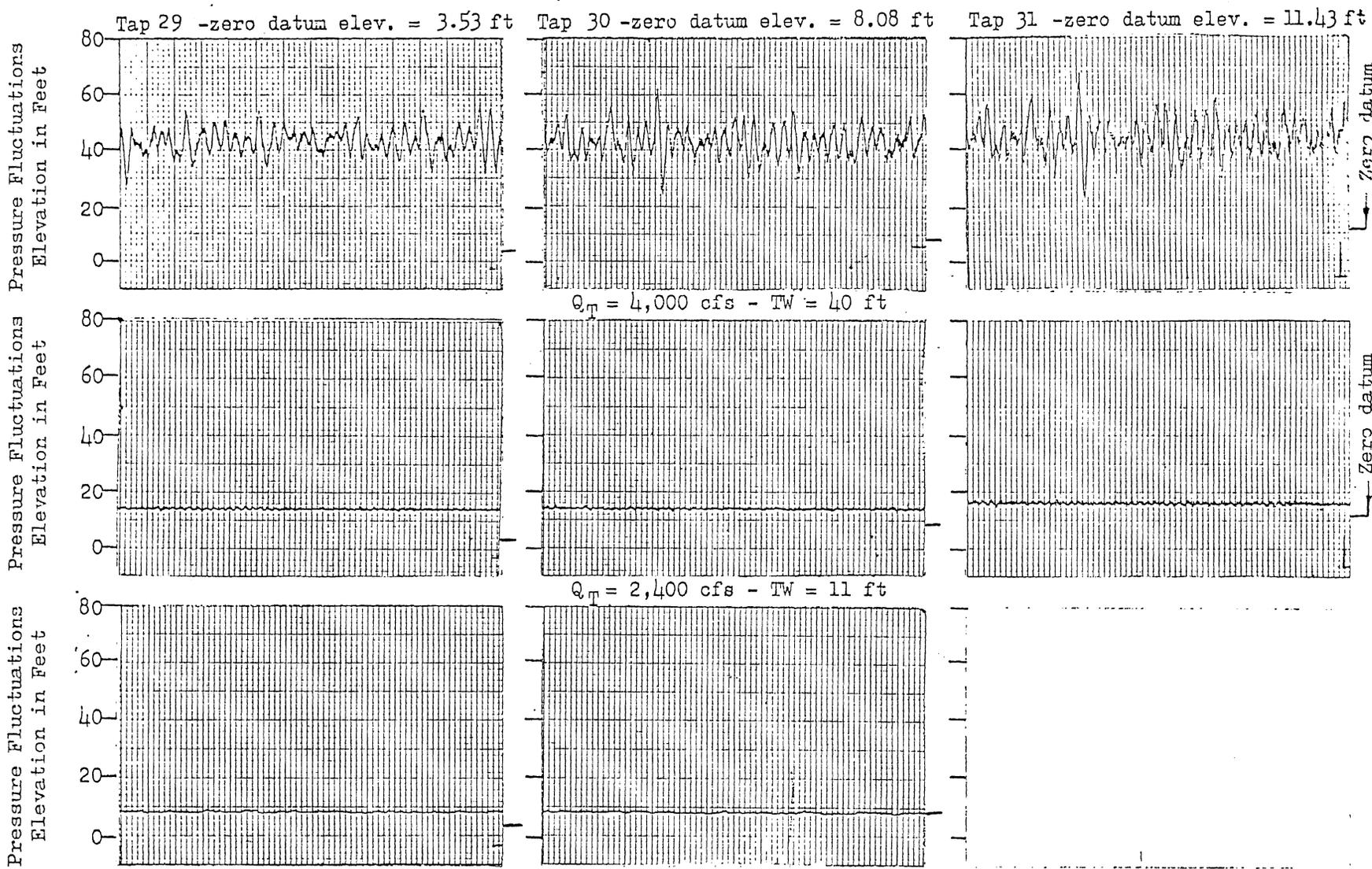
CULVER-GOODMAN MODEL STUDIES  
 Type A Dropshaft Scale 1:21.5  
 Typical Pressure Fluctuations  
 $Q_{DS} = 300$  cfs

SAINT ANTHONY FALLS HYDRAULIC LABORATORY UNIVERSITY OF MINNESOTA		
DRAWN KJA	CHECKED <i>[Signature]</i>	APPROVED
SCALE	DATE 5/2/77	NO. 260A2313-65



CULVER-GOODMAN MODEL STUDIES  
 Type A Dropshaft Scale 1:21.5  
 Typical Pressure Fluctuations  
 $Q_{DS} = 300$  cfs

SAINT ANTHONY FALLS HYDRAULIC LABORATORY UNIVERSITY OF MINNESOTA		
DRAWN KJA	CHECKED <i>WCB</i>	APPROVED
SCALE	DATE 5/2/77	NO. 260A2313-68



CULVER-GOODMAN MODEL STUDIES  
 Type A Dropshaft    Scale 1:21.5  
 Typical Pressure Fluctuations  
 $Q_{DS} = 300 \text{ cfs}$

SAINT ANTHONY FALLS HYDRAULIC LABORATORY UNIVERSITY OF MINNESOTA		
DRAWN KJA	CHECKED <i>WAB</i>	APPROVED
SCALE	DATE 5/2/77	NO. 260A2313-70

$Q_{DS}$ cfs	$Q_T$ cfs	T.W. Elev. ft	Min. Elev. ft	Avg. Elev. ft	Max. Elev. ft	Min. Elev. ft	Avg. Elev. ft	Max. Elev. ft
			Tap 24 Tap 24 is at Elev. 1.83 ft (zero datum)			Tap 27 Tap 27 is at Elev. 0.38 ft (zero datum)		
400	0	0	3	4	4	0	1	6
400	0	4	3	4	4	0	1	6
400	0	8	4	6	8	2	5	8
400	0	12	12	13	13	10	12	12
400	0	20	16	20	30	17	20	24
400	0	40	37	42	46	38	40	46
300	0	0	2	2	3	-2	0	2
300	0	4	2	3	4	-2	0	2
300	0	8	5	6	7	6	7	7
300	0	12	11	12	12	12	13	13
300	0	20	18	20	21	18	20	25
300	0	40	34	40	47	36	42	48
200	0	0	2	3	4	-1	0	2
200	0	4	2	3	4	0	1	2
200	0	8	8	8	8	6	6	6
200	0	12	11	12	12	12	12	12
200	0	20	19	20	21	19	20	21
200	0	40	33	40	50	37	42	45
100	0	0	2	3	3	-1	0	0
100	0	4	2	4	4	1	2	3
100	0	8	8	8	8	8	9	9
100	0	12	12	12	12	12	13	13
100	0	20	20	20	21	22	22	23
100	0	40	38	40	44	40	44	48

CULVER-GOODMAN MODEL STUDIES  
 Type A Dropshaft Scale 1:21.5  
 Summary of Pressure Fluctuations

SAINT ANTHONY FALLS HYDRAULIC LABORATORY UNIVERSITY OF MINNESOTA		
DRAWN KJA	CHECKED <i>[Signature]</i>	APPROVED
SCALE	DATE 5/4/77	NO. 260A2313-80

$Q_{DS}$ cfs	$Q_T$ cfs	T.W. Elev. ft	Min. Elev. ft	Avg. Elev. ft	Max. Elev. ft	Min. Elev. ft	Avg. Elev. ft	Max. Elev. ft	Min. Elev. ft	Avg. Elev. ft	Max. Elev. ft
			Tap 12 Tap 12 is at Elev. 9.33 ft (zero datum)			Tap 13 Tap 13 is at Elev. 9.33 ft (zero datum)			Tap 14 Tap 14 is at Elev. 9.33 ft (zero datum)		
300	0	0	5	13	30	13	15	23	11	13	15
300	0	4	5	13	30	13	15	25	11	13	14
300	0	8	3	13	25	13	15	25	11	13	13
300	0	12	5	13	30	9	11	18	10	13	14
300	0	20	5	18	30	19	20	24	18	18	20
300	0	40	30	43	53	34	40	47	30	38	48

CULVER-GOODMAN MODEL STUDIES  
 Type A Dropshaft Scale 1:21.5  
 Summary of Pressure Fluctuations

SAINT ANTHONY FALLS HYDRAULIC LABORATORY UNIVERSITY OF MINNESOTA		
DRAWN KJA	CHECKED <i>[Signature]</i>	APPROVED
SCALE	DATE 5/4/77	NO. 260A2313-81

Q <sub>DS</sub> cfs	Q <sub>T</sub> cfs	T.W. Elev. ft	Min. Elev. ft	Avg. Elev. ft	Max. Elev. ft	Min. Elev. ft	Avg. Elev. ft	Max. Elev. ft	Min. Elev. ft	Avg. Elev. ft	Max. Elev. ft
			Tap 15 is at Elev. 9.33 ft (zero datum)			Tap 16 is at Elev. 9.33 ft (zero datum)			Tap 17 is at Elev. 9.33 ft (zero datum)		
300	0	0	11	13	14	10	13	13	10	13	15
300	0	4	13	15	16	10	12	14	10	11	15
300	0	8	13	16	18	10	12	15	10	11	11
300	0	12	15	16	18	10	12	15	10	10	12
300	0	20	20	21	23	18	19	23	15	18	20
300	0	40	34	41	50	35	42	48	33	38	48
			Tap 18 is at Elev. 9.27 ft (zero datum)			Tap 19 is at Elev. 7.52 ft (zero datum)			Tap 20 is at Elev. 5.26 ft (zero datum)		
300	0	0	13	13	15	10	11	13	8	8	8
300	0	4	13	13	14	10	10	12	8	8	8
300	0	8	12	13	13	10	10	13	8	8	8
300	0	12	11	12	13	11	12	13	8	8	10
300	0	20	18	21	23	19	21	23	20	21	23
300	0	40	33	42	50	36	43	48	38	43	48

CULVER-GOODMAN MODEL STUDIES  
 Type A Dropshaft Scale 1:21.5  
 Summary of Pressure Fluctuations

SAINT ANTHONY FALLS HYDRAULIC LABORATORY UNIVERSITY OF MINNESOTA		
DRAWN KJA	CHECKED <i>[Signature]</i>	APPROVED
SCALE	DATE 5/4/77	NO. 260A2313-82



Q <sub>DS</sub> cfs	Q <sub>T</sub> cfs	T.W. Elev. ft	Min. Elev. ft	Avg. Elev. ft	Max. Elev. ft	Min. Elev. ft	Avg. Elev. ft	Max. Elev. ft	Min. Elev. ft	Avg. Elev. ft	Max. Elev. ft
			Tap 21 Tap 21 is at Elev. 3.10 ft (zero datum)			Tap 22 Tap 22 is at Elev. 0.87 ft (zero datum)			Tap 23 Tap 23 is at Elev. 0.00 ft (zero datum)		
300	0	0	4	4	4	2	2	2	-1	1	2
300	0	4	4	4	4	2	2	2	0	1	1
300	0	8	4	4	5	6	6	7	5	6	7
300	0	12	10	11	12	11	12	12	11	12	12
300	0	20	17	20	24	20	20	22	18	19	21
300	0	40	34	41	51	33	40	46	34	40	48
			Tap 25 Tap 25 is at Elev. 8.08 ft (zero datum)			Tap 26 Tap 26 is at Elev. 15.23 ft (zero datum)					
300	0	0									
300	0	4									
300	0	8									
300	0	12	11	12	12						
300	0	20	19	20	22	19	22	26			
300	0	40	37	41	47	36	40	51			

CULVER-GOODMAN MODEL STUDIES  
 Type A Dropshaft Scale 1:21.5  
 Summary of Pressure Fluctuations

SAINT ANTHONY FALLS HYDRAULIC LABORATORY UNIVERSITY OF MINNESOTA		
DRAWN KJA	CHECKED <i>[Signature]</i>	APPROVED
SCALE	DATE 5/4/77	NO. 260A2313-83

Q <sub>DS</sub> cfs	Q <sub>T</sub> cfs	T.W. Elev. ft	Min. Elev. ft	Avg. Elev. ft	Max. Elev. ft	Min. Elev. ft	Avg. Elev. ft	Max. Elev. ft	Min. Elev. ft	Avg. Elev. ft	Max. Elev. ft
			Tap 28 is at Elev. 1.23 ft (zero datum)			Tap 29 is at Elev. 3.53 ft (zero datum)			Tap 30 is at Elev. 8.08 ft (zero datum)		
300	0	0									
300	0	4									
300	0	8	4	6	7	5	8	8			
300	0	12	11	12	12	10	12	12	10	11	12
300	0	20	18	20	22	19	20	21	17	19	22
300	0	40	36	41	49	34	40	47	35	40	44

Q <sub>DS</sub> cfs	Q <sub>T</sub> cfs	T.W. Elev. ft	Min. Elev. ft	Avg. Elev. ft	Max. Elev. ft	Min. Elev. ft	Avg. Elev. ft	Max. Elev. ft	Min. Elev. ft	Avg. Elev. ft	Max. Elev. ft
			Tap 31 is at Elev. 11.43 ft (zero datum)			Tap 32 is at Elev. 14.73 ft (zero datum)			Tap 33 is at Elev. 15.73 ft (zero datum)		
300	0	0									
300	0	4									
300	0	8									
300	0	12									
300	0	20	17	19	20	17	19	22	18	20	22
300	0	40	36	38	43	36	40	44	38	40	46

CULVER-GOODMAN MODEL STUDIES  
 Type A Dropshaft Scale 1:21.5  
 Summary of Pressure Fluctuations

SAINT ANTHONY FALLS HYDRAULIC LABORATORY UNIVERSITY OF MINNESOTA		
DRAWN KJA	CHECKED <i>[Signature]</i>	APPROVED
SCALE	DATE 5/4/77	NO. 260A2313-84

- 73 -

CHART 27

Q <sub>DS</sub> cfs	Q <sub>T</sub> cfs	T.W. Elev. ft	Min. Elev. ft	Avg. Elev. ft	Max. Elev. ft	Min. Elev. ft	Avg. Elev. ft	Max. Elev. ft			
			Tap 24 Tap 24 is at Elev. 1.83 ft (zero datum)			Tap 27 Tap 27 is at Elev. 0.38 ft (zero datum)					
400	800	8	8	9	10	10	10	11			
400	2400	11	13	14	16	14	16	19			
400	4000	40	28	45	60	29	43	55			
300	800	8	8	8	9	10	10	10			
300	2400	11	13	14	17	14	15	17			
300	4000	40	32	47	64	32	44	58			
200	800	8	8	8	9	10	10	10			
200	2400	11	12	14	17	13	15	21			
200	4000	40	31	46	64	29	44	58			
			Tap 12 Tap 12 is at Elev. 9.33 ft (zero datum)			Tap 13 Tap 13 is at Elev. 9.33 ft (zero datum)			Tap 14 Tap 14 is at Elev. 9.33 ft (zero datum)		
300	800	8	- 2	10	28	10	12	16	8	11	13
300	2400	11	- 3	11	28	10	13	16	10	12	16
300	4000	40	38	48	60	38	45	55	40	46	57

CULVER-GOODMAN MODEL STUDIES  
Type A Dropshaft Scale 1:21.5  
Summary of Pressure Fluctuations

SAINT ANTHONY FALLS HYDRAULIC LABORATORY UNIVERSITY OF MINNESOTA		
DRAWN KJA	CHECKED <i>JTB</i>	APPROVED
SCALE	DATE 5/4/77	NO. 260A2313-85

- 74 -

CHART 28

Q <sub>DS</sub> cfs	Q <sub>T</sub> cfs	T.W. Elev. ft	Min. Elev. ft	Avg. Elev. ft	Max. Elev. ft	Min. Elev. ft	Avg. Elev. ft	Max. Elev. ft	Min. Elev. ft	Avg. Elev. ft	Max. Elev. ft
			Tap 15 Tap 15 is at Elev. 9.33 ft (zero datum)			Tap 16 Tap 16 is at Elev. 9.33 ft (zero datum)			Tap 17 Tap 17 is at Elev. 9.33 ft (zero datum)		
300	800	8	11	12	13	14	15	16	12	13	14
300	2400	11	12	14	15	15	16	18	14	15	16
300	4000	40	39	44	53	42	50	58	40	46	52
			Tap 18 Tap 18 is at Elev. 9.27 ft (zero datum)			Tap 19 Tap 19 is at Elev. 7.52 ft (zero datum)			Tap 20 Tap 20 is at Elev. 5.26 ft (zero datum)		
300	800	8	12	12	12	11	12	12	5	6	7
300	2400	11	14	15	16	17	18	19	14	16	18
300	4000	40	40	46	54	40	50	62	38	48	57
			Tap 21 Tap 21 is at Elev. 3.10 ft (zero datum)			Tap 22 Tap 22 is at Elev. 0.87 ft (zero datum)			Tap 23 Tap 23 is at Elev. 0.00 ft (zero datum)		
300	800	8	6	7	8	6	8	12	3	6	10
300	2400	11	15	16	17	14	15	16	10	14	16
300	4000	40	36	46	55	38	50	64	34	46	57

CULVER-GOODMAN MODEL STUDIES  
Type A Dropshaft Scale 1:21.5  
Summary of Pressure Fluctuations

SAINT ANTHONY FALLS HYDRAULIC LABORATORY UNIVERSITY OF MINNESOTA		
DRAWN KJA	CHECKED <i>[Signature]</i>	APPROVED
SCALE	DATE 5/4/77	NO. 260A2313-86

- 75 -  
CHART 29

Q <sub>DS</sub> cfs	Q <sub>T</sub> cfs	T.W. Elev. ft	Min. Elev. ft	Avg. Elev. ft	Max. Elev. ft	Min. Elev. ft	Avg. Elev. ft	Max. Elev. ft	Min. Elev. ft	Avg. Elev. ft	Max. Elev. ft
			Tap 25 Tap 25 is at Elev. 8.08 ft (zero datum)			Tap 26 Tap 26 is at Elev. 15.23 ft (zero datum)					
300	800	8	9	10	11						
300	2400	11	12	14	16						
300	4000	40	32	46	59	24	40	59			
			Tap 28 Tap 28 is at Elev. 1.23 ft (zero datum)			Tap 29 Tap 29 is at Elev. 3.53 ft (zero datum)			Tap 30 Tap 30 is at Elev. 8.08 ft (zero datum)		
300	800	8	7	8	9	8	8	9	8	8	9
300	2400	11	12	14	16	13	14	15	13	14	15
300	4000	40	33	43	54	28	43	59	24	44	62
			Tap 31 Tap 31 is at Elev. 11.43 ft (zero datum)			Tap 32 Tap 32 is at Elev. 14.73 ft (zero datum)			Tap 33 Tap 33 is at Elev. 15.73 ft (zero datum)		
300	800	8									
300	2400	11	14	16	18						
300	4000	40	22	46	68	27	40	55	22	40	62

CULVER-GOODMAN MODEL STUDIES  
 Type A Dropshaft Scale 1:21.5  
 Summary of Pressure Fluctuations

SAINT ANTHONY FALLS HYDRAULIC LABORATORY UNIVERSITY OF MINNESOTA		
DRAWN KJA	CHECKED <i>WOB</i>	APPROVED
SCALE	DATE 5/4/77	NO. 260A2313-87